THE TRIBOLOGICAL BEHAVIOUR OF GLASS FILLED POLYTETRAFLUOROETHYLENE (PTFE) UNDER DRY AND WATER LUBRICATION

BY

NKOSANA V. KLAAS

A dissertation submitted to the Faculty of Engineering and the Built Environment of the University of Cape Town in fulfillment of the requirements for the degree of Master of Science in Applied Science.

Department of Mechanical Engineering

Centre for Materials Engineering

University of Cape Town

2003

ACKNOWLEDGEMENTS

I would like to express my sincere gratitude to the following people for their significant contribution during this research project:

- Dr K. Marcus, my supervisor for all his invaluable advice, encouragement and guidance throughout the duration of my project

- Mrs Carolyn Kellock, a technical division manager at Chemplast Marc Etter (Pty) ltd for providing me with the relevant information and material.

- Mrs M. Waldron, Electron Microscope Unit (EMU) for her assistance in using the electron microscopes

- Mr G Newins and Mr P Jacobs (technical staff) for their patience and assistance in the preparation of my specimens

- Centre for Materials Engineering (CME) staff and students for their support and words of encouragement during the duration of this project

- Mr T Ntsoane at Ithemba Labs for his x-ray diffraction expertise and assistance

- Professor T. von Moiltke at the University of Pretoria for his work on the x-ray photoelectron spectroscopy (XPS)

- I would like to express my gratitude to the members of my family who have given me all the support I needed throughout the period of this thesis.

- A special thanks to Chemplast Marc Etter (Pty) Ltd and the NRF for their financial support.

NOMENCLATURE

PTFE	Polytetrafluoroethylene
LDPE	Low Density Polyethylene
UHMWPE	Ultra-High Molecular Weight Polyethylene
DSC	Differential Scanning Calorimetry
EDS	Energy Dispersive Spectroscopy
XRD	X-Ray Diffraction
XPS	X-Ray Photoelectron Spectroscopy
ESCA	Electron Spectroscopy for Chemical Analysis
SSG	standard specific gravity
ΔH_f	heat of fusion
ΔH_v	molar heat of vaporisation
K_0	specific wear rate
Mn	number average molecular weight
Mw	weight average molecular weight
R_a	centre-line average surface roughness
S	breaking strength
SEM	Scanning Electron Microscope
V	velocity
W	load
ν	Poisson's ratio
τ	shear strength
μ	friction coefficient
ϵ	elongation to break
η	viscosity
θ	temperature

ABSTRACT

This study was aimed at establishing the tribological behaviour of 25 % wt glass fibre filled polytetrafluoroethylene (PTFE) under dry sliding conditions. The experimental work was extended to compare and include its wear behaviour with other fillers such as bronze, carbon and graphite and to conduct tests under under water lubrication. Polyester-based materials, Vesconite and Vesconite Hilube, were used in this study for comparison purposes as well. The worn polymer pin surfaces and the counterfaces were studied by means of optical microscopy, scanning electron microscopy (SEM), energy dispersive spectroscopy (EDS), x-ray photoelectron spectroscopy (XPS) and surface profilometry. X-ray diffraction (XRD) and differential scanning calorimetry (DSC) were employed to study the changes in crystallinity and morphology of PTFE composite wear surfaces during the sliding process.

The effect of the different forms of glass, viz. glass fibres, glass beads (hollow and solid beads) and glass flakes on the friction and wear behaviour of PTFE was investigated. The effect of additions of small amounts of additive such as molybdenum disulphide, MoS_2, and pigments on the wear rate of glass fibre filled PTFE was also investigated. The results show that the addition of glass fillers to PTFE reduce the wear of PTFE by three orders magnitude while keeping the coefficient of friction more or less unchanged. The reduction in wear upon addition of the glass to PTFE was attributed to the formation of a coherent and adherent transfer film to the counterface during the sliding process. The transfer film formed by unfilled PTFE was quite patchy and non-adherent to the metal counterfaces.

The glass fibres and solid glass beads showed the lowest wear results whilst hollow beads showed the highest wear results under both low and high pressures due to crumbling and crushing of the beads during the sliding process. The glass flake filled PTFE showed relatively high but stable wear results up to 4.5 MPa above which wear rates increased dramatically. A marginal increase in wear was achieved by

using high aspect ratio glass fibres to the PTFE matrix. No correlation between the size of glass reinforcement and wear rate was established. The addition of MoS_2 to the glass fibre filled PTFE significantly improved the wear resistance. This was attributed to a low shear strength layer formed by this solid lubricant on the metal counterface during the sliding process. The mechanism by which glass fillers reduced wear is thought to be via the deposition of polymer fragments into the asperity valleys of the counterface. Mechanical interlocking of polymer fragments into asperities, results in a coherent film that is further enhanced by the formation of chemical bonds at the counterface and thus forming an adherent film. XPS analysis showed the presents of extra peaks in the fluorine spectra and it was determined that metal fluorides are formed during sliding.

Bronze filled PTFE showed higher wear rates than glass, carbon and graphite PTFE. The wear rate of glass filled PTFE composites was found to be higher than those of Vesconite and Vesconite Hilube by two orders of magnitude when tested in water. The high wear rates of the glass filled PTFE in water can be ascribed to the easy separation of the glass fillers from the polymer matrix in water and to the absence of the transfer film. At low pressures of about 2 MPa Vesconite Hilube showed lower wear rates compared with glass filled PTFE under dry sliding conditions but this difference decreases with increasing pressure. Another feature of this work is the fact that the dry wear rates for glass filled PTFE was similar for the reciprocating and pin on disk tests, further illustrating the significance of the role of the transfer film.

TABLE OF CONTENTS

CHAPTER 1

GENERAL INTRODUCTION

1.1 INTRODUCTION

Polymers and polymer composites are steadily gaining ground over the conventionally used metals, and more specifically in the field of engineering applications in tribology. Recent advances in technology and a better understanding of their wear behaviour have made it possible for polymers and polymer composites to be used in place of metals in various tribo-systems. Therefore, today engineers and designers have a wide variety of polymer products available to improve the performance and life span of critical parts such as bearings and seals. Polymer bearings are found in a wide range of industrial applications and currently many light stressed journal and sliding bearings are polymer-based. A major reason for the application of polymer materials in tribo-systems such as bearings is their capacity to mate against metals without the need for external lubrication. As such, they surpass metals under conditions where lubrication is impossible or undesirable. The performances of the tribo-components depend mainly on the following factors: nature of the bearing material, application parameters, counterface specifications as well as wear modes and their mechanisms.

The friction and wear behaviour of polymer bearings depend on the degree of adhesion between the counterface and the polymer bearing, the cohesive strength of the polymers and the thermal events in the frictional area while high ***pv*** values are applied[1]. Generally, polymers have low melting points and low thermal conductivities. Therefore, the frictional heat that is generated when the polymers are rubbed against metal counterfaces is not readily dissipated, resulting in possible distortion of the polymer components and sometimes failure or seizure of the whole system. A good bearing material is therefore one that exhibits both low coefficient of friction and low wear rates when mated with the metal surface. In addition, polymer bearings should have

melting points so as to avoid distortion and dimensional instability. Figure 1.1 shows a material performance pyramid that ranks the most commonly used thermoplastics in tribo-contacts according to their temperature performance[2]. Fluoropolymers such as PTFE, fluorinated ethylene-polypropylene copolymer (FEP) and polyvinylidene fluoride (PVDF), are widely used in mechanical as well as tribological parts and components. These polymers are used, for example, in gaskets and seals since they exhibit superior durability, longevity and high temperature stability. The important properties of these materials are given in appendix A. The advances in technologies coupled with an understanding and manipulation of the microstructure of polymers to influence properties, has led to an increase in the number of polymers that can be used in tribo-systems. Nylon- and polyester-based components are used extensively in industrial and marine applications where fluoropolymer components do not perform that well.

The most common fluoropolymer is PTFE and its use range from cookware to aerospace equipment and industrial machines. Fluoropolymer demand in the United States of America is forecast to increase by 5.3 % per year to nearly $1.7 billion in 2006. Figure 1.2 shows a pie chart representation of the US fluoropolymer demand in 2001. A significant portion of the fluoropoymer demand is dependent upon continued product development, which paves the way for new applications. Across a spectrum of end use markets, the fluoropolymer demand is driven chiefly by the superiority of these materials over other polymers and rubbers. Their use will continue to grow as emerging conditions necessitates the performance characteristics that these materials exhibit. The high melting point of the polytetrafluoroethylene (PTFE) of 327 °C and its low coefficient of friction when slid against metal counterfaces make this polymer particularly useful in dry sliding tribo-systems[1,2].

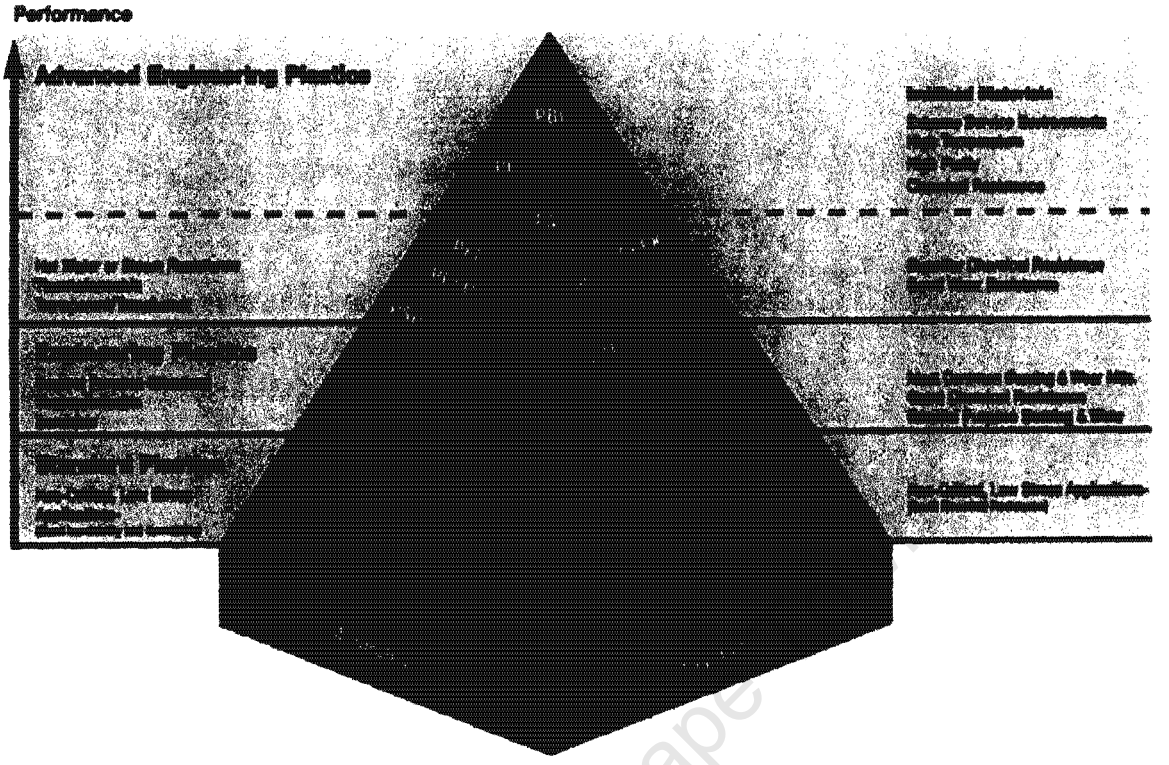

Figure 1.1: **The material performance pyramid ranking the thermoplastics that are extensively used in tribo-systems according to their temperature performance [After ref. 1].**

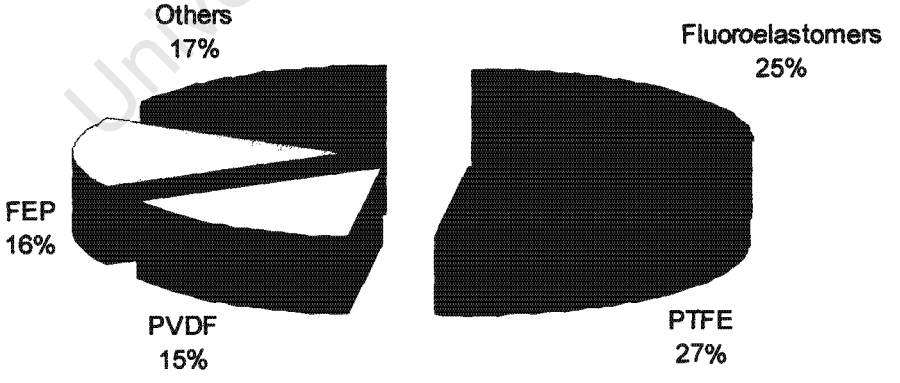

Figure 1.2: **The US fluoropolymer demand in 2001 that amounted to $1.3 billion broken down into different segments [After ref. 2].**

1.2 RESEARCH MOTIVATION

In many industries today there is major emphasis on the selection of a good polymer bearing material that will not only last long in service but also be reliable and one that requires minimum maintenance. Due to the advances in technology and an increase in the body of knowledge, there is an increasing demand for polymer bearing materials that could perform well under harsh conditions e.g. in aerospace. For this reason, there is a drive towards polymer materials that are self-lubricating and so require no lubrication which could lead to contamination. For the proper selection of dry running polymer materials, tribological data on the material combinations in question are required. The tribological behaviour of a material in a given contact situation may strongly depend on its actual composition and structure. A general theory to predict this behaviour from first principles is not available; therefore tribological characterisation of materials has to be based on experimental results. Thus, the tribological behaviour of filled PTFE composites under different sliding conditions should provide relevant and sufficient information that can then be used in making new formulations in a quest to improve the performance of these components even more.

1.3 RESEARCH OBJECTIVES

The main objectives of this study are to:

- Elucidate friction and wear mechanisms of different glass filled PTFE composites under dry and water lubrication
- Establish the effect of processing on the wear of PTFE
- Establish the effect of the form and size of glass on the wear of PTFE
- Determine the effect of additives and pigments on friction and wear of PTFE
- Detemine the ***pv*** limits of reprocessed glass fibre filled PTFE composites
- Compare the wear performances of glass filled PTFE with other materials
- Establish microstructural properties that give rise to the friction and wear behaviour observed

1.4 OUTLINE OF THE THESIS

The work that was carried out in the current study is reported in different chapters. Chapter two gives a background on the salient factors that affect the tribological behaviour of polymer bearings. Chapter three gives a description of the experimental techniques employed in this study as well as the material preparation. The results obtained in this investigation are given in chapter four and discussed in chapter five. Concluding remarks drawn from the observations are listed in chapter six followed by recommendations made for future work related to this present study.

CHAPTER 2

LITERATURE REVIEW

2.1 PERFORMANCE REQUIREMENTS OF TRIBOLOGICAL COMPONENTS IN MODERN INDUSTRIES

All rotating or sliding machinery, including motors and pumps, require support, alignment and sealing to maintain correct operation. Bearings and seals are used to provide this support[3]. Bearings locate, guide and support these rotating parts, preventing excessive axial or radial movement. The support and alignment of rotating parts is critical to the proper operation of the machine and contributes to the simple design and construction of sealing components. In all machinery plants, the loss of energy from friction is one of the major design and operating difficulties. A reduction of this mechanical friction and its consequent wastage of energy is the major reason for lubrication since proper lubrication does not only reduce loss of energy but also prolongs the life of machinery. In many cases it extends operational characteristics into higher speed and power regions. Thus, it is critical that some form of lubrication be present between contacting surfaces in relative motion in order to prolong the service lives of the tribo-components. Therefore, the proper choice of a bearing material becomes crucial. Bearings are classified as thrust and journal types but may be further divided to sliding surface (friction) or rolling (antifriction) types[4]. The main requirements of good bearing materials include the:

- availability of supply and practicability of servicing the material
- material should be uniform and posses a low coefficient of friction

- material should possess sufficient strength, appropriate wear factors and endurance
- material should have high thermal conductivity and be heat resistant
- should be a non-swelling material and be hard enough to resist abrasion
- should be able to carry the load yet the material should have impact resistance and not be brittle nor score the journal
- repair and maintenance costs of the material should not be excessive

The advances in new technology have made increasing demands on performance and reliability of the tribological components. These new developments have seen polymer bearings being more extensively been used in place of the conventional metal bearings. For a bearing to last in service, it is essential that the bearing be able to dissipate the frictional heat due to rubbing to the shaft. Figure 2.1 shows a schematic diagram of a typical bearing illustrating the important parts where heat energy is dissipated.

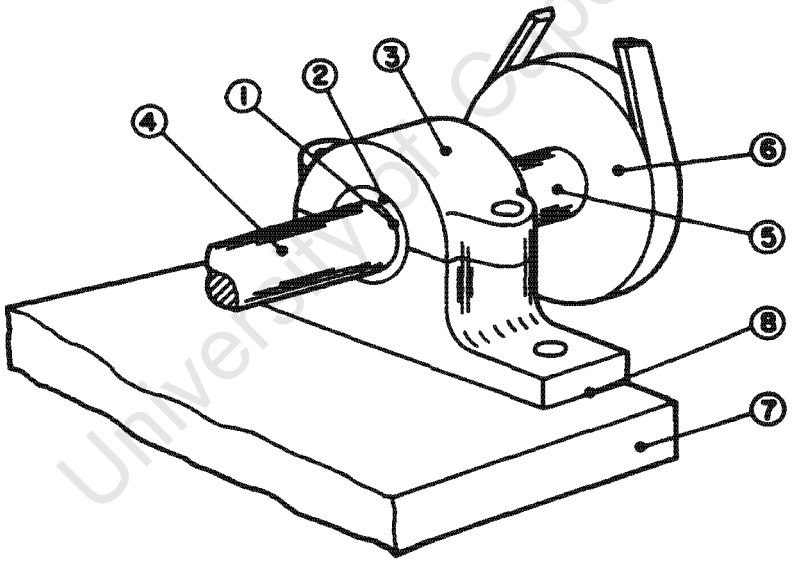

Figure 2.1: Schematic representation of a simple bearing assembly showing how the heat generated is conducted and dissipated at the (1) bearing surface, (2) bearing, (3) housing, (4) left hand part of the shaft, (5) right hand part of the shaft, (6) pulley wheel, (7) base and (8) joint.

2.2 PTFE As A Bearing Material

Polytetrafluoroethylene (PTFE) has gained international recognition as a versatile, high performance material that has traditionally been limited to specialty applications in high-end markets. It has unique properties that often make it the engineering polymer of choice for many of today's most demanding applications. PTFE's unique set of high performance properties has particularly found success in the chemical processing and valve industry in applications such as valve seats, seals bearings, gaskets, diaphragms, gears, impellers, vanes and friction pads. The communications and electronic industries consume PTFE parts in applications such as beads, connectors, insulators, radars and antenna products. PTFE components also serve the automotive, marine, medical, military, and food processing industries. The important properties that make PTFE a polymer of choice for these applications are summarised in table 2.1.

Table 2.1 Typical properties of PTFE resins.

D4894/4895	MPa	13.8
D4894/4895	%	140
D790	MPa	345 - 620
D256	J/m	106
D2240	-	50 - 65
E228	mm/mm.°C	$1x10^{-4}$
D435	W/m .K	0.25
D4591	kJ/kg.K	1.4
D621	%	10
D648	°C	73
D570	%	< 0.01
-	-	excellent
-	-	excellent
-	-	0.05 - 0.08
D4894/4895		2.1 - 2.3

The selection and use of PTFE and its composites as bearing materials to solve a combination of complex wear and friction bearing as well as structural issues, has both advantages and disadvantages. Some of these are summarised below:

Advantages

- PTFE is a low friction material for long life bearings and exhibits self-lubricating characteristics making it an ideal material for unlubricated applications where conventional lubrication is impractical or inconvenient. An example of this would be in the food industry where lubrication can lead to contamination of the product.

- The static and dynamic friction coefficients of PTFE are similar so there is no noise or stick-slip action in PTFE bearings, bushes and seals. PTFE also has high dimensional stability and does not swell in water in contrast to most synthetic polymers and so can be used in lubricated environments as well[3,4].

- PTFE bearings may be used where maintenance is infrequent therefore maintenance cost is greatly reduced. The temperature range for continuous use of PTFE is quite broad ranging from -260 to 260 °C, which makes PTFE one of the few materials that can be used at cryogenic environments. Thus, it is often used in spacecraft and satellites that operate in extreme environments.

- PTFE bearings may be used where long bush and pin life is required and due to PTFE's exceptional resistance to chemical attack, may be used in harsh environments where chemical attack is a problem.

Disadvantages

- PTFE exhibits high wear rates when slid against metal counterfaces and this somewhat impairs its use in tribosystems. When subjected to constant tensile stress or pressure, PTFE tends to cold flow or creep. Due to these properties,

PTFE parts subjected to higher levels of mechanical stress are either encapsulated, thus preventing their escape, or PTFE compounds with clearly enhanced pressure resistance properties are formulated.

- Although the impact strength of PTFE is high, its tensile strength, wear resistance and creep resistances are low in comparison to other engineering polymers. Glass fibres, bronze, carbon and graphite are sometimes added to improve specific properties. The mechanical properties have been further enhanced with the introduction of chemically modified PTFE systems such as the Hostaflon® TFM resin series by Hoechst Celanese[5].

- Due to its high molecular weight ($1x10^8$ g/mol) and high viscosity of about $0.1x\ 10^{11}$ Pa.s at 380 °C, PTFE cannot be processed by the conventional melt-processing techniques such as injection moulding. Instead, the granular grades of PTFE are processed by compression followed by a sintering technique which parallels powder metallurgy and ceramic processing[6]. The components fabricated in this way are much more expensive than those processed by conventional methods. Thus, PTFE components tend to be more expensive than other polymer components.

- The low thermal conductivity and high expansion coefficient of PTFE, common to all synthetic thermoplastics, means that frictional heat is not readily dissipated in the bush or bearing and so adequate clearance between the polymer bearing and the shaft is vital.

2.3 SYNTHESIS OF PTFE

PTFE is a straight-chain vinyl polymer that is made from the monomer tetrafluoroethylene (TFE) by free radical vinyl polymerisation as illustrated in figure 2.2 below. The white product formed from polymerisation has an extremely high molecular weight and is made up of repeating units or 'mers' that form a linear polymer chain structure $(-CF_2-CF_2-CF_2-)_n$[7,8]. Each mer is bonded strongly to two other mers, except for

mers at the very ends of the linear polymer molecule (see figure 2.2). The fluorine atoms are much bigger than the carbon atoms and so the carbon backbone of the linear molecule is completely sheathed by the electron cloud of fluorine atoms. The ensheathment and the angles at which the carbon-fluorine bonds are disposed, causes the centres of the electronegativity and the electropositivity to be perfectly balanced across the polymer chain cross section. As a result, no net charge difference prevails.

The non-polar nature of the polymer is partly responsible for its lack of chemical reactivity. The fluorine atoms are also responsible for the low surface energy and exceptional frictional characteristics of PTFE. The high C-F and C-C bond strength are among the strongest in single bond organic chemistry such that the bond forces between two adjacent polymer chains are significantly lower than the forces within one chain. Thus, the polymer must absorb considerable energy to disrupt the intra-chain bonds.

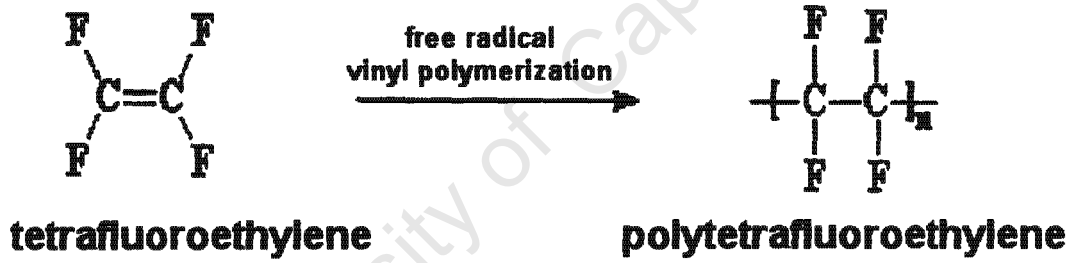

Figure 2.2: Schematic representation of the PTFE polymerisation process.

2.3.1 Monomer Preparation

Various stages are encountered in the monomer preparation and these are given by the following balanced chemical equations:

$$CaF_2 + H_2SO_4 \rightarrow CaSO_4 + 2HF$$
$$CH_4 + 3Cl_2 \rightarrow CHCl_3 + 3HCl$$
$$CHCl_3 + 2HF \rightarrow CHClF_2 + 2HCl$$
$$2CHClF_2 \Leftrightarrow CF_2CF_2 + 2HCl$$

The pyrolysis of chlorodifluoromethane to PTFE (last step) is a non-catalytic gas-phase reaction carried out in a flow reactor at atmospheric pressure and yields as high as 95 % polymer[9].

2.3.2 POLYMERISATION

Two basic polymerisation processes are used to obtain three different classes or forms of PTFE, which are also processed by different techniques[9]:

(a) Suspension polymerisation is used to produce granular resins and
(b) Dispersion polymerisation is used to produce fine powder resins as well as aqueous dispersions

Granular resins result from polymerisation of TFE alone with an initiator and with or without a small amount of dispersing agent. Vigorous agitation during the early stages of the process is maintained throughout to produce a precipitated resin, commonly referred to as granular resin. Fine powder resins are made by polymerising TFE in an aqueous medium in the presence of both the initiator and emulsifying agents. The dispersion remains sufficiently stable throughout the process and coagulates into a fine agglomeration, which floats on the aqueous solvent. Upon drying, the agglomeration form fine PTFE powder. The dispersion is made by the same polymerisation process used for fine powder resins. The difference is that in aqueous–dispersion polymerisation, precipitation of the resin particles is avoided[10].

The two polymerisation methods produce distinctly different products, even though both are chemically high molecular weight PTFE polymers. The granular resins may be moulded to various forms, while the resin produced by the aqueous dispersion method cannot be moulded but is fabricated by dispersion coating or by converting to powder

for paste extrusion. Granular resins on the other hand, cannot be paste-extruded or dispersion-coated. Therefore, these different forms of PTFE are used in different applications. Granular PTFE resins are used for moulded parts, billets and sheets and for extruding pipes and rods. Fine powders are used for thin walled tubing and tapes. The crystallinity of polymerised PTFE can be as high as 95 %. Granular resins are of particular importance in the current study as the unfilled PTFE material that is studied is of this type. Thus, the mechanical properties as well as the tribological properties mentioned in this thesis refer to granular resins. The way in which these properties are influenced by molecular structure is discussed below.

2.4 MOLECULAR STRUCTURE OF PTFE

In the solid state PTFE may be described as semicrystalline with a melting point of 327 °C. A semicrystalline polymer consists of interdispersed crystalline and amorphous regions. The morphological structure of many semicrystalline polymers is often termed spherulitic because of the spherulites that crystallise from the molten state. Although PTFE is a semicrystalline polymer, its morphological structure is not yet fully understood. Studies have been conducted over the past few years to further understand the morphological structure of PTFE [11,12]. These studies show that PTFE has extended chain crystals similar to that of polyethylene (PE) and it consists of bands or lamellae with the interdisperse amorphous and crystal regions[13].

However, the tribological behaviour of PTFE is found to be much different to that of PE. The studies show that the microstructure of PTFE consists of long and narrow bands with striations running along the width of the band giving it a smooth molecular profile which leads to low friction and easy formation of thin films, transferred onto the counterface during sliding against metal counterfaces. Researchers proposed and agreed that PTFE has a unique morphological structure, known as the banded structure[6,10,14,15,16]. This model for PTFE morphology has since been used by various researchers to explain the transfer characteristics as well as the high wear rates exhibited by PTFE when rubbed against metal counterfaces[8,10,11,17]. The banded microstructure of PTFE is shown in figure 2.3 below. Transmission electron microscopy

shows that the thickness of the crystalline slices separated by the amorphous regions is about 200 Å. Since the tribological behaviour of a polymer is critically depended on the structure of the polymer, the molecular morphology is expected to have a significant impact on the tribological performance of PTFE-based materials.

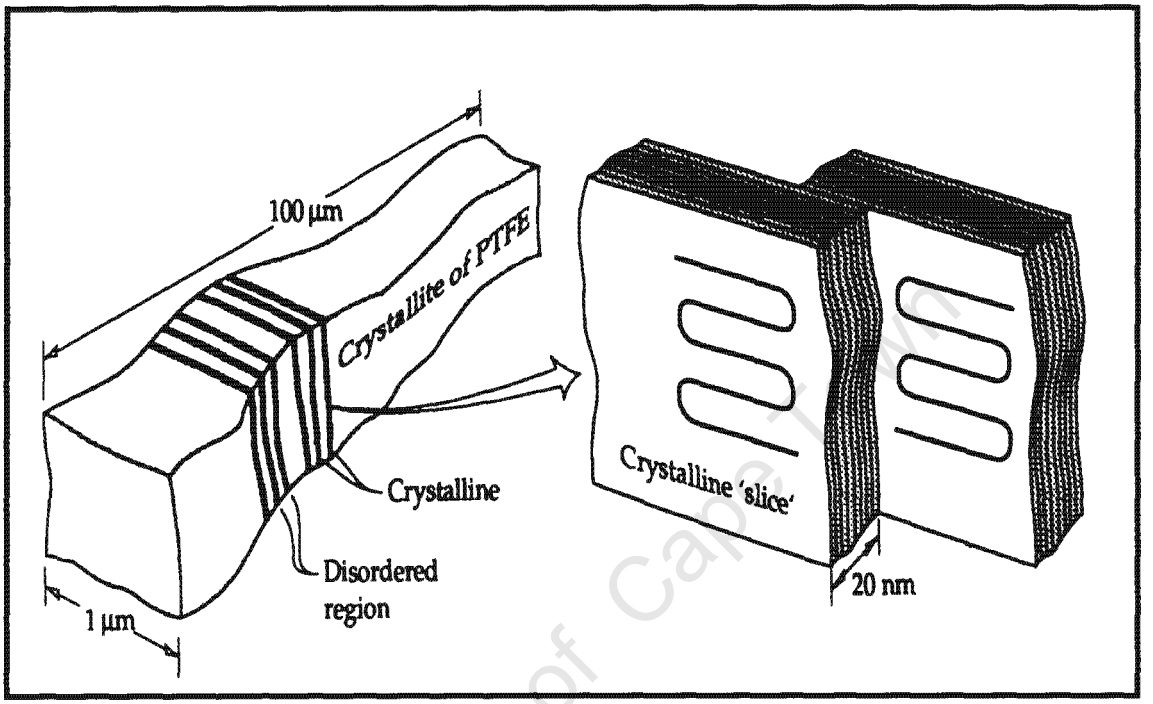

Figure 2.3: Banded structure of PTFE characterised by alternating crystalline and amorphous slices of striae and the slipping of lamellae [After ref. 13].

When PTFE is rubbed or slid against a much harder material, its chains undergo scission, creating polymer fibrils and active groups that chemically react with the counterface. This results in a strong transfer film on the substrate. When the bulk polymer interact with this transfer film, anisotropic deformation of the polymer unit cell occurs resulting in easy shear between chains[18].

2.4.1 Chain Morphology

PTFE has an unusual crystal structure in that it has a number of crystal forms and also possesses considerable molecular motion within crystals well below the melting point. The multiple forms of PTFE are influenced by temperature, pressure and thermal history.

In turn, these forms significantly influence the physical, electrical and processing properties of the polymer. It is well documented that the hydrogen analogue of PTFE, i.e. PE, has a planar, zig-zag molecular conformation while PTFE assumes a helical conformation up to 150 °C[13,18]. The reason for the helical structure is to accommodate the much larger fluorine atoms. The polytetrafluoroethylene molecule has 13 or 15 chemical repeat units (-CF_2- groups) and undergoes thermally activated structural transformations at 19, 30 and 150 °C[18]. The first two transition temperatures are particularly important due to their proximity to the ambient temperatures[19]. Below 19 °C shearing causes PTFE crystals to slide pass each other and retain their identity. Above 19 °C, the molecules are loosely packed and shearing result in the unwinding of molecules, creating PTFE fibrils[20].

Clark and Osswald investigated the first order transition that occurs at 19 °C, where PTFE undergoes crystal to crystal transformation from phase II to IV which prevails up to 30 °C[21,22]. Phase IV is characterised by the 15/7 conformation in a hexagonal unit cell. They asserted that PTFE undergoes this transition mainly because the polymer molecules want to assume the lowest energy conformation such that the fluorine atoms run helically on the surface. Thus, the PTFE chain resembles a rigid, cylindrical rod with a smooth surface. They further argue that this mutual arrangement of molecules is such that the lowest energy state is reached if the larger fluorine atoms replace the hydrogen atoms (in the PE structure), then the crystals assume a helical shape. In PTFE therefore, the crystals form helices as in all isotactic polymers with bulky side groups. PTFE has different stable helix geometries at different temperatures as stated above. These changes are accompanied by changes in crystal volume. A 13/6 morphological structure of PTFE is shown in figure 2.4.

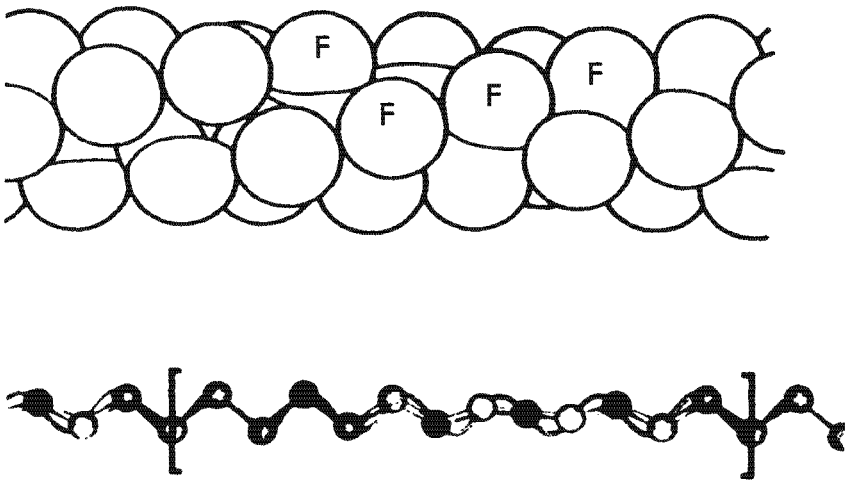

Figure 2.4: The repeat units of PTFE conformation (13/6) as well as the helical definition of the carbon backbone [After ref. 23].

2.5 POLYMER PROPERTIES

The thermal as well as mechanical properties of polymers depend on three main factors that also determine whether the polymer will be glassy, rubbery or leathery in nature. These factors include:

- The flexibility of the macromolecule
- The magnitude of the forces between the molecules and
- The stereoregularity of the macromolecules[23]

2.5.1 CRYSTALLINITY

The degree of crystallisation in a polymer may vary depending on the molecular weight as well as the crystallisation temperature. The inability to attain a fully crystalline structure is mainly due to the long chain structure of a polymer. Some of the twisted and entangled segments of chains that get trapped in between crystalline regions do not undergo the conformational reorganisation to become fully crystalline[24]. All the available

experimental and theoretical evidence indicate that granular PTFE is a linear polymer with a high degree of crystallinity. The crystallinity of as polymerised PTFE is reported to be higher than 90 %[4]. However, the high crystallinity is never regained after sintering and values of between 50-70 % are often recorded instead. The degree of crystallinity is known to affect the mechanical behaviour of polymers. Crystallisation improves the strength, density and modulus (stiffness) of polymers by reducing the degree of molecular randomization. There are several ways of determining the degree of crystallinity in polymers. These include:

(i) Differential scanning calorimetry (DSC): the enthalpy of fusion is compared to the literature value for 100 % crystallinity

$$X_c = \left(\frac{\Delta H_f}{\Delta H_f^*} \right) \qquad [2.1]$$

where ΔH_f is the heat of fusion of the sample and ΔH^*_f is the heat of fusion of 100 % crystalline PTFE

(ii) Wide angle x-ray diffraction (WAXD): WAXD can be used to measure the degree of crystallinity, X_c, from the ratio of the areas under the crystalline and amorphous reflections, A_c and A_a, respectively

$$X_c = \left[1 + \frac{A_{amorph}}{A_{cryst}} \right]^{-1} \qquad [2.2]$$

(iii) Density: literature values for the density, ρ of 100 % amorphous and 100 % crystalline are employed to calculate the degree of crystallinity (X_c) from the measured density of the sample as follows:

$$X_c = \left[\frac{\rho_{sample} - \rho_{amorph}}{\rho_{cryst} - \rho_{amorph}} \right] \qquad [2.3]$$

PTFE is insoluble in many solvents, thus making determination of molecular weight using conventional molecular weight measurements by Gel Permeation Chromatography (GPC) impossible[19]. The crystallinity can be related to density and molecular weight of the polymer since the rate of crystallisation decreases with increasing molecular weight. Thus, samples prepared from high molecular weight polymer and cooled from the melt at a constant, slow rate have lower standard specific gravities than those prepared from low molecular weight polymer cooled at the same rate. Higher specific gravity (SSG) therefore implies greater crystallinity and hence, smaller molecular weight as illustrated by equation 2.4.

$$SSG = 2.612 - 0.058 \log_{10} \overline{M_n} \qquad [2.4]$$

The evolution of the crystallinity is described by the Avrami equation:

$$X_c = 1 - \log(-Kt^n) \qquad [2.5]$$

K is a crystallisation rate constant and n a factor which adds the dependence of time of the nucleation step and dimensionality of the growth process. Thus, the determination of crystallinity of PTFE and its composites would provide useful information on the properties of the materials. In addition, the molecular weight of PTFE composites may be inferred from the degree of crystallinity. The molecular weight, in turn gives information on the nature of the polymer chains. The density of the PTFE and its composites is also expected to play a crucial rule in determining the tribological performances of these materials. Therefore, by using equation 2.4 the density of the PTFE and its composites may be compared directly to the measured densities using the pycnometer.

2.5.2 Mechanical Properties

The properties of polymers are mainly dependent on two factors: the flexibility of the polymer chain, and the interaction of the chain with its neighbours[25]. Mechanical properties such as yield stress and stiffness depend to a large extent on the density while the length of the polymer molecules has a significant effect on properties such as

toughness and wear resistance[26]. PTFE is tough and moderately flexible with a high elongation to break. It retains its toughness at very high and very low temperatures and therefore does not embrittle at liquid helium temperatures. It has excellent weathering resistance and is stable in air to at least 260 °C for continuous use. For linear polymers such as PTFE, their density as well as molecular weight, determine most of their properties. The lengths of chains influence the mechanical, chemical and physical properties of polymer. The properties that are associated with intermolecular forces of attraction are expected to increase as the homogeneous series in the paraffinic structure is extended. Properties such as polymer stiffness, tensile and impact strength and resistance to creep show these trends. As a molecular weight is increased, however, other properties become unacceptable, e.g., a high viscosity means it is difficult to work the polymer or injection mould and this would imply higher process temperatures to get the desired flow needed[26].

2.5.2.1 EFFECT OF MOLECULAR WEIGHT ON MECHANICAL PROPERTIES

The effect of molecular weight on the mechanical properties of polymeric materials may be best understood by knowing how polymer chains are distributed in a polymer molecule. Molecular weight of polymers is not uniformly defined but is an average value. This is so because the individual molecules generally posses different chain lengths. During polymerisation not all chains grow to be the same length and therefore there is a distribution of chain lengths that results in [27]:

- A distribution of molecular lengths in the bulk polymer
- An average molecular weight

A polymer with a distribution of chain lengths is described as polydisperse. Many industrial polymers show a similar molecular distribution curve as shown in figure 2.5. The number average from this curve is found by dividing chains into series of molecular weight ranges and then determining number fraction of chains within each range, i.e.

$$\overline{M_n} = \frac{\sum m_i}{\sum n_i} = \frac{\sum n_i M_i}{\sum n_i} \qquad [2.6]$$

where n_i is the number of molecules having molecular weight M_i. From light scattering determination, a method that depends on size rather than number of molecules, a weight average molar mass, M_w is obtained. The weight average molecular weight is found in a similar manner as the number average molecular weight[22,24,25]:

$$\overline{M_w} = \frac{\sum m_i M_i}{\sum m_i} = \frac{\sum n_i M_i^{\,2}}{\sum n_i M_i} \qquad [2.7]$$

One kind of weighting is the viscosity average molecular weight, M_v, that is derived from solution viscosity measurements and is calculated using:

$$\overline{M_v} = \left[\frac{\sum m_i M_i^{\,\alpha+1}}{\sum m_i} \right]^{\frac{1}{\alpha}} \qquad [2.8]$$

where α is the intrinsic viscosity of the polymer and is a material property. The viscosity average molecular weight is usually closer to the weight average than to number average molecular weight as shown in figure 2.5. An elegant way of determining MWD is by Gel Permeation Chromatography (GPC), the principle of which is that the polymer chains of different lengths behave differently when a solution passes through the column packed with a gel with uniform and appropriate pore sizes. However, this conventional technique of determining molecular weight does not work for viscous and insoluble polymers such as PTFE as described in section 2.5.1.

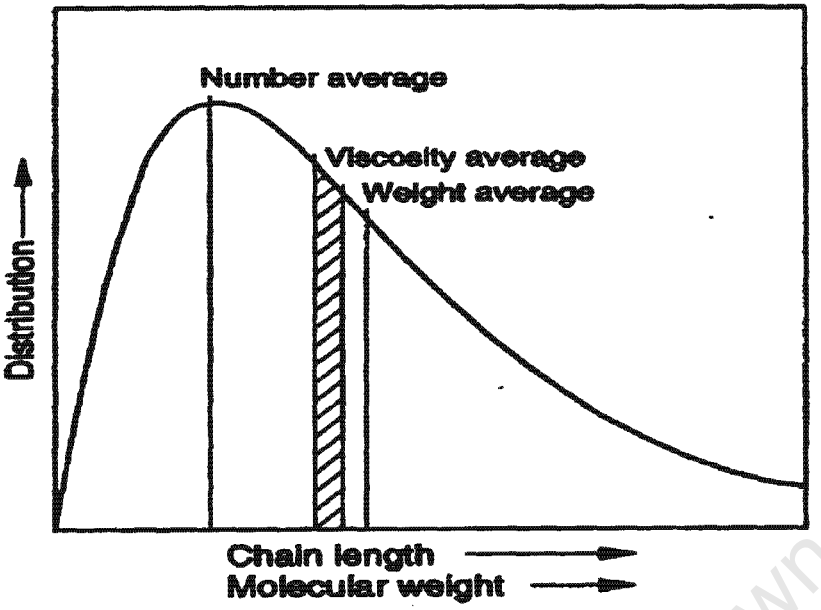

Figure 2.5: Typical distribution of synthetic polymer molar mass [After ref. 24].

2.5.3 THERMAL PROPERTIES

The effect of molecular weight on mechanical properties is best understood by examining the relationship between modulus and temperature. The thermal resistance of PTFE has a range of – 260 °C to + 260 °C. It can also withstand temperatures up to 300 °C for a short period. However, continuous operating temperatures depend on stress factors. Also, the thermal conductivity of PTFE is very low rendering it a good thermal insulator. The thermal conductivity of PTFE is known to increase with an increase in temperature but the increase is fairly small at moderate temperatures and becomes high at higher temperatures[27]. Researchers have found that the thermal conductivity of PTFE between – 180 °C and +150 °C is about 0.22 W/m.K[28,29]. The thermal conductivities of polymers are very low, of the order of one-hundredth that of the steel, and the dissipation of frictional heat is therefore very poor[30,31]. The low thermal conductivities of polymers result in large temperature gradients in the material and could cause a reduction in mechanical properties such as strength and stiffness or even degradation of the polymer.

The linear thermal expansion coefficients of polymers on the other hand are very high compared with those of metals. Polymers therefore tend to expand more when exposed to the heat source than do metals. This, coupled with the low thermal conductivities make modification of these materials necessary for sliding operations, like bearings and seals where dimensional stability and heat dissipation are critical.

2.5.3.1 GLASS TRANSITION TEMPERATURE

The glass transition temperature is a temperature or range of temperatures below which a linear and amorphous polymer is in a glassy state and above which it is rubbery. For semicrystalline polymers, the glass transition temperature always occurs at temperatures below the crystalline melting point (T_m). Thus, upon heating the semicrystalline polymer, it will pass through the T_g the chains come out of their ordered arrangement and begin to move around freely at T_m. The properties of polymers change profoundly at the T_g, including the coefficient of thermal expansion, heat capacity, refractive index, mechanical damping and electrical properties[7,11]. It has been empirically established that the glass transition temperature can be related to the polymer melting point by:

$$T_g = 0.66T_m \qquad [2.9]$$

where T_g and T_m are given in units of Kelvin. This relation, however, does not apply to all polymers.

2.5.4 POLYMER MELT RHEOLOGY

Rheology is the study of the flow and deformation of polymers. In particular, the relationship between stress, strain, time and temperature of polymeric materials is vitally important in this study. Polymer melts are viscoelastic i.e. they will exhibit a response to an applied stress, which is a combination of elastic and viscous strains[20]. Thus, under certain conditions they will behave like a liquid, and continually deform under an applied stress. Under other conditions they behave like an elastic solid, and will recover when the stress is removed. The most important and relevant facet of viscoelasticity is creep. Creep is a time dependent strain increase to a constant applied stress. Viscosity is a

measure of the internal friction that arises when there are velocity gradients within the system i.e. resistance to flow. The dynamic viscosity η, is expressed as the ratio between shear stress and the rate of shear. Since polymers do not exhibit Newtonian behaviour and are pseudoplastic, as the shear rate increases the polymer melt appears to yield. With Newtonian fluids, the viscosity is constant and independent of shear rate. Pseudoplastic materials exhibit the property of shear thinning i.e. decreasing viscosity as the shear rate increases. Various factors such as shear rate, molecular weight, temperature and pressure affect the melt viscosity of thermoplastics. There are a number of empirical mathematical equations describing the relationship between stress and strain rate of polymers, one of which is the power law model:

$$\frac{d\varepsilon}{dt} = K(\sigma)^n \qquad \textbf{[2.10]}$$

where ***K*** and ***n*** are material parameters. If n = 1 the expression reduces to Newton's Law of Newtonian fluids (i.e. shear stress is directly proportional to shear strain rate). Viscosity is sensitive to molecular chain length. Polymers of low molecular weight will therefore have low viscosity and so are easier to form. The viscosity of most polymer melts range between 10^2 and 10^7 Pa.s and therefore processing techniques such as extrusion as well as injection moulding can be employed to process them. At viscosities, higher than 10^4 Pa.s, normal extrusion becomes difficult and special techniques need to be employed[32].

2.6 PROCESSING OF PTFE

PTFE is one of the few known polymer materials that have very high molecular weights rendering them difficult to process[16,19,20]. Conventional melt processing methods such as extrusion and injection moulding cannot be used for these polymers because of their high melt viscosities of the order 10^{10} Pa.s at the processing temperatures[19]. This polymer is also very sensitive to shear in the amorphous state and tends to melt fracture. PTFE is processed by compression and sintering which is often employed in powder metallurgy to process ceramics and metals. Components manufactured in this

way tend to be expensive and may contain microscopic voids and fissures arising from the porous nature of the unsintered particles and the molecular re-arrangement caused by sintering[25]. The correct choice of polymer grade and the careful use of fabricating techniques should be employed to minimise the formation of voids.

2.6.1 Compression Moulding

Due to the high molecular weight and high viscocity, PTFE is processed by a two-stage process of compression followed by sintering known as free sintering. This powder processing technique is a compromise between powder flow and good strength. The particle shape, size, size distribution and internal structure are all critical in the processing of good quality PTFE components[10]. The free sintering compression moulding process consists of two phases, compression and sintering. During the first phase, the powder is compressed in a mould at room temperature to form a preform. The compaction, involves mixing the powder with a lubricant / binder and moulding it to shape by compressing it in a closed rigid die to form a 'green compact'[33]. At this stage the compact is highly porous but has enough rigidity to support its own weight and to permit gentle handling. Also during this stage of the process (compaction), particle rearrangement, elastic deformation at contact points and finally the compression of the material take place. In the second phase the compacted polymer product or preform is heat treated (sintered) to a well-defined temperature above the crystalline melting point of 327 °C for it to pass completely into the "gel state"[34]. The pre-moulded parts are usually sintered at 380°C in electrically heated, circulating air ovens according to specified programs and are allowed to expand and contract freely. Sintering can be divided into three stages:

- heating
- dwell time at sintering temperature
- cooling

The heating up and dwell time depend on the article being made, while the rate of cooling (which must be slow to avoid stress crack formation) influences the crystallinity of the finished article and so determines its properties[35]. During the first stage of free

sintering a component is heated to peak temperature in the shortest time without cracking. At this stage, the component has almost zero tensile strength and is highly prone to cracking due to residual and thermally induced stresses[34]. During the holding period (dwell time), the temperature should be the same throughout. During this stage coalescence and crystallisation take place leading to a decrease in porosity and an increase in density. The last step of the sintering process, determine the physical properties of the component. Slow cooling is ensures that desired crystallinity and the other properties related to it are achieved[10,35]. Factors such as the size, size distribution, shape of the particles, apparent density as well as powder flow, affect the performance of the final PTFE component. Free sintering is the cheapest method of fabricating PTFE components. However, components made in this way tend to have low creep resistance and higher porosity.

2.6.2 Pressure Sintering

This process is similar to free sintering and the preform is prepared in the same way[6]. The difference between these two processing methods is that, for pressure sintering the preform is not removed from the mould as in free sintering. The mould and the article being moulded are instead heated up in the oven without pressure till the sintering temperature is reached[6,35]. A pressure that is less than the compacting pressure is then applied to avoid built up of internal stresses that can result in stress cracking. The pressure is applied throughout the remainder of the sintering process. Pressure sintering however, is much more expensive than free sintering. Moreover, the pressure sintered components tend to lack homogeneity and consequently properties are highly anisotropic. Pressure sintered components also tend to suffer from discoloration which is usually required for aesthetic purposes.

2.7 Friction And Wear of Polymers

In bearing applications, like other tribological applications, wear and friction generated between the shaft and the bearing play a critical role in determining how long the bearing will survive in service. The objective therefore is a design that will give an

acceptable friction level and rate of wear. This is usually achieved by ensuring that there is a form of lubrication separating the two surfaces in relative motion. More often this is not achieved because ensuring adequate fluid lubrication is either difficult, impossible or even undesired[36]. Polymers can be used successfully in these applications since they exhibit the following important characteristics:
They

(1) can be used without any lubrication
(2) have low coefficients of friction
(3) are relatively light
(4) show no noise emission and
(5) are relatively cheap

This section therefore describes some fundamental areas in tribology that have a direct and significant effect on the performance of a bearing. The nature of friction, the mechanisms of wear, bulk mechanical and chemical properties of the polymer, transfer film mechanisms as well as other operating parameters all affect friction and wear. Tribology is defined as the science and technology of interacting surfaces in relative motion and the practices related thereto. The word ***tribology*** is derived from the Greek word ***tribos*** meaning rubbing[37]. Thus, it is the study that deals with the design, friction, lubrication and wear of interacting surfaces in relative motion such as bearings, artificial prosthetic joints, brakes, clutches, driving wheels, cams, gears and seals[38]. The friction and wear appearing in these operations constitute the largest energy losses, so research in tribology may lead to substantial economic savings and better performance of machines.

2.7.1 Friction Processes

Friction is the force that resists motion of two solids in relative motion. It plays a crucial role in determining how long a particular bearing is going to last in service. Friction arises from an adhesive force between contacting asperities and a deformation force that is needed to plough asperities of the harder material through the softer material.

The Amontons-Coulomb laws of dry sliding friction are often used as guiding rules in engineering applications. However, many deviations from these laws have been reported in the literature, so that further studies of the dependence of the coefficient of friction on sliding parameters need to be carried out[39].

2.7.1.1 THE LAWS OF FRICTION

The friction force, F_f, is proportional to the normal load, W, between the bodies. Alternatively, the ratio between the frictional force, F_f, and the normal load, W is known as the coefficient of friction and is denoted by the symbol μ[40].

$$F_f = \mu W \qquad [2.11]$$

(i) The friction force is independent of the apparent geometric area of contact and

(ii) The friction force is independent of sliding velocity (low velocity)

Thermoplastic polymers and their composites are viscoelastic materials and their deformation under load is viscoelastic. They usually do not obey law number (i) very well and the frictional force for these materials is thus not linearly dependent upon the applied load. The following relation is frequently used:

$$F_f = kW^n \qquad [2.12]$$

or

$$\mu = kW^{(n-1)} \qquad [2.13]$$

where k and n are constants, with n values between 2/3 and 1[41]. According to equation 2.13, the friction coefficient of PTFE composites decrease with an increase in load. When the load is increased further the temperature at the interface will rise leading to an increase in viscoelastic deformation and the reduction in mechanical strength as well as load carrying capacity of the PTFE composites. The Amontons-Coulomb laws are however open to misinterpretation. Therefore, a physical picture of the mechanics of

solid friction is needed from which the influencing factors and the relevant properties of the sliding components can be compiled. This treatment should include both an explanation of the forces necessary to overcome friction as well as the processes by which energy is dissipated. The friction model that is widely used by many researchers today is that of Bowden and Tabor[42] and later modified by Czichos[43]. Bowden and Tabor proposed that during dry sliding of tribosystems, mechanical energy is introduced into the contact zone by the formation of the real area of contact. This energy is then transformed mainly by the effect of deformation, ploughing and adhesion. This dissipation phenomenon encompasses the effects of thermal dissipation, storage or emission. These various aspects of friction are summarised in figure 2.6.

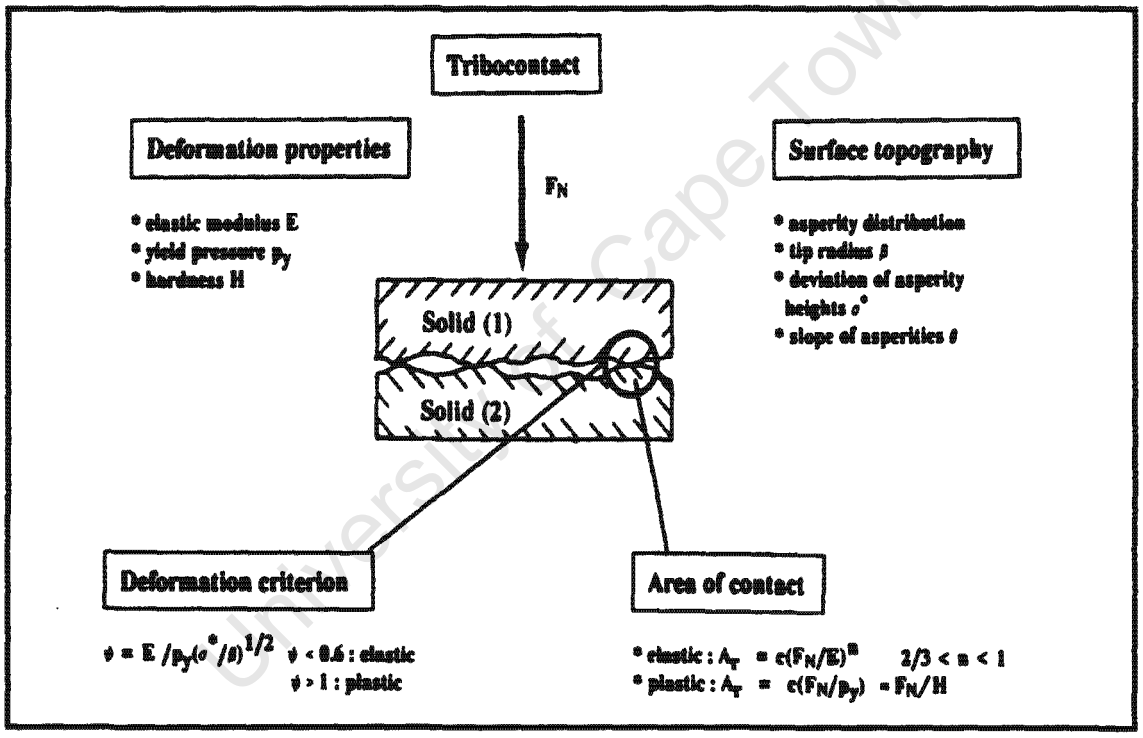

Figure 2.6: The surface characteristics of two solid surfaces in tribocontact. The asperities that provide the only contact points are clearly illustrated. [After ref. 39].

The salient aspects of the Bowden and Tabor friction model are discussed in sections 2.7.1.2 to 2.7.1.5.

2.7.1.2 THE REAL AREA OF CONTACT

Various studies have shown that the surfaces of tribosystems are not smooth but have asperities of certain height distribution (usually Gaussian) which deform elastically or plastically under a given load. For metals there is a crucial parameter,(the plasticity index), below which only plastic deformation occurs. However, for polymers with a near Gaussian distribution of asperity heights, the area of contact is linked to the applied load. At low interfacial loads, contact occurs only at the highest asperity tips but as load is increased the number of contact spots also increase as new contacts are now created with lower asperities (see figure 2.6). The summation of the individual spots gives the actual area of contact, A_r, which is quite smaller that the nominal area, A_0, as illustrated in figure 2.7. Explaining this microscopic model of friction, Czichos classified different contributions to friction into two categories[37]:

(i) Deformation processes and
(ii) Adhesion processes

These processes, are not independent of each other, under one set of conditions one process may dominate so that the other contributions may be neglected. Despite all these advances there is no experimental method yet available for determining the true area of contact between surfaces in static or sliding contact[44].

2.7.1.3 JUNCTION GROWTH

Friction is however, not only affected by the normal load, the tangential force plays a prominent role as well. If a tangential force is applied to one of the bodies in contact, the junctions formed at the regions of real contact will have to be sheared if sliding is to take place. If this force is insufficient, the junctions will deform but not break and sliding will therefore not take place. The phenomenon of junction growth between asperity contacts is based on the notion that when the normal load is acting on the asperity is high enough for the asperity to plastically yield, the contact area will easily be increased if the tangential force is introduced. The increase in the contact area will

result in a reduction in the normal pressure, since the same load is now carried over an increased area[45].

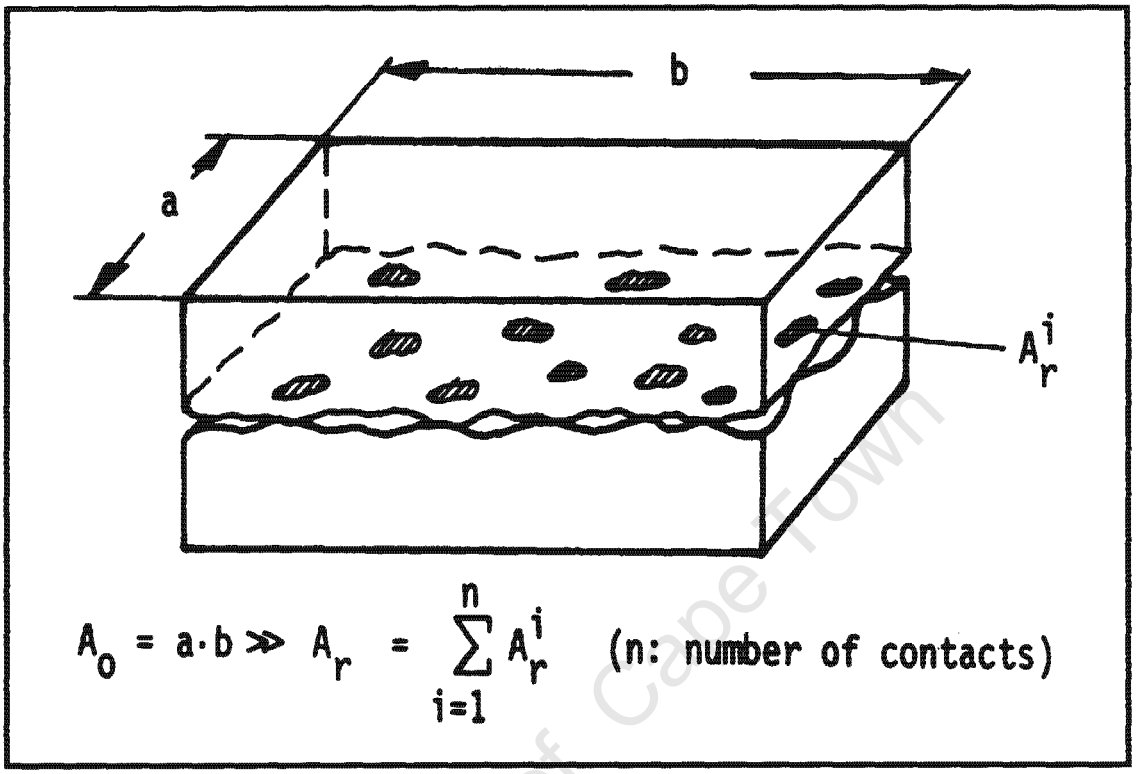

Figure 2.7: Two solid surfaces in tribocontact, clearly illustrating the difference between the apparent and real area of contact [After ref. 39].

2.7.1.4 ADHESION

The adhesion component of friction is often attributed to the molecular bonding of exposed surface atoms of both interacting surfaces[46]. Strong adhesion between the asperities has two main effects: (1) a large component of frictional force is generated and (2) the asperities could be removed from the surface to form wear particles or transfer films. During the relative sliding between polymeric materials and a hard surface, the separate chains in the surface layer attempt to link with molecules in the hard base, therefore forming local junctions (refer to figure 2.8). The sliding action causes these bonds to stretch, rupture and relax before new ones are formed. A strong

adhesion between tungsten and polymers such as PTFE and polyimide are reported in the literature[47]. These adhesive forces are strong enough to transfer polymer to the metallic surface when the two materials are separated. The strength of the adhesion is due to the presence of reactive non-metals, such as fluorine in the polymer.

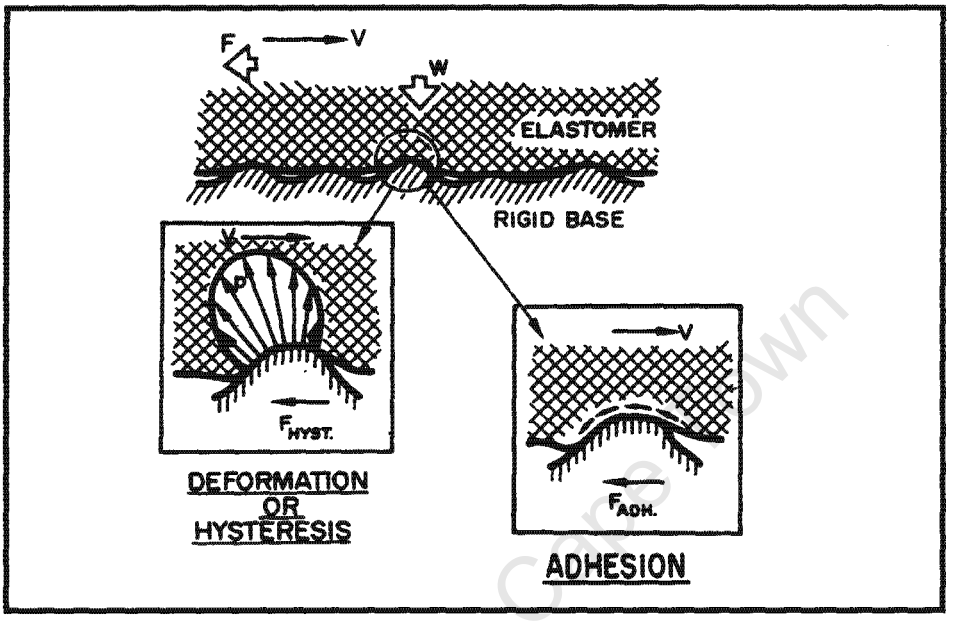

Figure 2.8: The principal components of polymer friction [After ref. 46].

2.7.1.5 DEFORMATION

While the adhesion component is due to electrostatic forces, Van der Waals forces and hydrogen bonds, the deformation component of friction is caused by the asperities of the harder metal penetrating into the softer material and 'ploughing' out a groove by plastic flow on the softer material[37,42,46]. The deformation component of friction can be isolated from the adhesion component by rolling a steel sphere over a PTFE surface. Resistance to rolling will be encountered which arises from energy dissipation in the bulk polymer beneath the sphere due to its viscoelastic response. Energy losses through hysteresis are a significant part of friction and if a fraction of the input energy is lost to viscoelastic hysteresis, it can be shown that the friction force, F_{def} will be given by:

$$F_{def} = 017\beta W^{\frac{4}{3}} R^{\frac{-2}{3}} (1-\upsilon^2)^{\frac{1}{3}} E^{\frac{-1}{3}} \quad [2.14]$$

where γ is the Poisson's ratio for the polymer,

W is the normal load

R is the radius of the sphere

E is the Young 's modulus and

β is the fraction of the total energy input

The friction processes do not only govern and dictate the heat generation at the tribo-contact but also affect and influence the amount of wear.

2.7.2 Wear Processes

Frictional interaction is accompanied by wear. Wear is defined as the removal of material from a solid surface as a result of the mechanical action exerted by another solid. It chiefly occurs as a progressive loss of substance of a body, occurring as a result of the relative motion at the surface[37]. There are distinct wear mechanisms involved in wear situation and these different wear mechanisms may be grouped into different categories. Evans and Lancaster list four main wear mechanisms that are most dominant in sliding motion and these are[30]:

(1) Adhesive wear
(2) Abrasive wear
(3) Surface fatigue and
(4) Thermal / oxidative degradation

These wear mechanisms may be further classified into two classes depending on the surface finish of the counter surface. The two classes of wear mechanism, involving surface and subsurface deformation have been termed interfacial and cohesive wear processes, with adhesive and chemical wear processes falling in the first category while abrasive and fatigue wear fall under cohesive wear processes. Other types of wear may be encountered, depending on the tribological environment. The four wear mechanisms mentioned above apply more to non-lubricated systems. In lubricated systems other types of wear such as corrosive wear, erosive wear, cavitation and impact chipping may

be encountered. Due to the polymeric materials low strength and elastic moduli (about one tenth of metals), ceramic or metallic counterfaces are often used as rigid bodies during sliding. Thus, all the deformation due to contact or sliding takes place within the polymer with the surface finish of the hard counterface having a strong influence and impact on the wear mechanism of the resulting wear[40]. Experimental results show that the phenomenon of wear in polymer-based materials is so complex and diverse that even in specific operating conditions, after the basic causes have been determined, it is difficult to establish and / or describe all its fine details[48]. It is found in practice that a single basic mechanism is always accompanied by the appearance of other types of wear. It is therefore necessary to confine our investigation only to the dominant wear processes that occur during the sliding motion. Thus, the wear modes that were deemed vital for this study are summarised in section 2.7.2.1 to 2.7.2.4.

2.7.2.1 ADHESIVE WEAR

Adhesive wear is the most common type of wear. It occurs as a result of strong adhesion due to the localised bonding between contacting solid materials leading to material transfer between the two surfaces or loss from either surface. The formation and subsequent shearing of welded junctions between two sliding surfaces result in the transfer of material to the harder surface and removal as wear debris[40,49]. The initial junction strength is a function of the interaction of the forces and the mechanical properties of contact. Adhesive wear occurs when the counterface is smooth and an incubation or running-in period often precedes steady state wear at which wear rate is often proportional to the normal applied load over a large range. For this type of wear to occur it is necessary for the surfaces to be in intimate contact with each other. Adhesive wear is many times greater for unlubricated than for effectively lubricated surfaces since surfaces which are held apart by lubricating films and oxide film reduce the tendency for adhesion to occur.

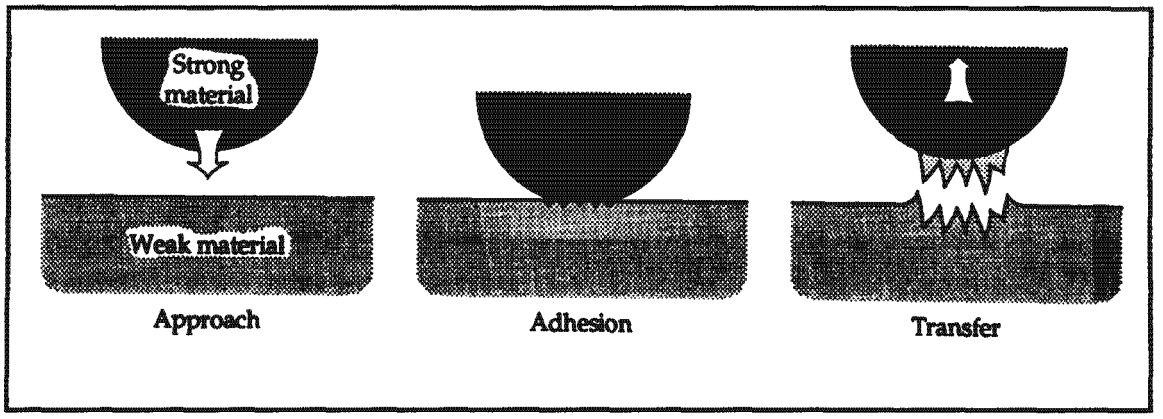

Figure 2.9: The adhesive wear of dissimilar materials rubbing against each other [After ref. 49].

Adhesive wear is particularly important for self-lubricating polymers that have a smooth molecular profile, such as PTFE. The smooth profile implies that the sliding of the polymer transfer film is easy and that the friction values are minimal[47].

2.7.2.2 ABRASIVE WEAR

Abrasive wear occurs in contact situations where there is direct physical contact between the two surfaces and where one of the surfaces is considerably harder than the other. It is due to hard particles or hard protuberances forced against and moving along a softer surface[50]. Abrasive wear is typically categorised according to the type of contact, as well as contact environment, into two-body abrasion and three-body abrasion. In two-body abrasion the harder surface asperities press into the softer surface, ploughing and removing the softer material, e.g. when polymers slide against rough metal surfaces or abrasion paper[51]. In three-body abrasive wear, the particles are loosely bound and move relative to one another while sliding across the wearing surface. Abrasion in polymers is accompanied by the tribo-chemical processes that are initiated mainly by degradation and is comparable with a "micro-cutting" process[43]. Thus, the wear debris formation occurs by ploughing, cutting and cracking mechanisms induced by the hard asperities of the counterface. Briscoe and Evans derived a mathematical model describing the abrasive wear of hard surface asperities removing polymer by shearing or cutting as[30,47]:

$$z = K(\frac{W}{H})\tan\theta \qquad [2.15]$$

where:

z is the volume of material removed per unit sliding distance,

W is the normal load,

H is the hardness,

k is the probability of formation of a wear particle,

θ is the base angle of the indenting asperity.

The abrasion deformation of polymers is partly elastic and partly plastic with the roughness of the counterface determining the relative proportions[51]. Relating wear to the mechanical properties of polymers, Lancaster and Ratner have shown that a single traversal wear of various polymers over steel counterfaces is proportional to $1/\sigma\varepsilon$, where σ is the rupture stress and ε is the elongation to break[52,53]. The cohesive energy density that indicates the strength of secondary bonding in polymeric materials was also shown to be related to the abrasive wear behaviour of polymers. Figure 2.10 shows that the abrasive wear of various thermoplastics is inversely proportional to the square roots of their cohesive energies.

Despite the associated increment in the breaking strength σ in many composites, the product $\sigma\varepsilon$ may become less than that of the parent polymer because of the reduction in ε. Friedrich reported that adding short fibres do not improve the wear rate of thermoplastics if the wear mechanism is highly abrasive in nature[54]. Since abrasive wear takes place when the abrading material is rough and harder than the surface to be abraded, it can be prevented either by eliminating the hard, rough constituent or by making the surface to be protected harder still materials[55].

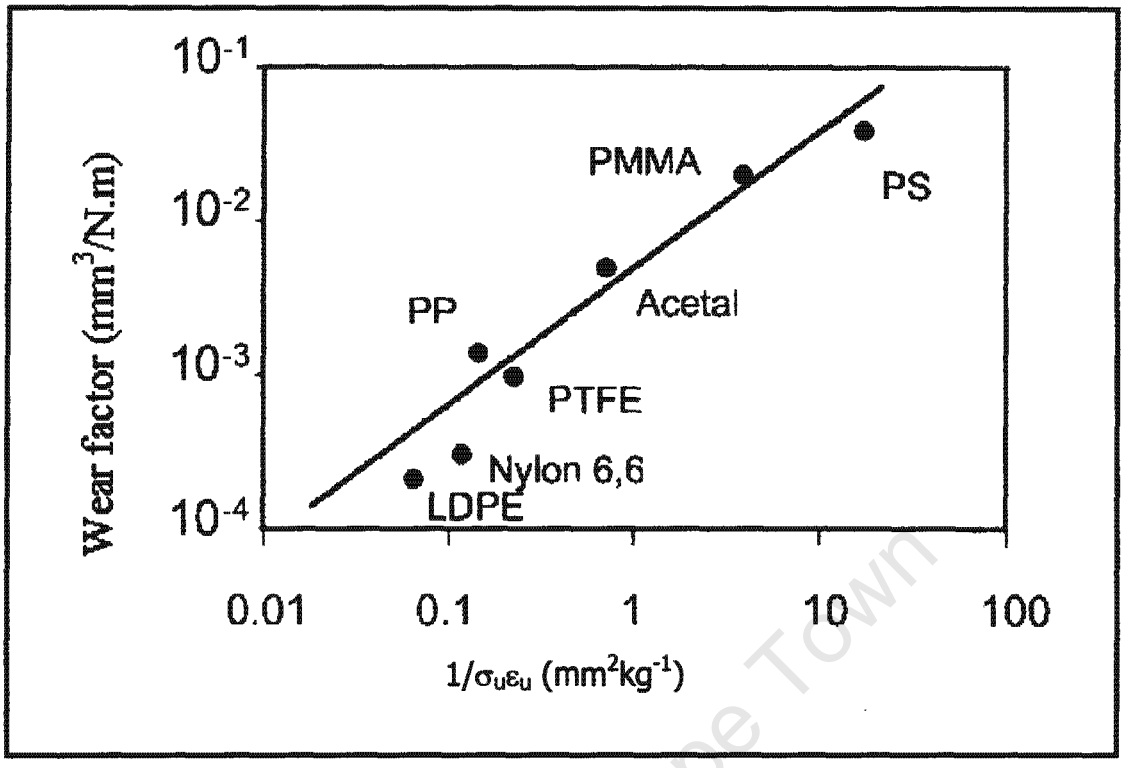

Figure 2.10: The Ratner-Lancaster correlation between the wear rates of thermoplastics under predominantly abrasive conditions and the reciprocal of the product of the stress and strain at tensile rupture. The tests were performed over rough steel counterface with the surfaces finish of 1.2 μm R_a [After ref.40].

In the presents of considerable adhesion and a number of traversals of the same portion of the same surface, another mode of wear, fatigue wear may dominate.

2.7.2.3 FATIGUE WEAR

Fatigue wear is the loss of material from solid surfaces due to repeated application of stress, by cyclic rotation across the surface or by the reciprocating sliding motion[56]. Under these conditions, the material in the surface layers become fatigued, micro fissures develop and cause microscopic crumbling and the formation of wear particles and subsequent loss of material from the solid surfaces. The basic mechanism involved in fatigue wear is shown in figure 2.11. In a simple model of fatigue wear, the wear rate could be determined by Paris equation:

$$\frac{da}{dN} = A(\Delta K)^n \qquad [2.16]$$

where

a is the crack length

N is the number of cycles

ΔK is the range of stress intensity to which the growing crack is exposed during each cycle

da/dN is the increase in crack length per stress cycle and

A and n are empirical constants.

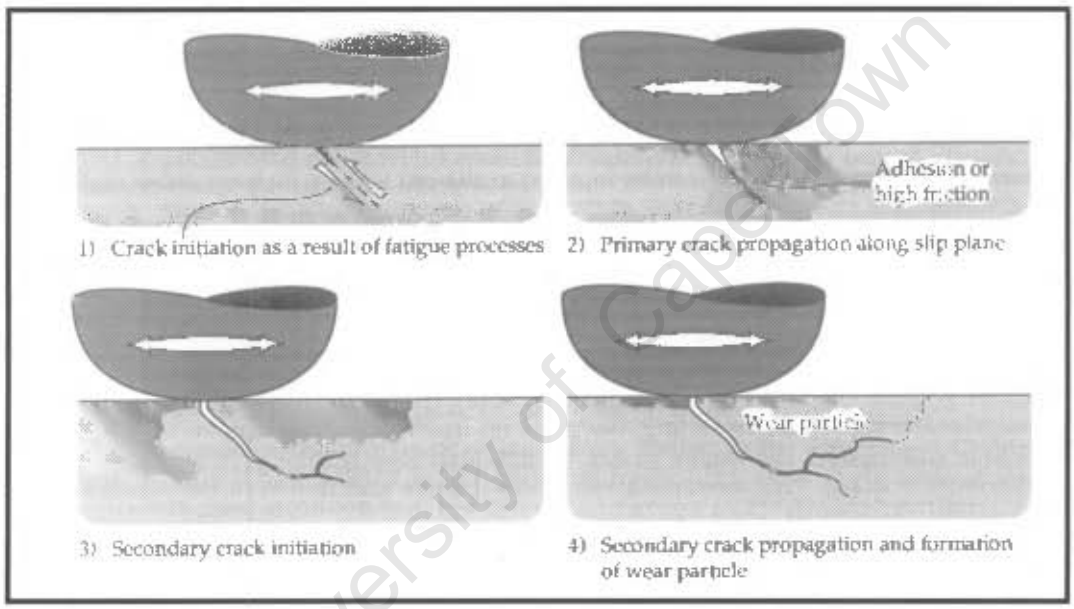

Figure 2.11: Diagrammatic representation of the fatigue wear mechanism [After ref. 49].

The last wear mode that usually manifests itself in chemically active environments, is the chemical wear.

2.7.2.4 CHEMICAL WEAR

Chemical wear occurs in chemically active systems in the presence of applied stress. Some form of chemical degradation is often present in all wear processes usually in a form of mild chain scission[23]. When this type of wear occurs, polymer materials may

crack before accepted critical values of stress are reached. The role and the mechanism of chemical wear in tribological processes, especially those involving polymers are not yet fully understood. This is partly due to the fact that the role played by chemical reactions in the overall wear process is not clear[47]. The other complications relate to the uncertainty on the precise effects played by the effects of strain activation, the catalytic effect of clean metal surfaces and the part played by fillers.

2.8 TRIBOLOGICAL CHARACTERISTICS OF PTFE

Studies reveal that PTFE exhibits very low coefficients of friction and retains useful mechanical properties at temperatures from –260 to +260 °C for continuous use. The investigations carried out by Pooley and Tabor showed that the friction of PTFE and high density polyethylene (HDPE) were very different from those of other thermoplastic polymers having bulky side groups in the molecular chain[57]. They suggested that the low friction and light transfer of these two polymers during sliding was due to their smooth molecular profiles. The smooth profile of the polymer chains facilitates adjacent polymer chains to slide past each other easily.

However, Tanaka and Miyata reported that the transfer of HDPE was similar to the other spherulitic semicystalline polymer materials and different to the extremely thin PTFE film of about 2.5 nm thick[58]. The field ion microscopy studies with PTFE sliding against tungsten reveal that the polymer transfers to the counterface by the mechanism of end-caps of the polymer chain adhering to the metal surface with carbon to metal bonding (refer to section 2.7.1.4). Therefore, there appears to be a broad consensus that the wear behaviour of PTFE is to a large extent influenced by its structural characteristics, such as the smooth profile of the polymer chains, the banded microstructure, crystallite size as well as the interchain distance in the unit cell. Therefore, the molecular structure of PTFE (discussed in section 2.4) has a major effect on its transfer and friction behaviour. PTFE exhibits the lowest coefficient of friction than any known polymer when slid or rubbed against metal counterfaces. Friction values of less than 0.05 are often quoted for bearings that operate at low velocities[27]. However, low coefficient of friction alone is not enough for a successful operation of a bearing as described in

section 2.1, other factors including the wear behaviour under a specified environment should be taken into account. Thus, a comprehensive study on the effect and influence of various factors on the tribological behaviour of PTFE is essential. Therefore, the following chapter is devoted to the analysis of the factors that affect, principally, the wear rates of polymers and polymer composites. These factors are narrowed to include only the so called "application parameters" such as bearing pressure, sliding velocity, temperature and counterface roughness. Other factors that are mainly concerned with the operating environments such as water together with the nature and form of filler are also discussed.

2.8.1 Factors Affecting Friction And Wear of PTFE Composites

There are many factors or parameters that affect the friction and wear performance of polymer composites in sliding operations[36]. Some of these are lumped as the 'application parameters' as mentioned in section 2.8. All these factors contribute to the wear behaviour of polymers and a change in one of them can often cause changes in one or more of the others.

2.8.1.1 THE EFFECT OF LUBRICATION

Lubrication is the action of introducing a lubricant between sliding surfaces to reduce wear and friction. Therefore, the purpose of a lubricant is to separate surfaces in relative motion with a film of material that is thin and which is sheared without causing damage to the surfaces[43]. In modern lubrication practices therefore, the main concern is to reduce the wear that accompanies sliding and at the same time to design lubrication systems that will operate for long periods without inspection or maintenance[59]. Fluid lubricants are the most frequently used since fluids may be sheared an infinite number if times without failing from wear or fatigue. There are three basic forms of fluid lubrication, hydrodynamic hydrodynamic lubrication, thin film or mixed lubrication and boundary lubrication[43,59]. The differences between these are the thickness of the lubricant film (ranging from 10^{-4} m to 10^{-9} m), the interfacial height distribution of the fluid lubricant and the degree of geometric conformity. PTFE compounds do not need to be lubricated and that is one of their main attractions in use

for bearings[36]. Yet there can be circumstances where a lubricant or a process liquid may be used, e.g. when the sliding velocity is high and so generating high frictional heat. The coefficient of friction for almost all polymer compounds decrease when a lubricant is introduced while the wear rate often goes up. This behaviour is often attributed to the fact that under non-lubricated, dry conditions a very thin layer of PTFE is transferred to the mating surface and acts as an effective dry lubricant. The presence of the fluid prevents or hinders the formation of such a film resulting in high wear rates[11,60].

2.8.1.1.1 Transfer Film

The interchain sliding in linear thermoplastic PTFE is responsible for the self-lubrication of this polymer[61]. Transfer film formation during sliding or rubbing is a very important phenomenon for self-lubricating polymers such as PTFE. The formation of coherent and adherent transfer film on the counterface is associated with low friction while lumpy and non-coherent transfer is associated with high friction. Many spherulitic polymers, especially those with low crystallinity show this behaviour (lumpy transfer) at low to moderate sliding speeds and loads. However, at high sliding speeds and load all polymers show lumpy transfer as well as high friction[18]. It is found that in the absence of such a film as long as strong adhesion between the metal and the polymer is ensured, the wear takes place by bulk fracture, resulting in lumpy and large debris.

Explaining the mechanism by which the thin transfer film (about 100 Å thick) of PTFE is formed Pooley and Tabor proposed that the transfer film is basically formed by shear process[57]. They say during sliding the strong adhesion between the counterface and the polymer result in the fracture of the bulk material leading to small particles of polymer being detached. These polymer fragments accumulate through adhesion and mechanical interaction between the machinery marks on the counterface giving rise to lumpy transfer. These lumps are drawn during sliding to make a thin film on the counterface so that further interaction between the polymer and the counterface is between the film and the counterface. As sliding commences a relatively thin (about 0.1 μm) and highly drawn layer is deposited on the transferred[55]. However, PTFE is known to be chemically inert so it is not clear how it adheres to the metal counterface.

The studies conducted by Buckley on the adhesion of PTFE onto the tungsten counterface revealed that the adhesion was quite strong[56]. With the use of the field ion microscope (FIM), he surmised that the adhesion could be due to the formation of carbon-metal bonds. Subsequent studies by Jintang ***et al*** revealed the presents of fluoride ions on the metal surface rubbed by PTFE[62,63,64,65,66,67]. They surmised that the PTFE radicals (chain fragments) and the fluoride ions react and chemically bond with the metallic elements of the counterface thereby aiding the process of strong adhesive bonding. The addition of lamellar solid lubricants such as molybdenum disulphide (MoS_2) and graphite aid and enhances the transfer film formation. In the case of MoS_2 on steel, strong metal to sulphur bonds are thought to form between the MoS_2 particles and the steel surface[68,69]. These chemical bonds ensures that a MoS_2 layer is always present at the counterface so that the friction remains low even after prolonged sliding[68].

2.8.1.2 THE EFFECT OF FILLERS

Pure PTFE has a relatively low wear resistance partly because the PTFE particles are not bonded in a real melt but are more or less mechanically connected in a sintering process. When PTFE is slid against a clean counterface, the polymer readily forms a thin transfer film on the counterface which does not normally adhere strongly to the counterface. The result is a high wear rate of the polymer. A significant improvement in wear resistance is achieved by incorporation of fillers in the PTFE matrix. The action of these fillers is not well understood but it appears that one of their beneficial effects is to attach securely the transfer layer to the counterface[10,11,13,18,41].

Fillers are generally added to polymeric materials to improve their properties and to reduce cost. They cover a wide range of particle sizes, shapes, as well as orientation in the composite and where necessary, undergo surface treatment to enhance compatibility with the polymer matrix. The purpose of the polymer resin is to bind the filler together and by the virtue of their cohesive and adhesive characteristics, the resins give the composite materials the ability to transfer load to and between fibres and protect them from environmental conditions.

Many types of fillers may be added to PTFE materials but the following fillers or combinations thereof are the most commonly used: glass fibres, carbon fibres, aramid (Kevlar®) pulp, graphite, metals (such as bronze or stainless steel), pigments and dyes in order to improve vital properties like compression resistance, wear resistance or thermal and electrical conductivity. Figure 2.12 shows the effect of different types of fillers and filler combinations on wear of PTFE composites when rubbed against mild steel[70]. The type, amount, shape and size of filler are important parameters that should be carefully considered when selecting a filler for PTFE. In the current investigation, glass is the filler of interest and therefore its impact on friction and wear of PTFE is of particular interest. There are various types and forms of glass and each form impact wear of the polymer matrix differently to others[71].

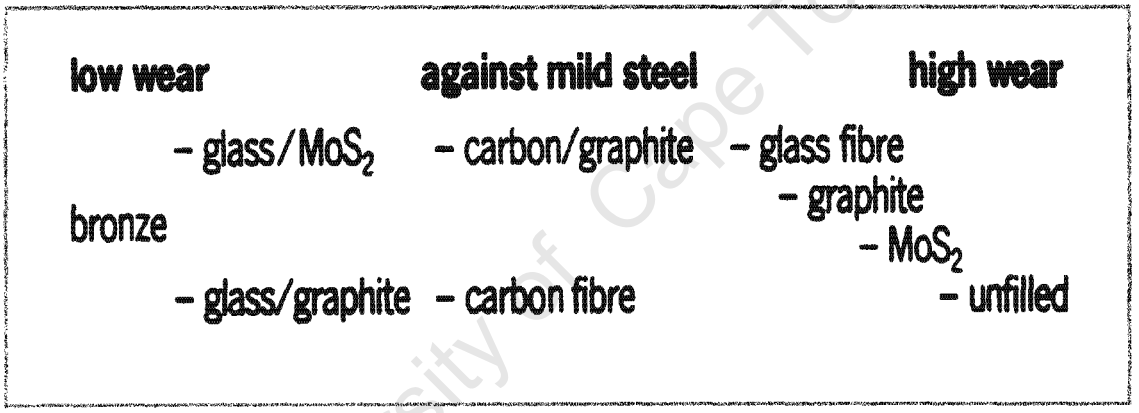

Figure 2.12: Effects of various fillers and filler combinations on wear of PTFE rubbed against mild steel [After ref. 70].

2.8.1.2.1 Glass Fibres

Glass fibres used in reinforced compounds have high strength and can be coated with a binder and coupling agent to improve compatibility with the resin and minimise abrasion between the filaments. Moulded glass products may contain as little as 5 % and as much as 60 % glass by weight. Glass fibre reinforcement improves most mechanical properties of plastics by a factor of two or more. They are particularly useful in increasing the strength and stiffness of polymers, and hence are effective in reducing wear in dry sliding conditions involving adhesion transfer or fatigue. Solid lubricants

dispersed into a thermoplastic base resin greatly improve surface–wear characteristics[70]. Creep behaviour of PTFE is improved by the inclusion of short glass fibres at low and high temperatures and incorporation of graphite or molybdenum disulphide or both further enhances the excellent frictional characteristics. Generally, fillers extend performance characteristics and allow for wider application particularly in demanding thermal stability and load support situations. In addition, the frictional and thermal properties of PTFE remain generally unaffected with the inclusion of fillers. Research in the past years has been focussed on determining the optimum filler loadings in an effort to enhance the tribological performances of polymer composites. The optimum level of filler is found to vary depending on a type of filler and polymer, with glass fibres a 25 % wt glass is often quoted as an optimum[72]:

Although fillers improve the mechanical properties of polymers, there is no simple correlation that exists between mechanical properties, wear behaviour and frictional properties. However, it is found that the filler incorporation and fibre reinforcement done to improve the wear behaviour of the base polymer for a particular application may not be beneficial for other wear situations. Sometimes it can worsen the wear performance[73,74]. The studies also show that additives such as graphite improve adhesive wear behaviour by improving the thermal conductivity of the polymer and negating changes in viscoelastic properties with rising speed or load application[75]. The additives, such as graphite and molybdenum disulphide are added to facilitate easy sliding while maintaining good mechanical properties.

Studies carried out by Briscoe ***et al*** on the lubricated friction and wear of polymers reveal that absorption of fluid into the surface layers of polymers can change the mechanical properties and consequently influence the friction and wear of polymers[76]. Similar studies done by Watanabe on friction and wear behaviour of various PTFE composites sliding against stainless steel in an aqueous environment revealed that the wear of PTFE composites were much more in water than in air, and that the PTFE filled with only glass fibres were much greater than that of other composites in water[77]. Yamada and Tanaka indicated that one of the causes of the high wear of PTFE composites in water is the easier separation between fillers and PTFE matrix in an aqueous environment[78].

2.8.1.2.2 Glass Beads

Glass beads increase the wear factor of the mating surface and the coefficient of friction. In unfilled PTFE and in PTFE compounds with spherical fillers, properties are usually isotropic whereas the irregular or longitudinal fillers tend to orientate themselves during compression moulding so that properties in the mould direction (MD) differ from those in the cross direction (CD)[4]. Pigments are generally added to glass fibre filled polymers in very small quantities just as colourants. Depending on how they bind the matrix and glass, they could slightly affect wear properties.

2.8.1.2.3 Glass Flakes

In contrast to glass fibres that are chiefly added as reinforcement, the glass flakes impart properties such as corrosion resistance and excellent mechanical properties. The important dimension for the fibre reinforcement is its length to diameter ratio (commonly known as the aspect ratio). For flakes the area or area to thickness control the properties of the composite. Therefore, the properties of glass fibre filled polymers tend to be anisotropic, with properties stronger in the longitudinal direction. In addition, the fibre carry most of the load and the marked improvement in specific strength and modulus are achieved. Particles and flakes enhance properties less effectively than fibres. The advantage of using glass flakes over other forms of glass in polymer composites is its low warpage properties.

2.8.1.3 THE EFFECT OF LOAD AND VELOCITY

The wear rate of unfilled polymers is generally found to be independent of pressure up to some critical value which is typically one-third the compressive strength of the polymer. Many polymer bearing materials such as polyacetal (POM) and ultra high molecular weight polyethylene (UHMWPE) show this behaviour with limiting bearing pressure often being defined by creep limitations rather than wear performance for some polymers. Research shows that the coefficient of friction of PTFE rises slowly at very light loads and decrease with increasing load[79,80,81]. O'Rourke also reported that that the twenty five percent glass fibre filled PTFE compounds that he tested do not follow that same trend and there was no significant increase or decrease for these materials when load was increased[79]. Some researchers disagree with this and suggest

that the coefficient of friction of glass fibre filled PTFE does vary with load[82]. The coefficient of friction for both filled and unfilled PTFE is reported to increase steadily with sliding velocity up to about 0.7 m/s. This phenomenon is often explained by the strain rate sensitivity of PTFE based materials as well as the increase in real area of contact caused by shearing at the interface. Sliding velocity affect wear rate of polymer composite through its influence on the temperature at the counterface. Anderson showed that the steady state mean surface temperature, θ, attained at the bearing surface could be related to sliding velocity by:

$$\theta = R\mu P\, v \qquad [2.17]$$

where
μ is the friction coefficient
P is the bearing pressure
v is the sliding and
R is the thermal resistance of the bearing assembly[34]

2.8.1.4 THE EFFECT OF SURFACE TEMPERATURE

The influence of temperature on friction and wear of plastics-based bearing materials is of primary importance in the prediction of the service life of dry bearings. The mechanical properties of polymers and composites are strongly temperature dependent. Young's modulus and hardness are found to be much higher at low temperatures compared to room temperature or higher temperatures. Consequently, the friction and wear mechanisms of polymer composites are expected to change with temperature. Operating temperature is important in many plastic applications and with dry bearings in particular it is often the factor that limits performance. This is especially true of the thermoplastics bearings, where load capacity depends on the temperature rise and the allowable degree of deformation at the working temperature[36].

The bearing surface temperature can be viewed as having two components. Firstly, the mean surface temperature immediately beneath the bearing surface, which is readily measurable and determined by the ambient temperature and the overall efficiency with

which the bearing assembly dissipates frictionally generated heat, and secondly, the flash temperature. The flash temperature is associated with heat conduction from the asperities and is generated into the bulk of the mating components[83]. The flash temperature estimation either theoretically or experimentally is difficult. Lancaster showed that with unfilled thermoplastics the wear rates often fall as the temperature rises, but subsequently increase sharply as the softening point is approached[66]. This suggests that the changes in mechanical properties such as hardness of unfilled polymers are primarily responsible for their sliding behaviour at elevated temperatures. The studies of Tanaka ***et al*** revealed that the wear of unfilled PTFE between 20 °C and 380 °C was similar to those of other unfilled thermoplastics at elevated temperature, i.e. the wear rate increases sharply as the temperature approaches 327 °C[84]. The wear rates of filled and reinforced PTFE also, generally increase with increasing temperature[85,86].

Theiler ***et al*** carried out studies on the tribological performance of PTFE composites at cryogenic temperatures[67]. Their studies revealed that the coefficient of friction of PTFE composites decreases from room temperature to 77 K. They attributed this behaviour to an increase in hardness of the polymer composites at low temperature as well as the decrease in friction due to deformation. However, at an extremely low temperature (4.2 K) they measured quite high coefficients of friction for the composites. The variation of friction and wear of PTFE composites also depends on the influence of fillers and the way they modify the counterface during sliding. The temperature generated at the interface can rise due to either a high environmental temperature or frictional heat[36].

2.8.1.5 THE EFFECT OF COUNTERFACE ROUGHNESS

The surface roughness of the surfaces against which polymers and composites slide is another important parameter that influences the polymer wear rates. The surface roughness of the counterface tends to decrease with sliding time due either to the polymer transfer or the abrasive action of filler in a composite material. Anderson reported that the glass fibre-fibre filled PTFE grades were much abrasive than the carbon, graphite and bronze filled versions and that the abrasiveness increased slightly as the glass content increased[36]. The effect of counterface roughness on the friction

and wear of self-lubricating polymers such as HDPE, UHMWPE, POM and nylon was studied by numerous researchers[87]. The studies show that the afore-mentioned polymers and their composites exhibit a minimum wear rate at certain counterface roughness; the wear rate increase appreciably with an increase in roughness at roughness larger than that corresponding to the minimum wear. PTFE and its composites, on the other hand are generally insensitive to surface roughness more than 0.02 μm R_a as depicted in figure 2.13. The low wear exhibited by PTFE when the counterface is smooth is attributed to adhesion wear. However, the wear rate of PTFE incorporating MoS_2, graphite or bronze increase rapidly as the roughness increases beyond a certain critical value characteristic of each of the composites[88]. Thus it is essential that the roughness of the mating counterface be taken into account when sliding tests are conducted.

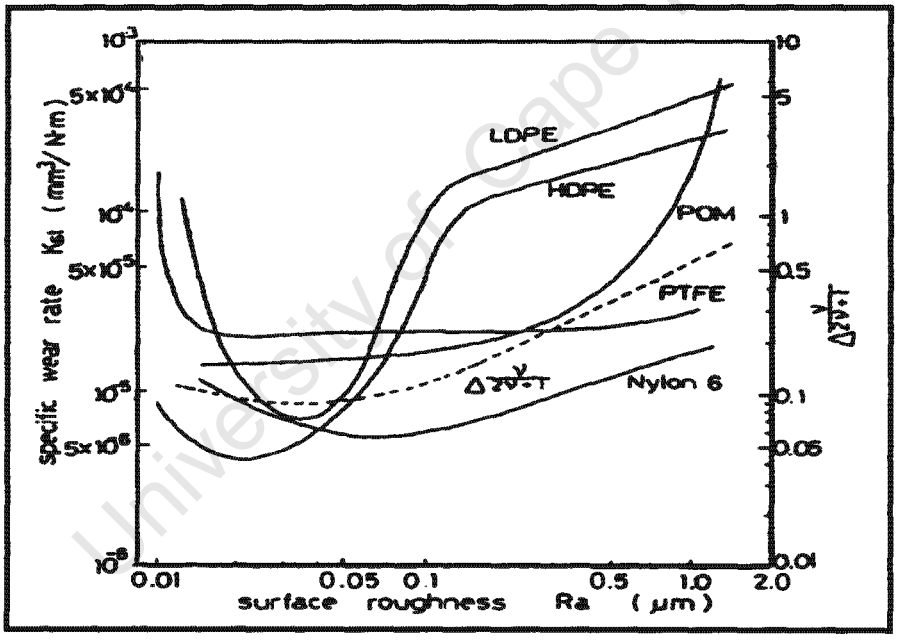

Figure 2.13: The variation of the specific wear rates of different polymers with steel surface roughness [After ref. 88].

2.8.2 THE *PV* FACTOR

The performance of polymer dry bearing composites depends on many parameters such that it is difficult to express it adequately by one single index[36]. The ***pv*** factor, a product of a sliding velocity and a bearing pressure is often used as a means of estimating the wear life of filled polymer bearings since it is related rate of wear as well as temperature rise at the composite-metal interface. The ***pv*** factor may be described in two ways:

(i) the limiting ***pv*** factor which is an upper bound to the useful operation of the bearing. This is the ***pv*** value at which the material exhibits excessive wear, usually due to interfacial melting or crack growth from ploughing. For polymers and composites, temperature is often the limiting factor and wear and friction tend to increase when a critical temperature (between the softening temperature and the melting temperature) is reached.

(ii) the ***pv*** value which gives a specified wear rate. This is generally quoted as the ***pv*** value to give 25 μm wear in 100 hours[32].

Materials in tribological interactions may therefore undergo either pressure or velocity induced failure. A pressure induced failure occurs when the loading of a polymer increases to the point at which the material creeps. A velocity induced failure on the other hand occurs at a point when the relative motion between the surfaces is such that thermal work at the material interface is sufficient to catastrophically increase the wear rate. However, the ***pv*** factor does not take into account the temperature of the environment, on which the temperature due to frictional heating is superimposed. Figures 2.14 (a) and 2.14 (b) show the effect of temperature on the wear of PTFE composites and idealised ***pv*** limits of different materials, respectively. Also, when a lubricant is introduced, a whole new set of factors come into effect and very high ***pv*** factors can be achieved for some polymer composites but this simplified approach to performance assessment becomes unworkable[34,38,89]. The decrease in wear of polymer materials when a lubricant is introduced in the interface is the prevention of the

solid/solid interaction during sliding resulting in low wear rates. However, the wear rates of some polymer composites such as glass fibre filled PTFE are known to increase sharply in water. This high wear rate is often attributed to the absence of the transfer film, being washed away by the lubricant. In the case of glass fibre, it is thought that the bond between the polymer matrix and glass fibres is not strong and in water the glass fibres separate easily from the matrix thereby leading to high wear rates.

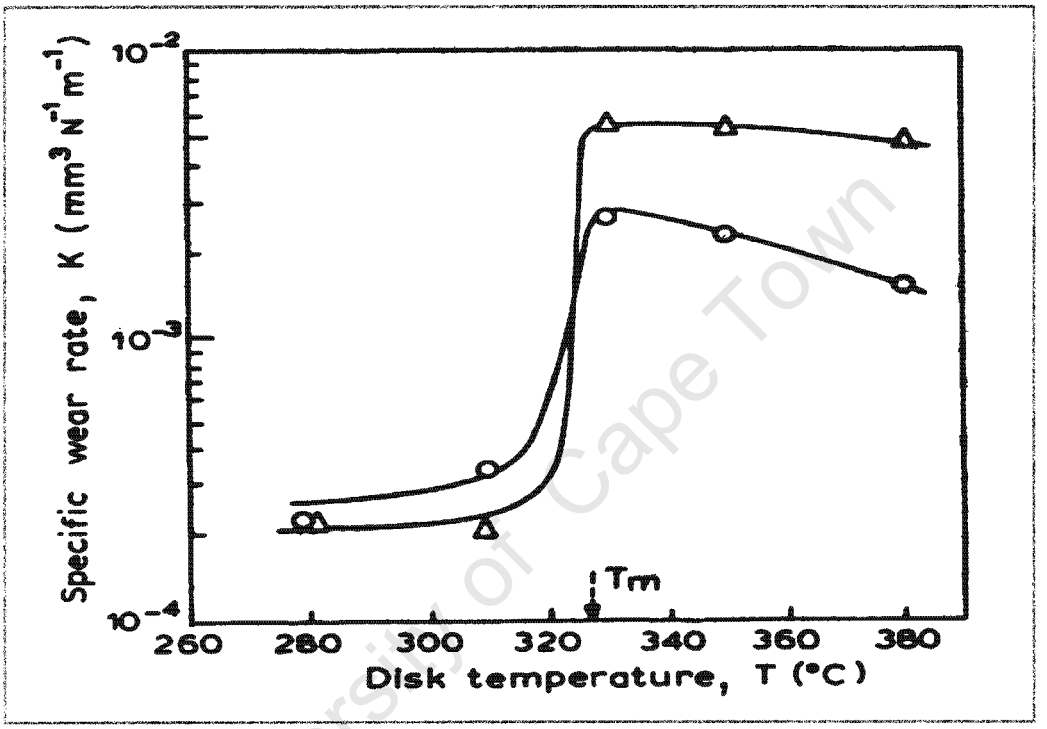

Figure 2.14 (a): Typical variation of the wear rates of PTFE composites with the temperature of the disk counterface [After ref. 13].

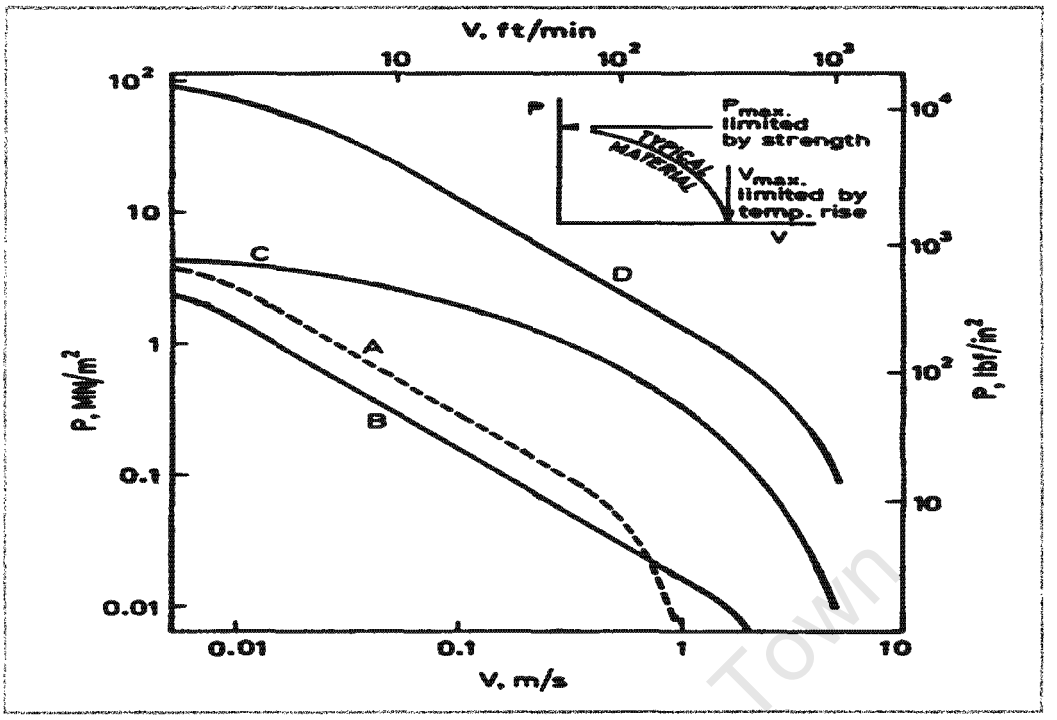

Figure 2.14 (b): **The relationship between the pressure and velocity of A-thermoplastics, B-PTFE, C-PTFE+fibres and D-porous bronze+PTFE+Pb. The curves represent the combinations of pressure and velocity under which the different materials may be successfully used. The region above each of the curves is a region of severe wear while the region below it is characterised by mild wear [After ref. 90].**

CHAPTER 3

EXPERIMENTAL TECHNIQUES

LABORATORY WEAR TESTING APPARATUS

3.1 INTRODUCTION

The tribological behaviour of polymers depends very strongly on the material combination, which part moves and which part stands still. It is therefore critical that the test system corresponds to the practical application in the closest possible manner. Since polymers generally have low thermal conductivity and high thermal expansion coefficients, the specimen may expand under frictional heat so allowances of these must made when the wear rig is designed. Various standard rigs with different contact geometries such as, block (or pin)-on-ring, sphere-on-prism and plain bearing-on-shaft are often employed. The present study seeks to simulate the real journal bearing contacts as well as simulation of linear guidance systems. The purpose therefore is to obtain for polymer-based materials reproducible measured values for wear and the coefficient of friction under specified and exactly defined test conditions in water lubrication and without lubrication.

3.2 WEAR TESTING RIGS

The standard friction and wear testing apparatus used in the present study to determine the tribological performances of glass filled PTFE materials are the:

(i) pin-on-disk – simulation of journal bearing contacts and
(ii) reciprocating sliding wear rig- simulation of linear guidance systems

The wear tests performed on the rigs are done under somewhat different sliding conditions due to speed limitations of the reciprocating sliding wear rig.

3.2.1 THE PIN-ON-DISK SET-UP

The pin-on-disk tribometer is the simplest friction and wear testing apparatus. It is a standard rig widely used because of its simplicity and convenience of use[90]. Figure 3.1 shows a typical pin-on-disk apparatus layout. The apparatus consists of a pin made from the material under investigation which is mounted on a balanced lever arm to ensure zero residual load. The pin is forced against the counterface disk that is mounted on onto a shaft driven by an electric motor by means of the lever arm system. Simply adjusting the pivot load can therefore alter the interfacial pressure. Friction may be measured by a strain gauge device located on the pivot arm or by a load cell restraining the tangential movement of the specimen clamp. This simple method facilitates the study of friction and wears behaviour of almost every solid state material combination with or without lubricant. A more detailed description of the pin-on-disk follows in section 3.2.1.1.

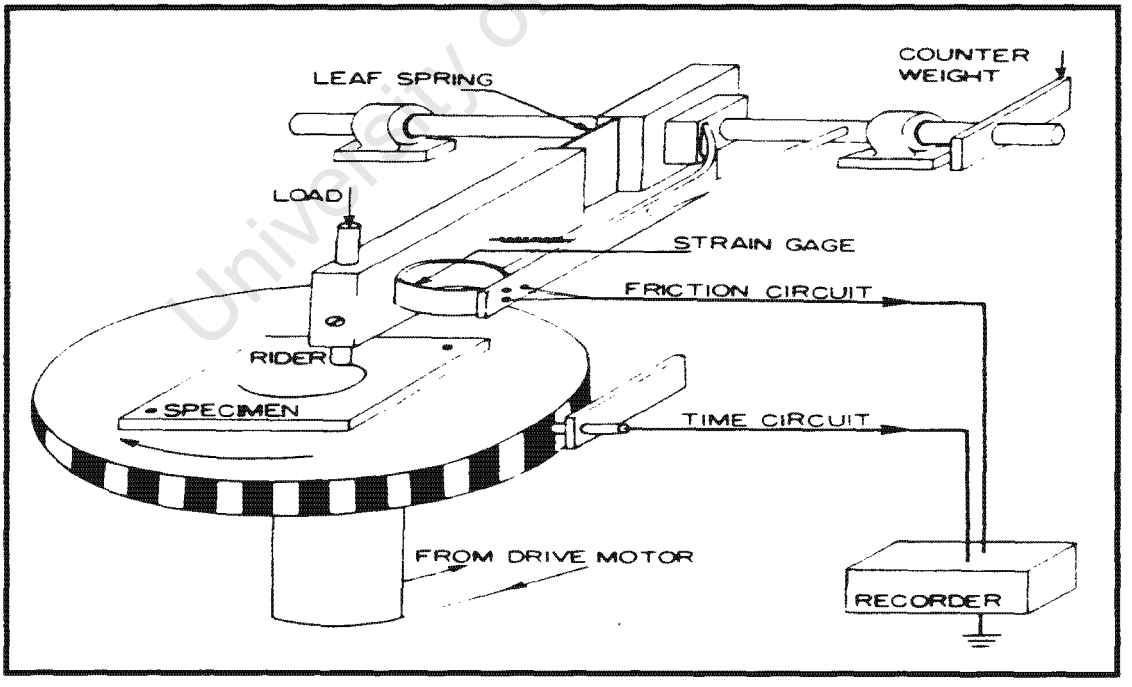

Figure 3.1: Schematic view of a basic pin-on-disk apparatus [After ref 89].

There are many benefits in using this type of system. These include:

- simple mechanical design
- basic testing of simple test specimens
- easy friction measurements
- no increase of sliding surface area due to wear
- uncomplicated loading technique
- initial ranking of materials

There are however some major disadvantages with this system as well. These include the following:

- wear debris is easily removed from the interface due to the outward flow of lubricant
- the counterface disk should be fairly large if linear motion is to be approached.
- the sliding velocity varies across the wear pin surface due to the circular motion of the counterface disk.
- the topography (and therefore roughness) of the counterface disk changes with the rotational angle of the disk.

3.2.1.1 THE PIN-ON-DISK WEAR RIG

The pin-on-disk sliding wear rig was chosen in the present study because of its simplicity and unspecialised nature of the tests. The results obtained in such tests would indicate the wear resistance under continuous, unlubricated conditions at moderate speeds and pressure. Figure 3.2 shows a picture of the pin-on-disk sliding wear rig. The rig was built in house and consists of a lever arm with counterweight to balance the weight of the arm to zero. A pin is screwed into the pin-holder that is attached to the arm and locked with a nut to avoid pin rotation during sliding. The dead weight load is placed onto the end of the arm and is amplified twice at the pin due to torque balance. The polymer composite pin slides against a martensitic stainless steel AISI 431 grade that is 140 mm in diameter and 18 mm thick. The disk is held at the base by four grub screws

and is rotated at constant velocity by a 0.75 kW AC electric motor. A cylindrical thrust bearing that can adequately support the loads up to 20 kg supports the base. The pulley below the base has eight bolts that serve as the magnetic pick-up points for an electronic counter. The number of revolutions that correspond to chosen sliding distance can then be selected and entered into the counter. The counter automatically switches off the motor when these are completed.

A – Chart recorder used to measure friction
B – Disk
C – Load
D – AC control box
E – R.T.M counter
F – Speed dial
G - Counter

Figure 3.2: Photograph of the pin-on-disk sliding wear rig.

An AC control unit controls the rotational velocity of the electric motor and changes the signal from a single phase AC current to a delta three phase AC current. It is therefore able to control the RPM of the motor by varying the frequency of the voltage. The

maximum RPM of the motor is 1400 with 3:1 pulley system. The radius of the wear track on the disk is also variable so that a wide range of sliding speeds can be attained, roughly 0.1 to 2 m/s. The coefficient of friction can be measured by the 20 kgf load cell that is mounted next to the lever arm such that the bolt head from the arm pushes with the frictional force against the pin of the load cell. The signal from the load cell is amplified and sent to a TOA chart recorder as voltage traces that are later converted to friction by first calibrating the load cell. A number of tests can be performed on a disk, each test using new and separate wear track that has a width equal to that of the wear pin specimen.

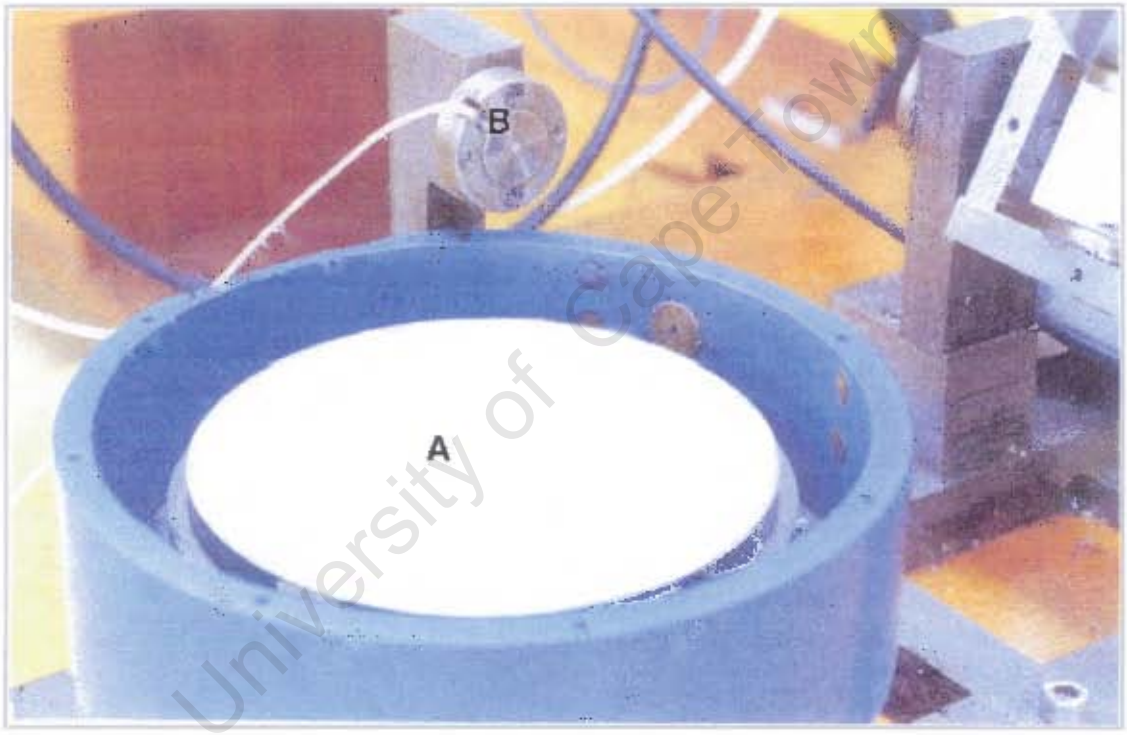

Figure 3.3: A close up photograph of the stainless steel disk counterface (A). The load cell (B) can be more clearly seen here than in figure 3.2.

Although the pin-on-disk wear system is built-in house, it has produced reliable friction and wear results over the past few years. Therefore, no major modifications were necessary before the rig could be used.

3.2.2 The Reciprocating Sliding Wear Set-up

The linear reciprocating sliding wear rig reproduces the reciprocating motion typical of many real world mechanisms, thus the apparatus is frequently used to test wear performances of materials. Figure 3.4 is a schematic illustration of the specimen motion typical for such a rig. In this type of reciprocating motion the counterface is mounted onto a shuttle base which is forced to reciprocate perpendicular to the stationary wear pin. The reciprocating wear testers do not suffer from any of the drawbacks mentioned in section 3.2.1 for the pin-on-disk. Also, the reciprocating technique is very useful for studying the variation over time of the static coefficient of friction – as opposed to the kinetic coefficient measured with the pin-on-disk geometry. However, although the type of motion associated with the reciprocating type apparatus is linear, the sliding velocity is sinusoidal and this may be undesirable in certain wear simulations.

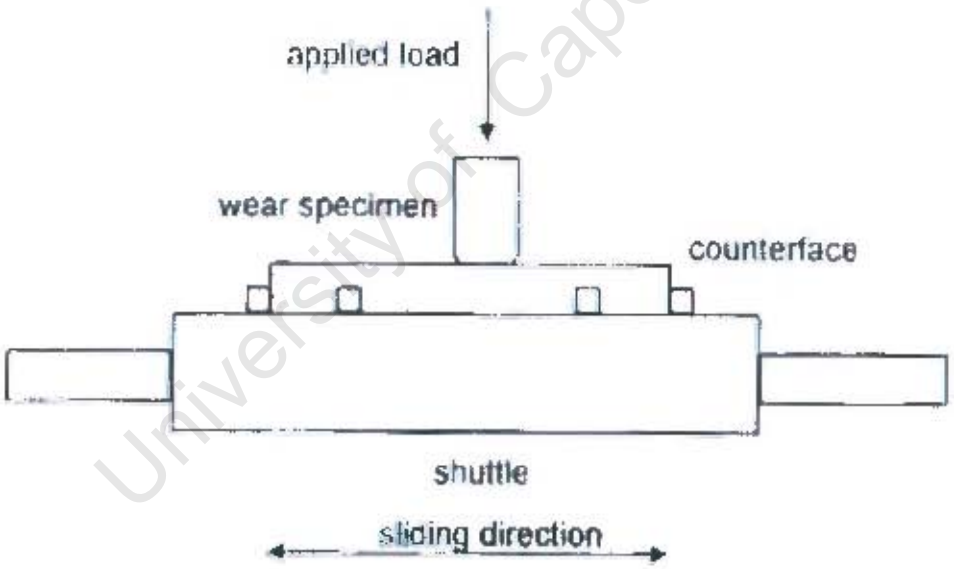

Figure 3.4: Schematic illustration of the reciprocating type of motion.

3.2.2.1 THE RECIPROCATING SLIDING WEAR RIG

The reciprocating sliding wear tester to be used for investigations of wear and friction of glass fibre filled PTFE grades is shown in figure 3.5. The assembly consists of a vertical backing plate that forms the central part of the rig. All the test components holding the specimens and facilitating load application are on the same side of the side of the plate. The other side of the vertical backing plate is bolted to gusset stands that hold it in position. All the mechanical drive components are located on this side of the plate and include a 1.5 kW electric motor that drives the crankshaft via a timing belt/pulley. The crankshaft is further connected to two connecting rods on either side, that drive the reciprocating shafts thereby forcing the shuttles and all parts associated with them to reciprocate. Two diaphragm type tension/compression load cells rated to 1000 N form part of the reciprocating shafts and therefore enable the friction measurements to be carried out. The lever arms are hinged onto brackets bolted onto the crankshaft side of the vertical backing disk. The applied load is carried to the wear pin via force transmission pins. These are located at a distance of 170 mm from the hinges while the dead weight are located 595 mm away from the hinges. The force exerted to the wear pin is thus approximately 3.5 times higher than the applied load. To find the actual load exerted on the wear pin, the lever arm mass, the counterweight suspension system, the force transmission pin as well as the wear specimen holder masses should be taken into consideration. Hence, the actual wear pin load is given by

$$F = 34.16M_{deadweight} + 64.26 \qquad [\mathbf{3.1}]$$

where F is in Newtons and M in kilograms. The system is also fitted with push button load cells types (Biomer Systems cc.) to ensure that load exerted on the force transmission pins is passed to the wear pins. Figure 3.6 shows the main elements of the reciprocating drive mechanism.

Figure 3.5: **The reciprocating wear testing apparatus with (1) dead weights/lever arm (2) wear pin holder and reciprocating shuttle (3) electric motor (4) pump control, speed control and cycle counter (5) strain gauge amplifier and (6) digital oscilloscope.**

Lubricated tests may be performed on this system by making use of the lubricant reservoir that is situated beneath the base plate. The lubricant of choice is pumped from the reservoir to the level of the reciprocating bath by a variable flow pump and the T-piece separates the flow into two flexible hoses that are connected to the perspex sides of the bath.

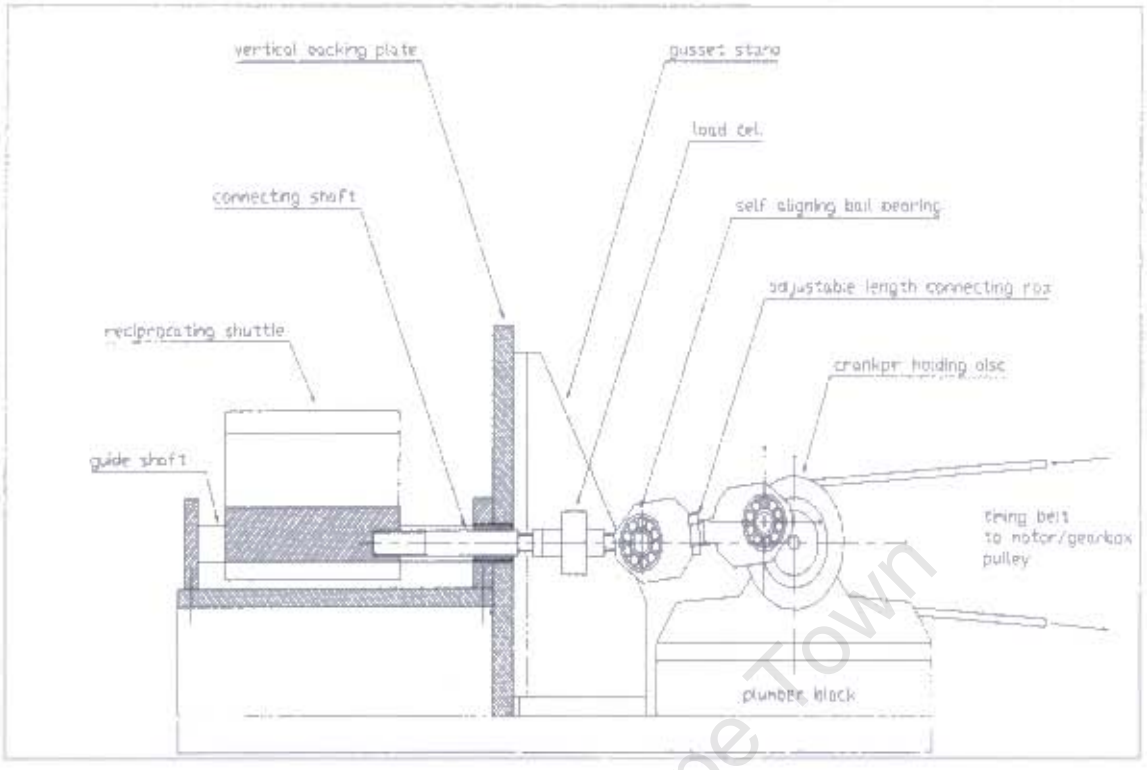

Figure 3.6: A drawing showing the main elements of the reciprocating drives mechanism [After ref 21].

The friction measurements are conducted by means of the diaphragm type load cells connected to the reciprocating shafts. Lock nuts secure the load cells in position and the signal from the load cell is amplified by means of the strain gauge amplifier and sent to 20 Ms/sec (DSO) 1604 oscilloscope. The oscilloscope may plot both kinetic and static coefficients of friction so the load cells had to be calibrated before they were installed. Figure 3.7 shows a typical friction plot from the oscilloscope. In figure 3.8 more pictures of the wear pin clamping mechanisms together with the lubricant entries to the shuttle bath. The reciprocating sliding wear rig is fairly new and was designed and built to overcome the disadvantages associated with the previous rigs that were used in the Centre for Materials Engineering before. Thus, it offers excellent and efficient way of measuring wear and friction of engineering materials.

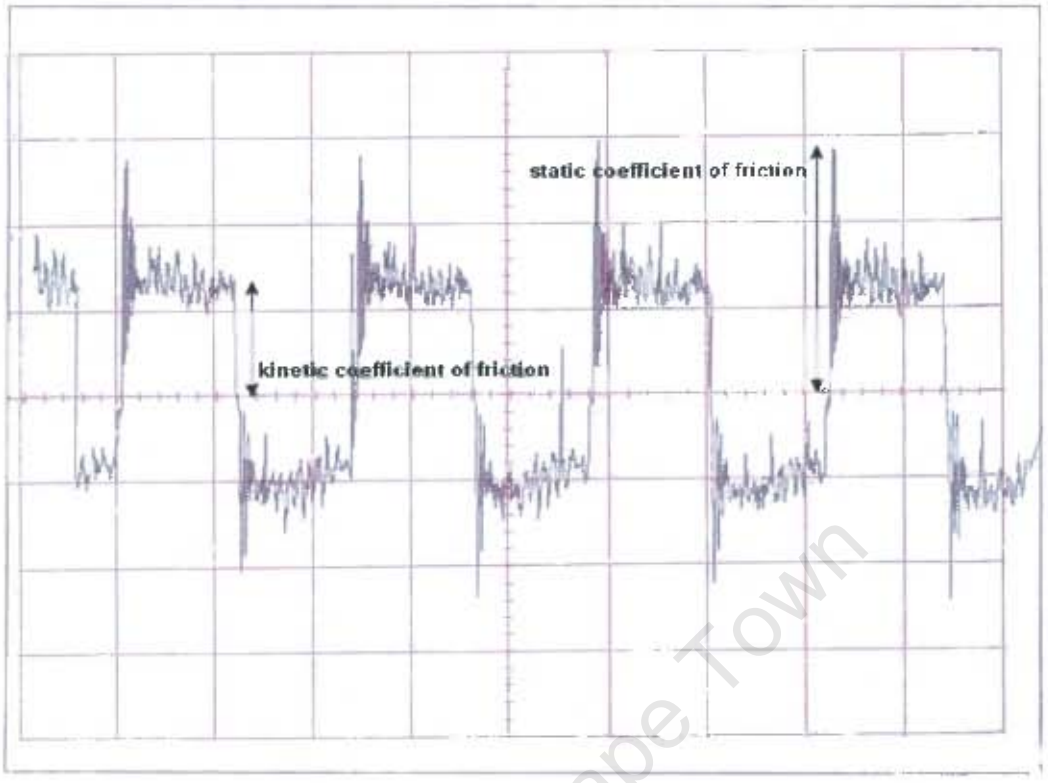

Figure 3.7: A typical load cell output versus time.

The advantages with this rig include:

- duplication of the relevant mechanisms to allow two tests to be performed simultaneously
- lubricant recirculation to ensure constant temperature
- easy to use and reliable lever arm/dead weight load up to 1000 N

The system is driven by a Renold Crofts 1.5 kW 380/240 V 3 phase, 4 Pole Electric Motor c/w. The primary transmission is by the Renold Crofts Ritepower 2D Gearbox ratio 7.52: 1. The speed is controlled by means of the Renold Croft Renvert Junior RVJ 150-2, AC Variable Speed Drive, 220 V single phase in, 220 V three phase out and can attain an average sliding velocity of 0.2 m/s.

(a)

(b)

(c)

Figure 3.8: **Pictures showing (a) the front view of the pin-counterface system with pin and counterface in position (b) the close view of the shuttle bath showing the stainless steel counterface and (c) a different view of the pin clamping mechanism in holding position with PTFE pin mounted inside.**

All the materials used for both the pin-on-disk and the reciprocating sliding wear rig had to be cut and machined to proper dimensions and shapes.

3.3 MATERIALS PREPARATION

3.3.1 THE POLYMER WEAR PINS

A total of 17 glass filled polytetrafluoroethylene (PTFE) grades were used in this study, with one unfilled PTFE grade used as a reference material. An extra polyester grade was also used for comparison purposes. The materials were obtained from the supplier, Chemplast Marc Etter (Pty) Ltd. The PTFE composites materials used are and their mechanical properties are given in table 3.1. The wear samples were cut and machined from the bulk materials or billets. Cylindrical and rectangular wear pins were then machined to appropriate dimensions suited for a particular wear rig. Reciprocating sliding wear pins were machined to rectangular pins with the dimensions, 10 mm x 10 mm x 25 mm. A small 45° camfer was then cut along the trailing edge of the pin wear surface so as to minimize rocking of the pin during the sliding process. The initial cross sectional area then becomes 90 mm^2. The pin-on-disk wear pins cylindrical pins on the other hand, were machined to a final diameter of 6.2 mm and a length of 25 mm. These are shown in figure 3.9.

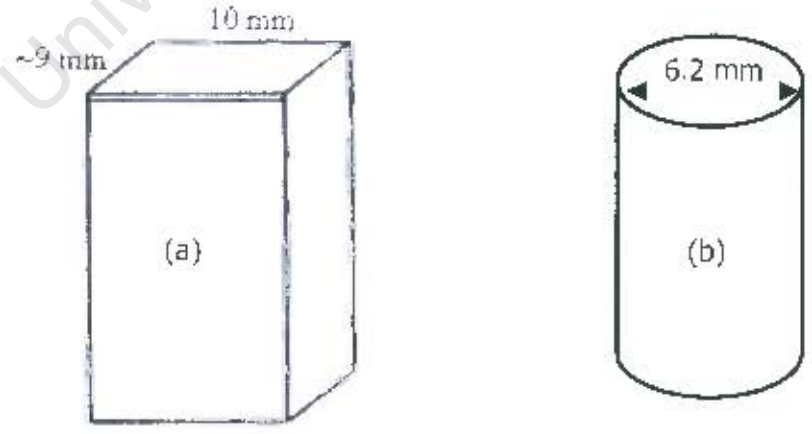

Figure 3.9: The geometry of wear pins for (a) reciprocating test and (b) pin-on-disk.

Table 3.1: The PTFE composites used and their mechanical properties*.

Material	Filler			Processing	Density g/cm³	Mechanical properties		
	Form	%wt	Size			Tensile strength MPa	%elongation	Hardness Shore D
PV1000		unfilled		Compression	2.18	30	350	55
PF1125	SGF	25	20-100 μm	Compression	2.17	19.5	262.8	62
PF1125 IN	LGF	25	0.8-2 mm	Compression	2.10	15.6	234.1	60
PF1125 PS	SGF	25	20-100 μm	Pressure sint.	2.21	5.9	80.5	49
PF1125 BP	SGF+pigm[a]	25, 0.5	20-100 μm	Compression	2.21	16.9	272	63
PFR1125	SGF	25	20-100 μm	Pressure sint.	2.19	11	26.95	63
PFR1125+0.5	SGF+pigm[b]	25, 0.5	20-100 μm	Pressure sint.	2.20	8.9	29.2	66
PF1727	SGF+MoS_2	25, 2	20-100 μm	Compression	2.21	17.9	122.6	75
PF6668 N	LGF+MoS	25, 2	0.8-2 mm	Compression	0.20	19.2	250.2	64
PF1717	SGF+MoS_2	12, 6	20-100 μm	Compression	2.25	21.8	270.9	60
PF2031	SGF+$BaSO_4$+pigm[c]	25, 5, 1	20-100 μm	Compression	2.19	15	222.7	63
PF2226	SGF+pigm[c]	25, 0.5	20-100 μm	Compression	2.19	17.8	232.9	64
PFR2226	SGF+pigm[c]	25, 0.5	20-100 μm	Compression	2.00	9.4	83.6	62
PF2226 B	SGF+pigm[b]	25, 0.5	20-100 μm	Compression	2.18	17.6	211.5	61
T097/02	SHGB	25	2-35 μm(D)	Compression	1.65	4.1	56.9	59
T096/02	HHGB	25	2-35 μm(D)	Compression	1.80	11.8	263.5	61
T101-02	SGB	25	2-35 μm(D)	Compression	2.18	17.4	279.6	62
T103-02	GFL	25	1-6 μm	Compression	2.14	15.4	56.5	68

*the mechanical properties were supplied by Chemplast Marc Etter

SGF: short glass fibres
LGF: long glass fibres
SHGB: soft hollow glass beads
HHGB: hard hollow glass beads
SGB: solid glass beads
GFL: glass flakes

[a]Cobalt zinc aluminate pigment
[b]Carbon pigment
[c]Cobalt chromium aluminate pigment

In addition to the glass filled PTFE materials, polyester-based materials Vesconite and Vesconite hilube were used in this study for comparison purposes. It should be noted that PF2226 and PF2226 B are similar materials, the difference is that PF2226 B crumbled after compression moulding and so it was compressed again.

3.3.2 The Stainless Steel Counterfaces

The counterfaces in both wear rigs were martensitic stainless steel which were machined from grade AISI 431. Rectangular bars with dimensions 70 mm in length, 12 mm width and approximately 10 mm thick were machined for the reciprocating sliding wear rig. These bars were then subjected to a heat treatment schedule resulting in a hardness of 460 HV30 as measured on an ESEWAY hardness tester. Disks with the diameter of about 14 cm were used for pin-on-disk measurements. Figure 3.10 and Figure 3.11 show a schematic of the rectangular metal counterface and a typical laser surface characterisation of the counterface, respectively.

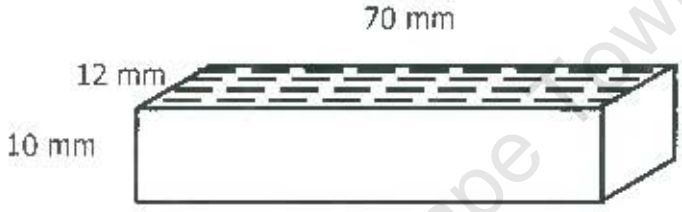

Figure 3.10: Schematic illustration of the stainless steel counterface.

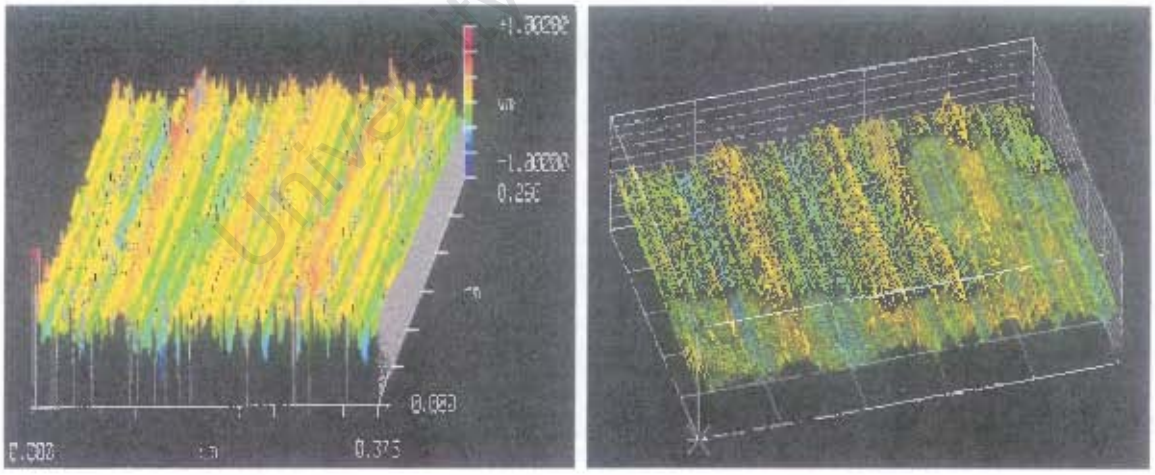

(i) (ii)

Figure 3.11: Typical laser surface maps of the ground stainless steel counterface showing (i) the oblique surface and (ii) three dimensional profile of the counterface [After ref. 23].

The stainless steel counterfaces for both rigs were surface ground to a final surface finish of 0.2 μm R_a. Also, the rectangular counterfaces were surface ground in a direction perpendicular to the sliding motion which resulted in a single scratch distribution normal to the sliding direction, as shown in figure 3.10 and figure 3.11.

3.4 TEST PARAMETERS

3.4.1 PRESSURE

The applied pressure and sliding velocity are very important parameters governing the wear and friction of polymers and so play crucial role in establishing how long a polymer bearing lasts in service. It should be noted that wear rates are independent of contact area and are proportional to load provided the wear mechanism remains the same. The applied loads used in the pin-on-disk were from 30 N to 75 N for all materials. These correspond to the nominal pressures of 1 MPa to 2.5 MPa. Further tests were conducted at higher pressures up to 4 MPa (120 N) for few selected grades. These load limits were selected so as to avoid creep behaviour of the grades as well as establishing the 'pv limits'. The applied loads used in the reciprocating sliding wear rig were from 235 N (2.6 MPa) to 577 N (6.4 MPa).

3.4.2 SLIDING SPEED

The sliding speed was varied for the pin-on-disk tests from 1 m/s to 2 m/s so that direct comparisons of wear performance results obtained in this study and results obtained by other researchers could be made. Bush simulation was done with the aid of the reciprocating sliding wear rig with an average sinusoidal velocity of 0.2 m/s. This velocity was held constant throughout tests, in other words only the applied load was varied with this rig. This velocity was chosen mainly because it allowed fairly rapid progression of the tests without significant frictional heating and also corresponded to the speed used by previous authors.

3.4.3 Counterface Roughness

The surface finish of the stainless steel counterfaces was maintained at 0.2 μm R_a before each test commences. Each test was performed on a single wear track so that the specimen comes into contact with the fresh surface, therefore, it was important to try and hold the roughness constant in these tests. A Taylor-Hobson Surtronic 3P surface profilometer was used to measure the surface roughness after they were ground and during tests intervals. Using this device, several surface roughness measurements were done perpendicular to the grinding direction and the average value recorded as well as the metal conterface profiles.

3.4.4 Temperature

All tests were conducted at room temperature so as to avoid the heat built up at higher temperatures and consequently deformation of the PTFE grades. Temperature at the interface was however not constant, but slightly changed with sliding distance (time) as a result of flash temperatures and frictional heat due to rubbing. The surface temperature was constantly monitored and measured by means of a Testo 826-T4 infrared thermal instrument. This was achieved by focussing the infrared probe normal to the disk counterface just after the test was finished. This device has an accuracy of ±2 °C.

3.4.5 Sliding Distance

Dry sliding wear tests were performed for all grades at different speeds and applied pressure. The total sliding distance covered each time varied depending on the rig used. The total sliding distance of 5 km was used for the reciprocating sliding wear rig and the total sliding distance of 30 km for the pin-on-disk. These distances were deemed sufficient to cover the 'bedding-in' (or running-in) effects that occur during the initial stages of sliding and the attainment of the stable wear. During the running-in period the counterface is being progressively modified by transfer film and abrasion by

any hard constituents in the bearing material. Thus, when dry a bearings is mated with an appropriate counterfaces, the counterface is effectively smoothed during running-in until it reaches some improved equilibrium surface condition which it then retains for the rest of the useful life of the bearing. The rate of wear during the running-in period for a particular counterface with appropriate surface finish is relatively higher than that of steady state. The main need in design is therefore to be able to predict the performance in the second equilibrium wear stage. Therefore, the wear rate quoted in the following pages is in fact the rate of wear after steady state has been attained. The tests were stopped at regular intervals so that friction, weight loss and surface temperature could be measured.

3.5 Experimental Measurements

3.5.1 Measurements of Specific Wear Rates

The tests samples were ultrasonically cleaned in methanol before and after each test. The weight loss measurements were subsequently done by means of a Satorius 2474 microbalance having an accuracy of 0.01 mg. The mass loss was converted to volume loss V which was plotted against sliding distance S. This method was preferred to measuring dimensional change as creep as well as unevenness in specimen surface could influence the latter after sliding. Specific wear rate K_o was obtained by dividing the steady state slope of the volume loss vs sliding distance graph by the normal load F

$$K = \frac{V}{F.S} (\text{mm}^3/\text{Nm}) \qquad [3.2]$$

The specific wear rates or wear factors could then be used to compare the wear performances of different polymer grades. The steady state wear is represented by A-B in figure 3.12 and O-A illustrates the 'running-in' region where the initial surface roughness plays a crucial role.

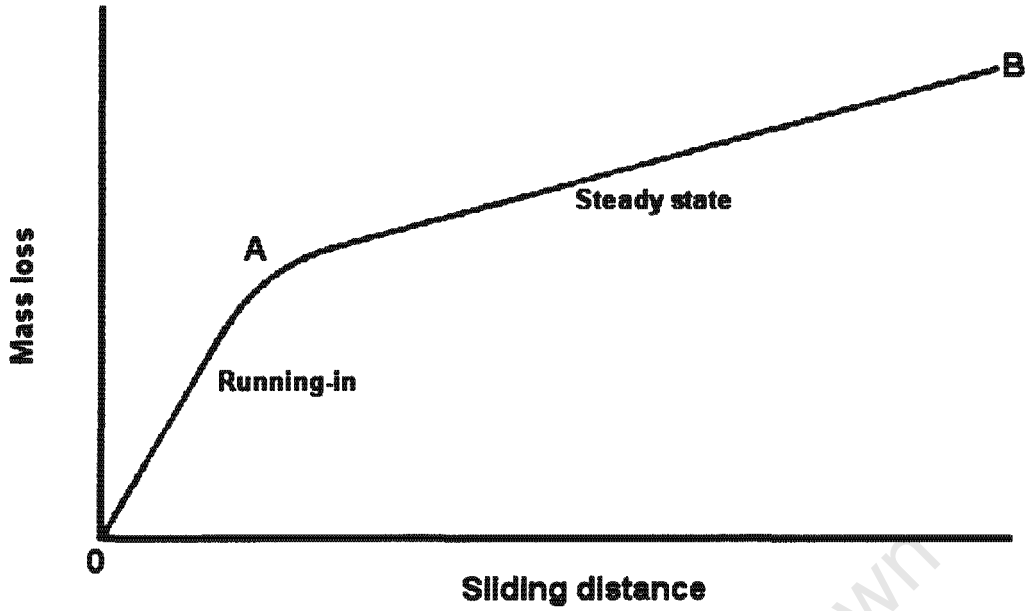

Figure 3.12: The typical graph that depicts the dry sliding wear behaviour of polymer bearings.

The attainment of the steady state is vital for self-lubricating materials such as PTFE in that the counterface is usually completely covered with the transfer film and consequently drop in wear rate.

3.5.2 Measurements of Surface Roughness

As described in section 3.4, the surface roughness measurements were done perpendicular to the grinding marks of the stainless steel counterface. The final surface finish of 0.2 μm R_a was obtained. The surface profile of the counterface before and after each test was also measured by means of the profilometer. Figure 3.13 shows a surface profile of the reciprocating sliding wear counterface before the sliding process. It can be seen from the figure that the roughness of the counterface is fairly uniform with few deep grooves resulting from machining process clearly illustrated by the circle on the figure.

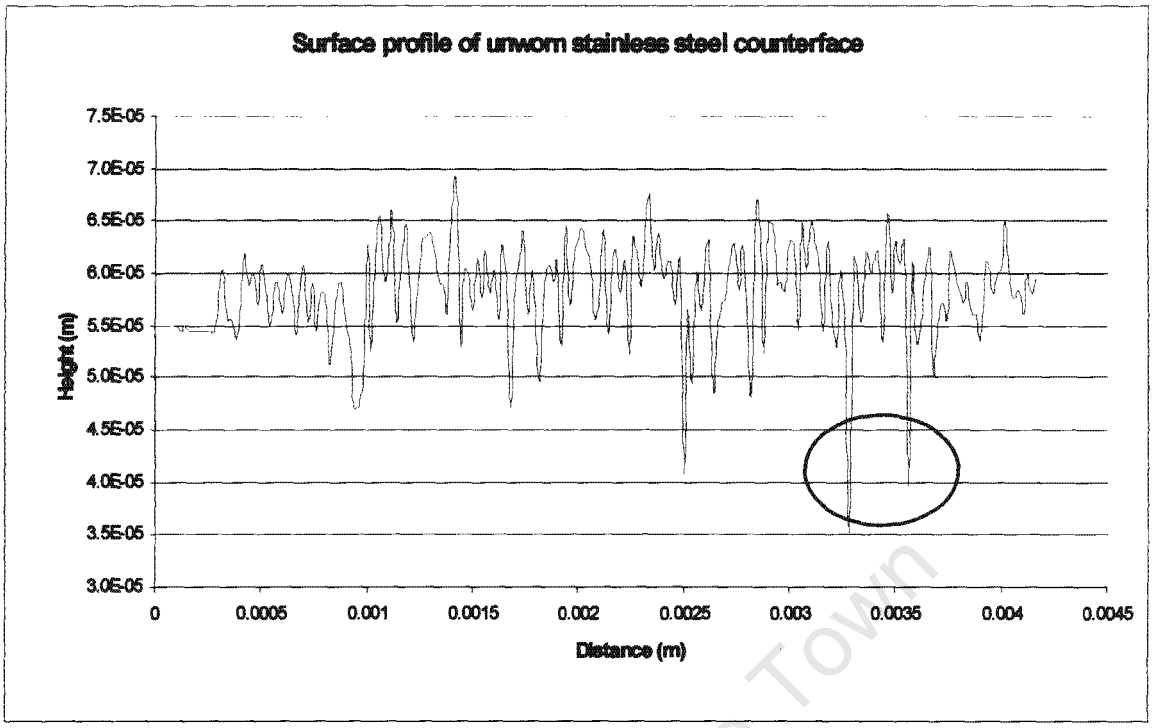

Figure 3.13: The typical surface profile of the metal counterface before being worn against PTFE composites. The circle indicates the presence of deep grooves on the counterface.

The measurement of surface roughness in this way gives a better understanding of the transfer film build up as well as the possible scratches caused by the abrasive glass fillers.

3.5.3 Measurements of Friction

An account on how friction was measured in both sliding rigs is given in sections 3.2.1 and section 3.2.2.1.

3.6 POLYMER CHARACTERISATION

3.6.1 OPTICAL MICROSCOPY

Worn polymer surfaces were initially studied by means of a Nikon light microscope and a Nikon camera that was attached to the microscope took photographs of these. A Reichart projection microscope was further used to study the PTFE and stainless steel counterface during test intervals. The polymer composite pins were ultrasonically cleaned with methanol for five to ten minutes before they were studied with the microscopes. This was done to make sure that there were no impurities or dirt on the composite surface that could contaminate and influence microstructural analysis. The optical microscope was extensively used in characterisation of the worn surfaces since specimens need no coating and so test could be interrupted and surfaces observed.

3.6.2 SCANNING ELECTRON MICROSCOPY (SEM)

Scanning electron microscope, Leo S440 Stereoscan was used to characterise the worn polymer samples. After each test, polymer samples were ultrasonically cleaned in methanol and mounted on an aluminium stubs using carbon dag. They were then gold-palladium coated in a Polaron E5100 Series II sputter coater. To make the specimen conductive, a conductive paint was applied to the sides of the specimen. A low acceleration voltage of about 10 kV was used to minimise radiation damage.

3.6.3 ENERGY DISPERSIVE SPECTROSCOPY (EDS)

The energy dispersive spectroscopy that was connected to the Leo S440 scanning electron microscope was used for the elemental analysis of the composite materials. The EDS results are fairly accurate despite the fact that the instrument cannot detect light elements such as oxygen and carbon.

3.6.4 X-Ray Diffraction (XRD)

The x-ray diffraction (XRD) facility at iThemba Laboratory for Accelerator-Based Science was employed to establish the crystallinity of the materials. A Bruker AXS was used to obtain the WAXS patterns using a Ni-filtered CuKα radiation source (λ_{cu}=1.5418 Å). A step size of 0.1° at 2 second interval was used for a scanning range from 5 and 60° with the sample holder rotating at 30 rpm. The degree of crystallinity was calculated as described by equation 2.2. The areas under the crystalline and amorphous peaks were calculated by the software package supplied with the x-ray machine.

3.7 Counterface Characterisation

3.7.1 Optical Microscopy

Complete analysis of the transfer film that is formed during the rubbing or sliding process on the metal counterface was done by means of the optical microscope. The tests were interrupted at regular intervals in order to measure the roughness on the counterface using surface profilometer as well as taking pictures of the metal surface. The profilometer connected to the computer gave surface profiles of the metal counterfaces before and after sliding, with all surface measurements were done at the centre of the metal surface.

3.7.2 Scanning Electron Microscopy

The stainless steel counterfaces were examined under scanning electron microscope after completion of the tests. Coating was necessary so for these materials due to the transfer film on the metal counterface.

3.7.3 X-Ray Photoelectron Spectroscopy (XPS)

For a better understanding of the tribological behaviour of the polymer composite, x-ray photoelectron spectroscopy analyses of the transfer film were carried out after the experiment. The objective was to examine possible chemical reaction between the PTFE composite and the stainless steel during sliding. X-ray photoelectron spectroscopy (XPS) or electron spectroscopy for chemical analysis (ESCA) uses the kinetic energy of the photoexcited electrons to derive the binding energy of the initial electronic state which is directly related to the ionisation energy of the appropriate atomic orbital. After sliding 20 km against BP6688 N (25 % glass fibre+2 % MoS_2+73 % PTFE) on a reciprocating sliding wear tester at room temperature under a load of 405 N (4.5 MPa), at an average sliding speed of 0.2 m/s, the counterface with transfer film was analysed using ESCA. The instrument used was a Perkin-Elmer 5400 with the Mg dual anodes operated under a voltage of 15 kV and 300 Watt. The tests were performed at the University of Pretoria.

3.8 Wear Debris Analysis

3.8.1 Differential Scanning Calorimetry (DSC)

Polymer wear debris was characterised by means of the Perkin-Elmer DSC 2 as well as the XRD in an effort to detect any likely internal changes in the material due to the sliding process. The degree of crystallinity is calculated from the heats of fusion (ΔH_f) based on measuring the area under the DSC melting peak above a preset baseline.

CHAPTER 4

EXPERIMENTAL RESULTS

FRICTION AND WEAR RESULTS

4.1 INTRODUCTION

This chapter presents the wear results, characterization and analysis of the wear behaviour of glass filled polytetrafluoroethylene (PTFE). The wear behaviours of filled PTFE (excluding glass) are included for comparison purposes. The reciprocating wear rig was used to evaluate the variation of wear rate with load at low sliding speeds. This in-house built apparatus is limited in terms of the sliding speed that can be attained. For this reason, a speed of 0.2 m/s was chosen and all the tests were subsequently performed at this speed. The pin-on-disk wear tests on the other hand were performed at 1.5 m/s and at 2 m/s. Since the loading, velocity, and wear type are different in the two wear rigs, they may not be compared directly. This chapter lists and presents all the friction and wear tests undertaken. Since the main focus of this study was on how the shape, size and glass content of the glass affect friction and wear of PTFE, it was deemed necessary to first characterise the glass. Various fillers such as carbon and graphite were also used in this study for comparison purposes.

4.2 FILLER CHARACTERISATION

4.2.1 GLASS FILLERS

Different forms of glass were used in this study with their content fixed at 25 % wt. These forms of glass are: glass fibres, glass flakes and glass beads. The glass beads were divided into two groups: hollow glass beads and solid glass beads. Within the hollow glass beads a distinction was further made between soft hollow glass beads and hard hollow glass beads, with the latter withstanding higher pressures in compression and crushing. The soft hollow beads crush at a pressure of about 70 MPa. The beads have different sizes with diameters ranging between 2 μm and 35 μm. The hard hollow glass beads and soft hollow glass beads were used in PTFE with the codes T096/02 and T097/02, respectively. The solid glass beads have a broader bead diameter distribution with the majority of the beads having diameters of less than 5 μm. The majority of the hollow glass beads, on the other hand have diameters of about 10 μm. Figure 4.1 shows the size variation in size of the solid and soft hollow glass beads. The red square on figure 4.1 (b) shows a broken bead, further illustrating the ease with which the soft hollow glass beads can be broken.

Small amounts (less than 6 % wt) of additives such as molybdenum disulphide and barium sulphate as well as tiny amounts of pigments were added to some of the PTFE materials as illustrated in table 3.1. The short glass fibres that were used in this study have similar sizes and are of type E. Their lengths vary between 20 μm and 100 μm with a few fibres having lengths that lie beyond this range. The fibre length distribution of these fibres was also broad with the majority of fibres having lengths of about 60 μm. These fibres were used for the materials such as PF1125 (see table 3.1). To investigate how the aspect ratio affect friction and wear of glass fibre filled PTFE, it was deemed necessary to include another type of glass fibre with relatively long fibres. Two PTFE composites, viz. PF1125 IN and BP6688 N are PTFE composites filled with 'long fibres' are used in this study for this purpose. The length of the 'long' fibres ranged between 0.8 and 2 mm. It must be noted that all the glass fibres used in this study can, in

general, be described as short fibres of the type E-glass. Henceforth, the terms 'short' and 'long' fibres will be used to make a distinction between these glass fibres. Micrographs depicting the differences in size between the glass fibres are shown in figure 4.1 (c) and (d). Since the glass fibre filled PTFE materials are processed by compression moulding, the fibres are randomly oriented within the billets from which pins are machined. There is thus no preferred orientation of the fibres along the length of the wear pin. One other form of glass that was used in this study is the irregular glass flake. Figure 4.1 (e) shows a SEM micrograph of the glass flakes used. The glass flakes are irregular, have a fairly broad particle size distribution with their sizes ranging between 1 and 8 μm.

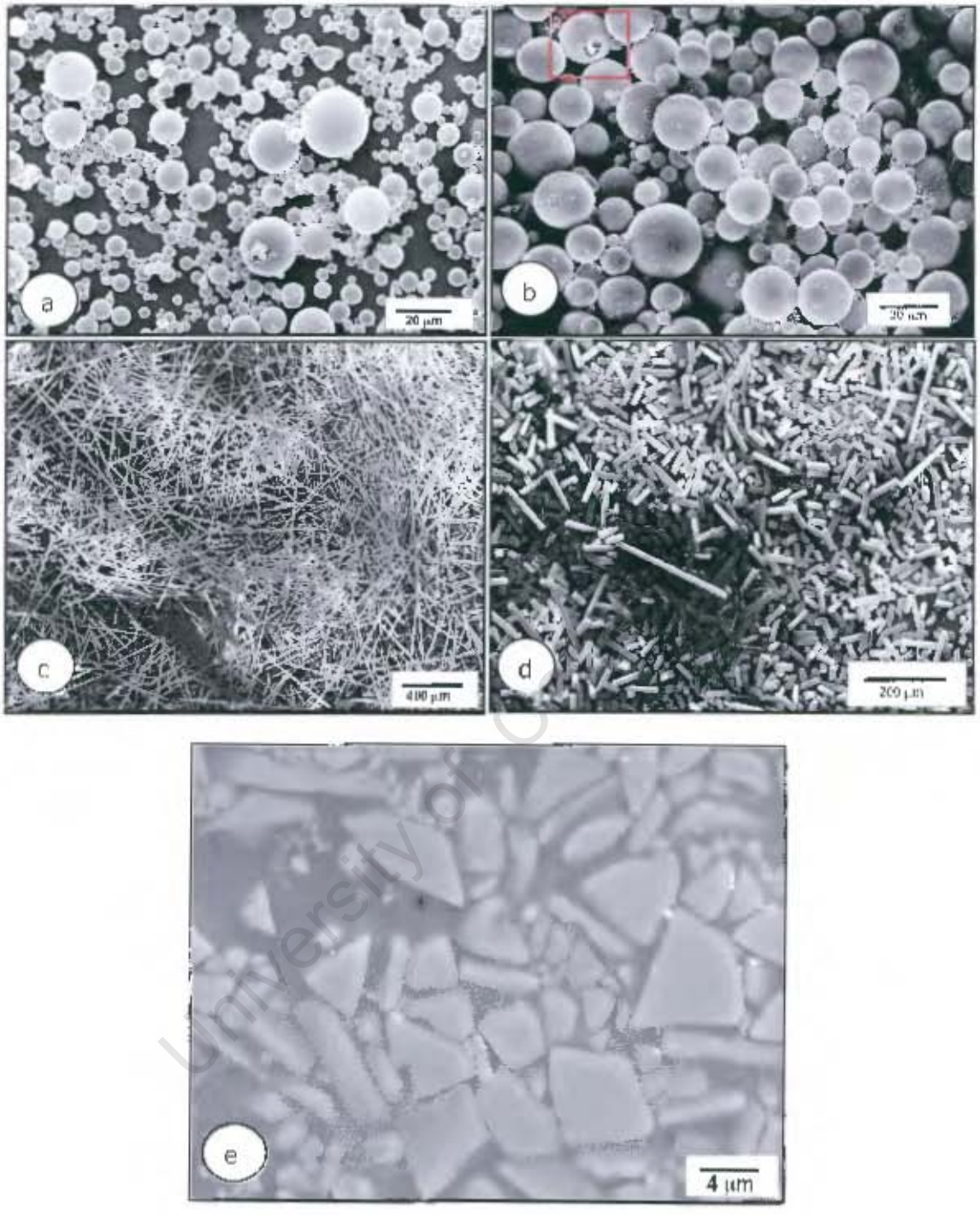

Figure 4.1: **SEM images showing (a) solid glass beads, (b) soft hollow glass beads, (c) long glass fibres ranging between 0.8 and 2 mm in size (d) short glass fibres ranging between 20 and 100 µm in size (e) glass flake of between 1 and 8 µm in size.**

4.2.2 Carbon, Graphite and Bronze

In addition to the glass fillers, other types of fillers were also considered for PTFE in sliding operations. To this end, carbon coke, graphite and bronze powders were used as fillers for PTFE in the quantities 25 % (PF 1325 I), 15 % (PF1415) and 60 % (PF1260), respectively.

4.3 Reciprocating Sliding Wear Results

Before sliding wear tests were performed on the reciprocating sliding wear rig, the reproducibility tests were conducted. Wear results from four wear tests that were performed on a stainless steel counterface, are presented in figure 4.2 (a) below.

4.3.1 Reproducibility Tests

Test Parameters

material couple used:	PF1125/AISI 431 stainless steel
reciprocating speed:	0.2 m/s (average)
counterface roughness:	R_a = 0.2 μm (ground ⊥ to the sliding direction)
load:	360 N (4 MPa)
sliding distance covered:	10 km
lubricant :	none
specimen dimensions:	9 mmx10 mmx24 mm

The test results for all four tests seemed to follow the same trend in that the wear rate initially increase rapidly during the 'bedding in' period and becomes steady after 1.5 km of sliding is covered. The steady state wear rates were therefore calculated from the slopes of the volume loss versus sliding distance curves from 2 km to 10 km and these are shown in table 4.1. It would appear from this table that the wear results are not

significantly different (8% difference) and the reproducibility of the wear rates were therefore deemed acceptable. Figure 4.2 (b) is the bar chart representation of the wear data obtained. The wear data used to generate the results in the table mentioned above can be found in appendix A. Since the steady state wear seemed to be achieved after 1.5 km of sliding, it was deemed necessary to reduce the sliding distance to 5 km for the actual tests.

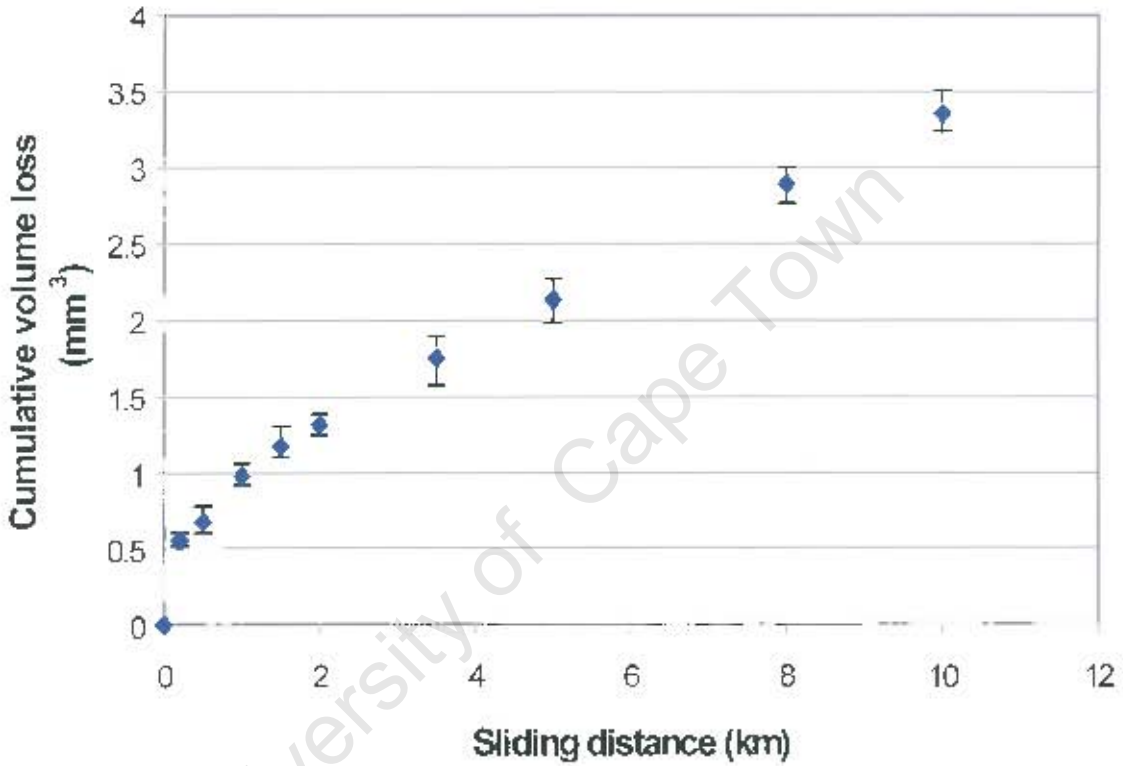

Figure 4.2 (a): **The average volume loss vs. sliding distance for the four tests with the 25 % wt glass filled PTFE, PF1125, showing the reproducibility of the results on the reciprocating wear rig.**

Table 4.1: The steady state reproducibility wear results for PF1125.

Test #	Surface roughness μm R_a	Steady state wear $mm^3/N.m$ $x10^{-6}$	Coefficient of friction (Steady state)
1	0.19	0.67	0.18
2	0.21	0.72	0.20
3	0.20	0.67	0.19
4	0.19	0.73	0.18
average		0.70±0.03	0.19±0.01

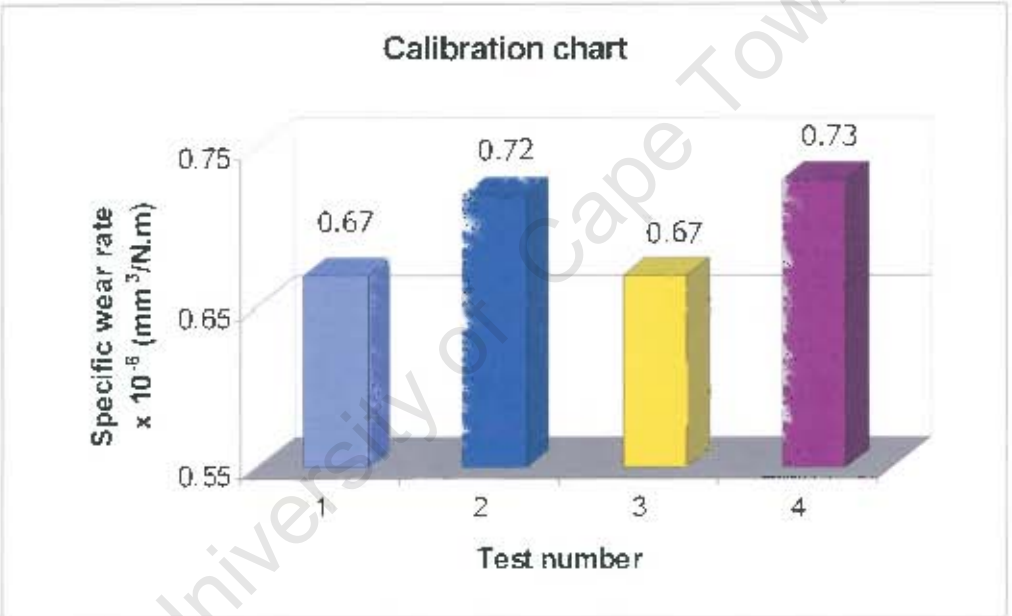

Figure 4.2 (b): Bar chart representations of the specific wear rates of PF1125.

4.3.2 Dry Friction and Wear Results

The sliding wear of PTFE composites were summarised in tables and graphs. Since most of the PTFE composite materials have glass fibre as filler, the glass fibre filled grades were divided into two groups and each group was plotted separately for convenience. The materials in either group are not fundamentally different; they are

grouped together so that they can be plotted easier. In doing so, materials that are much similar in terms of composition and/or processing e.g. PF2226 and PFR2226 which are similar in composition but differ in processing, were placed in the same group. The friction and wear results of the composites are then compared with a base grade viz. PF1125. PF1125 was chosen as the reference because it contains only the short glass fibres and no other additives and pigments.

4.3.2.1 GENERAL OBSERVATIONS CONCERNING THE TRIBOLOGY OF PTFE

The wear rates of the PTFE composites were characterised by a high initial wear rate during the first two kilometres of sliding followed by a much reduced linear and stable wear rate. Figure 4.3 shows a typical variation in volumetric wear of PTFE composites with sliding distance under a contact nominal pressure of 2.6 MPa. Each point in figure 4.3 represents an average of two values. From figure 4.3 (a) it is seen that the steady state wear rates for all the grades are fairly similar and of the order 0.3 – 0.6 x 10^{-6} mm^3/Nm (see table 4.1). It would also appear that the grades with MoS_2 have lower initial wear rates. From figure 4.3 (b) and table 3.1 it can be seen that PF1717, which has MoS_2 included, exhibited the lowest wear rate even though its running-in wear rate is higher than other materials. The reprocessed grade (PFR2226) and the grade that was twice compression moulded (PF2226 B) showed higher wear than PF2226, at a bearing pressure of 2.6 MPa. The differences in wear, however, diminished with an increase in pressure (see table 4.2). It is also evident that the addition of barium sulphate filler to glass filled PTFE (PF2031) did not improve the wear rate when it is compared to the base grade (PF1125). This was also found to be true at higher bearing pressures.

Glass bead filled PTFE and glass flake PTFE composites are shown in figures 4.3 (c). It would appear from the figure that the glass bead and flake filled PTFE grades also reach stable wear after 2 kilometres of sliding. The soft hollow glass bead filled PTFE grade (T097/02) showed much higher wear than the other glass bead and glass flake filled grades. At a pressure of 2.6 MPa, the soft hollow glass bead filled grade wear rate is about 6 times higher than the other glass bead and glass flake filled grades. At this

pressure, the solid bead and glass flake filled PTFE showed similar wear rates to the base grade, PF1125 (table 4.2).

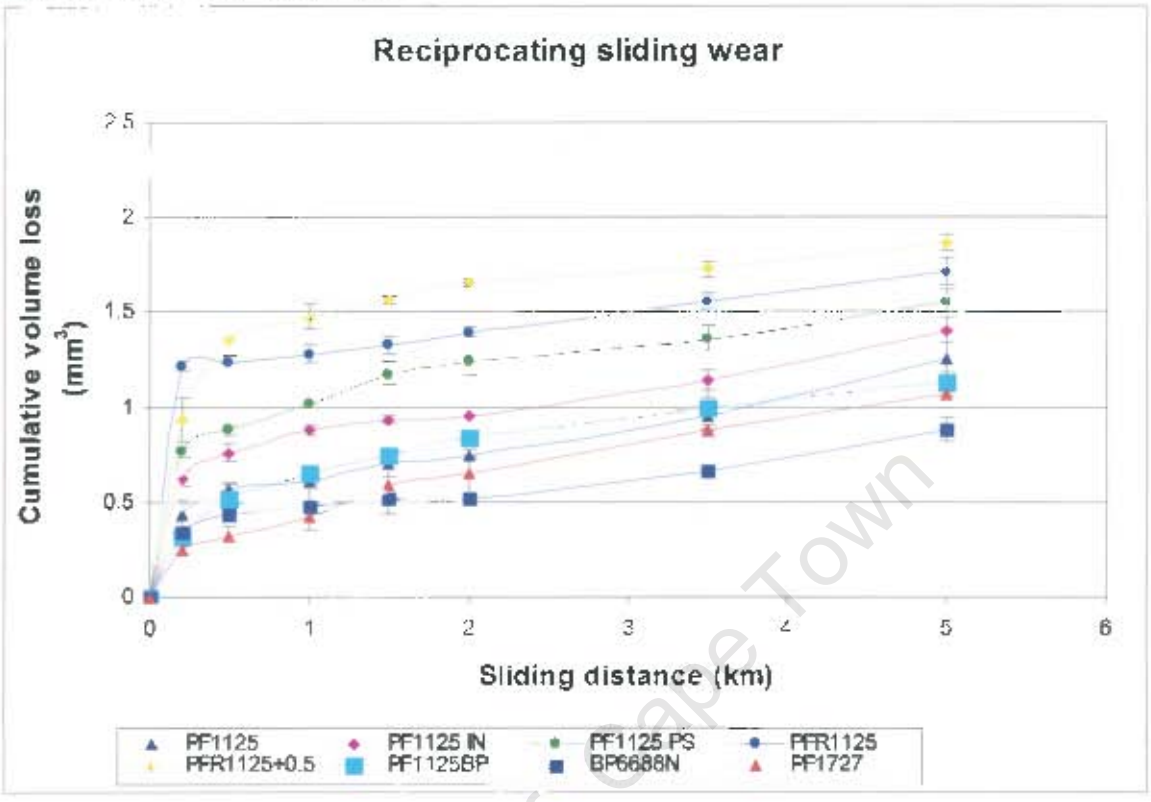

(a)

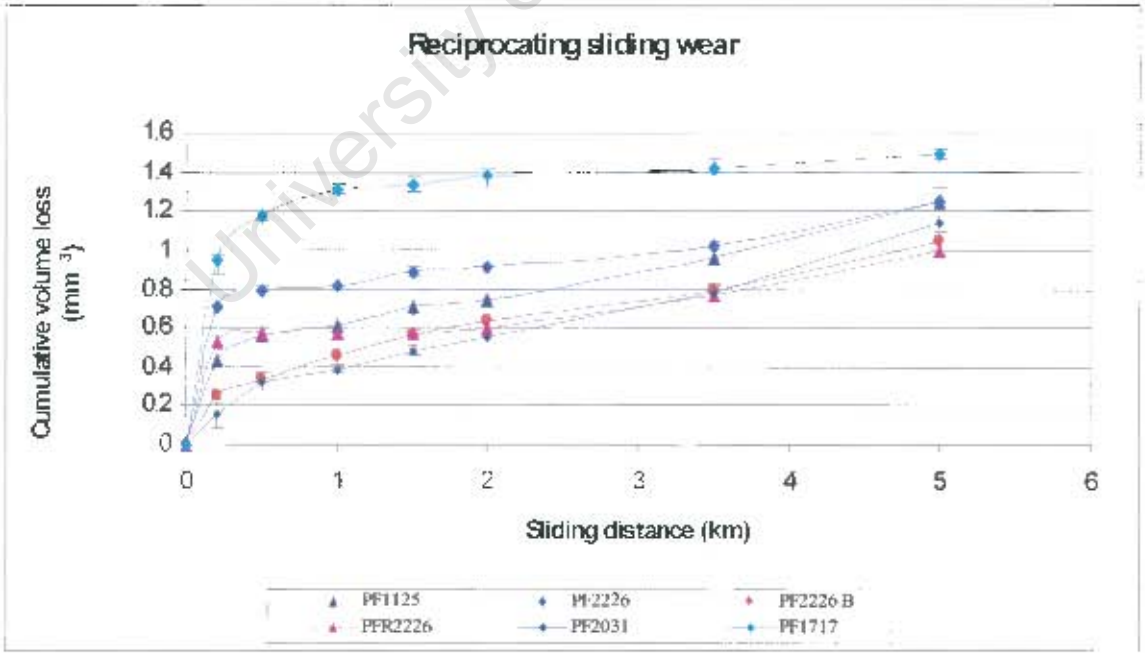

(b)

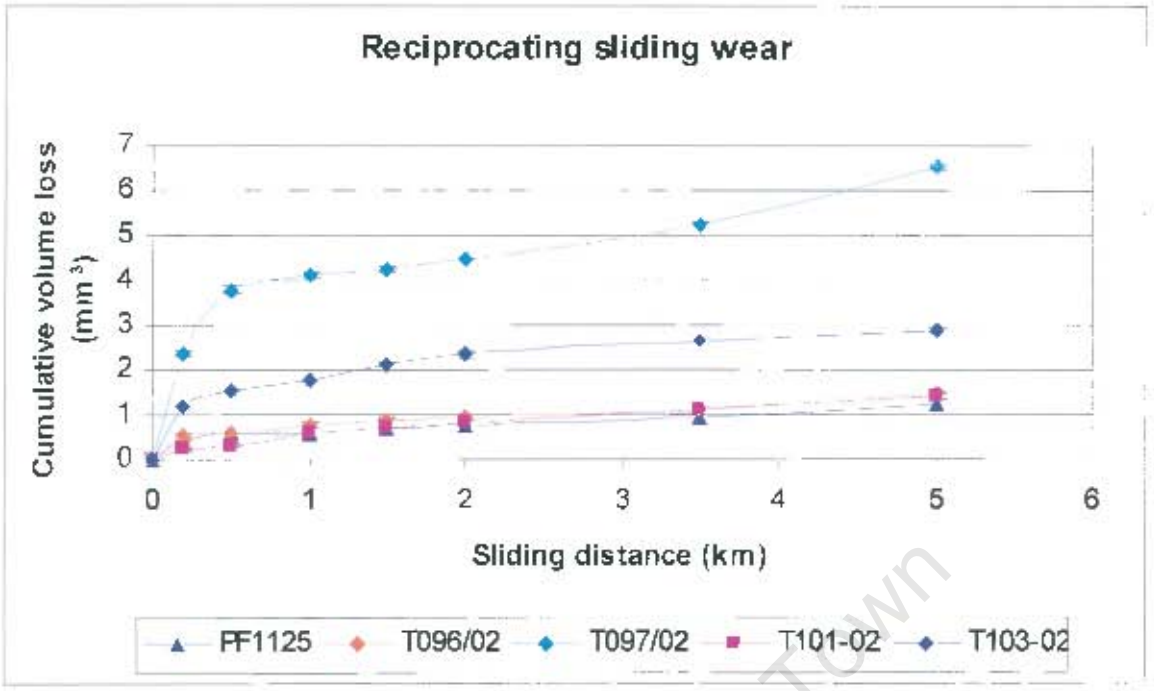

(c)

Figure 4.3: The reciprocating sliding wear curves obtained on rubbing the stainless steel counterfaces for 5 km at 0.2 m/s against (a) glass fibre filled PTFE (b) glass fibre filled PTFE and (c) glass bead/flake filled PTFE.

The high wear rate during the early stages of the sliding process is attributed to the transfer film formation on the stainless steel counterface. As sliding continues, the abrasive asperities of the counterfaces, where contact occurs, become less abrasive as more and more polymer composite fragments fill the asperity valleys, forming a transfer film. Therefore, steady state comes about as a consequence of the transfer film completely covering the counterfaces and thus reducing wear as further contact occurs between the composite surface and this film. The stability of volumetric wear during the steady state was accompanied by a similar steadiness in the dynamic coefficient of friction as well as the roughness of the stainless steel counterfaces. Figure 4.4 shows a typical graph depicting how the coefficient of friction and roughness vary with sliding distance. The figure clearly shows the effect of counterface modification on surface roughness and friction coefficient. The surface roughness decreases from 0.2 to about 0.09 um Ra whilst the kinetic friction coefficient increases from 0.12 to about 0.21.

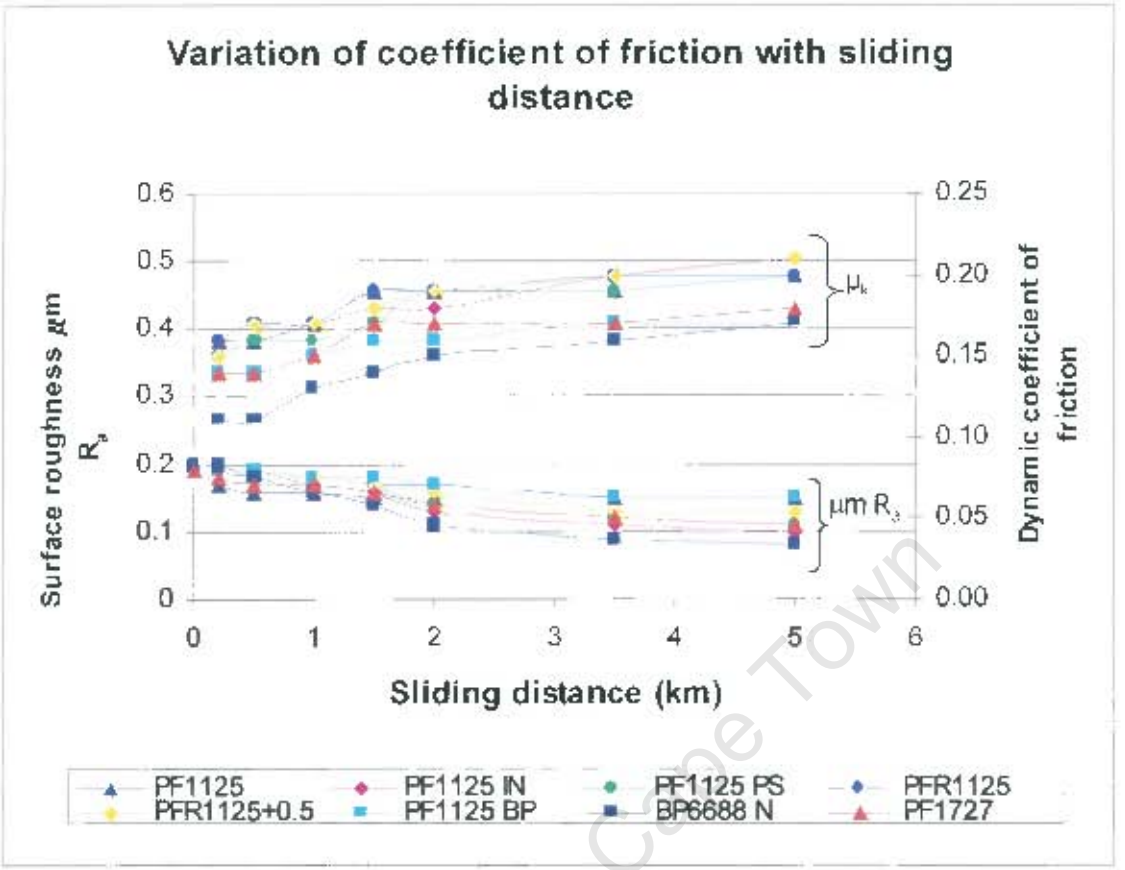

Figure 4.4: **Variation of the coefficient of friction and metal counterface roughness with sliding distance.**

4.3.2.2 THE TRANSFER FILM GROWTH AND WEAR MECHANISMS

The generation and growth of transfer film on the stainless steel counterface during sliding was monitored and studied by means of optical and scanning electron microscopy. Figure 4.5 shows the surfaces of the unworn stainless steel counterface before sliding. The grooves or scratches produced during the surface preparation process are clearly visible in these micrographs. The transfer film formed on the counterfaces rubbed against unfilled PTFE, PV1000 appeared to be different to those obtained upon rubbing against glass filled PTFE materials as shown in figure 4.6. Unfilled PTFE formed loosely adherent layered films on the counterface with the resultant flake-like debris that can be easily peeled off from the metal surface.

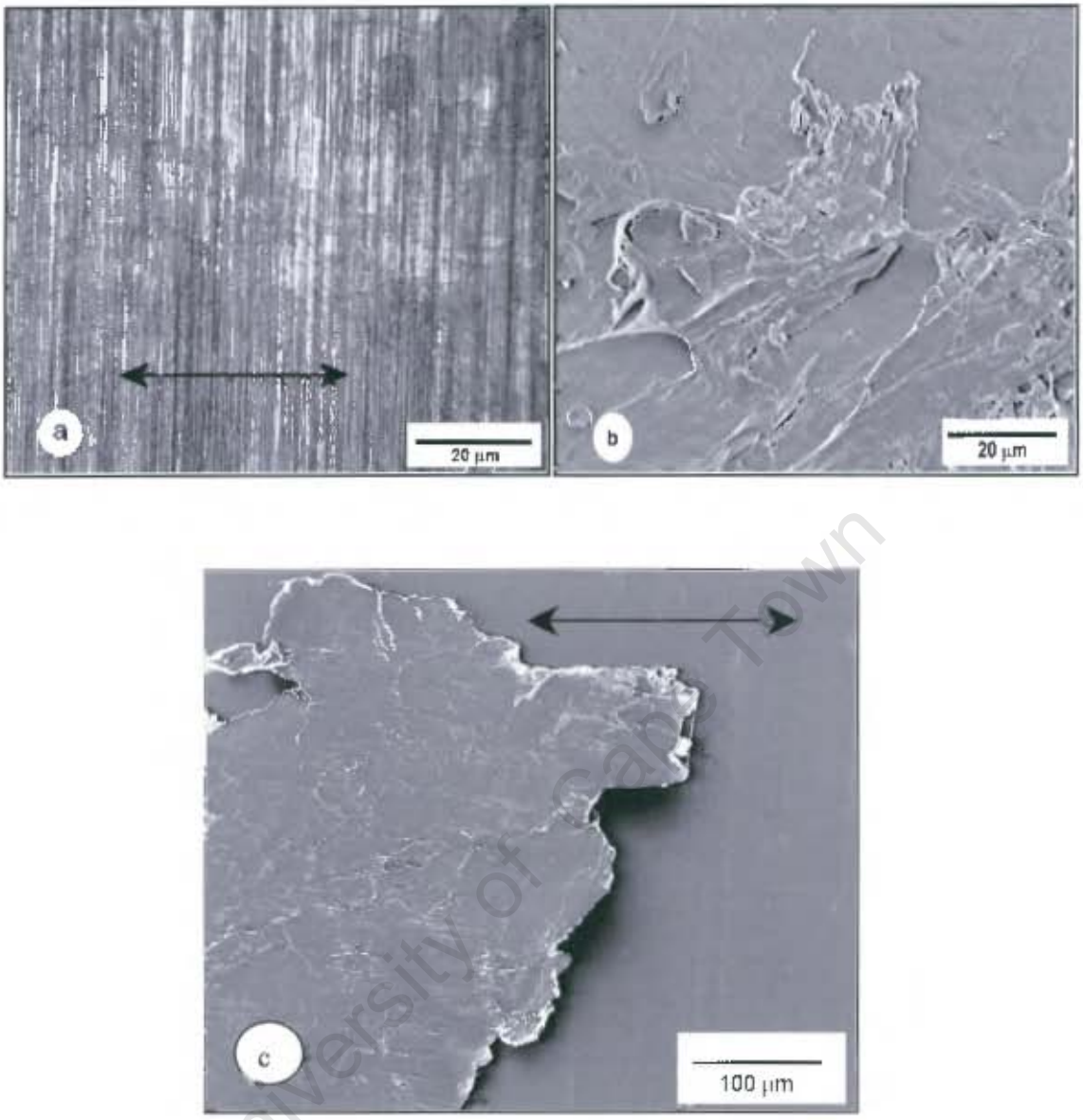

Figure 4.6: **(a) Optical micrograph depicting the non coherent transfer film formed on the stainless steel after rubbing approximately 3.5 km against unfilled PTFE, (b) shows the PTFE sheet being sheared off the pin surface, (c) SEM micrograph of the stainless steel counterface showing a magnified non-adherent PTFE transfer film. The arrows indicate the sliding direction.**

The build up of transfer film on the metal counterface on rubbing against the glass filled PTFE seems to be more gradual and leads to a uniform and adherent film. Unlike in the case with the unfilled PTTFE where small sheets are sheared off, smaller composite fragments are sheared and worked into the troughs or asperity valleys of the counterface. The gradual formation of the transfer film culminates in a coherent and adherent transfer film caused by the glass filler. It will later be shown that the mechanical interlocking of composite fragments into the asperity valleys are enhanced by chemical bond formation between the metal surface and the polymer, ensuring greater adherence of the film. The development and growth of the transfer film for glass fibre filled PTFE, PF1125, is shown in figure 4.7. The two regimes of transfer film development, viz. the '***bedding in***' and '***steady state***' are represented by figures 4.7 (a)-(b) and (c)-(f), respectively. In figures 4.7 (a) and (b) materials that is sheared off the polymer surface gets worked into the valleys between the asperities leading to a rapid decrease in surface roughness. Figure 4.7 (c) shows that once enough material is transferred, the glass fibres are exposed which then abrade the counterface leaving scratch marks in the sliding direction. In figures 4.7 (d) to (f) show that the counterface undergoes relatively few changes during the steady state wear regime.

SEM results show the process of transfer film formation is similar for all glass filled PTFE materials. However, as sliding progresses a coherent and adherent transfer film forms on the metal counterface and coat the glass fibres in the process. Therefore, after 5 kilometres of sliding the abrasive glass marks on the PTFE counterface are less pronounced. The transfer film formed when a solid lubricant, molybdenum disulphide was added to the glass fibre filled PTFE appeared to be more coherent and resulted in less wear than other glass filled grades. Glass beads generally showed thicker transfer films and consequently higher wear rates.

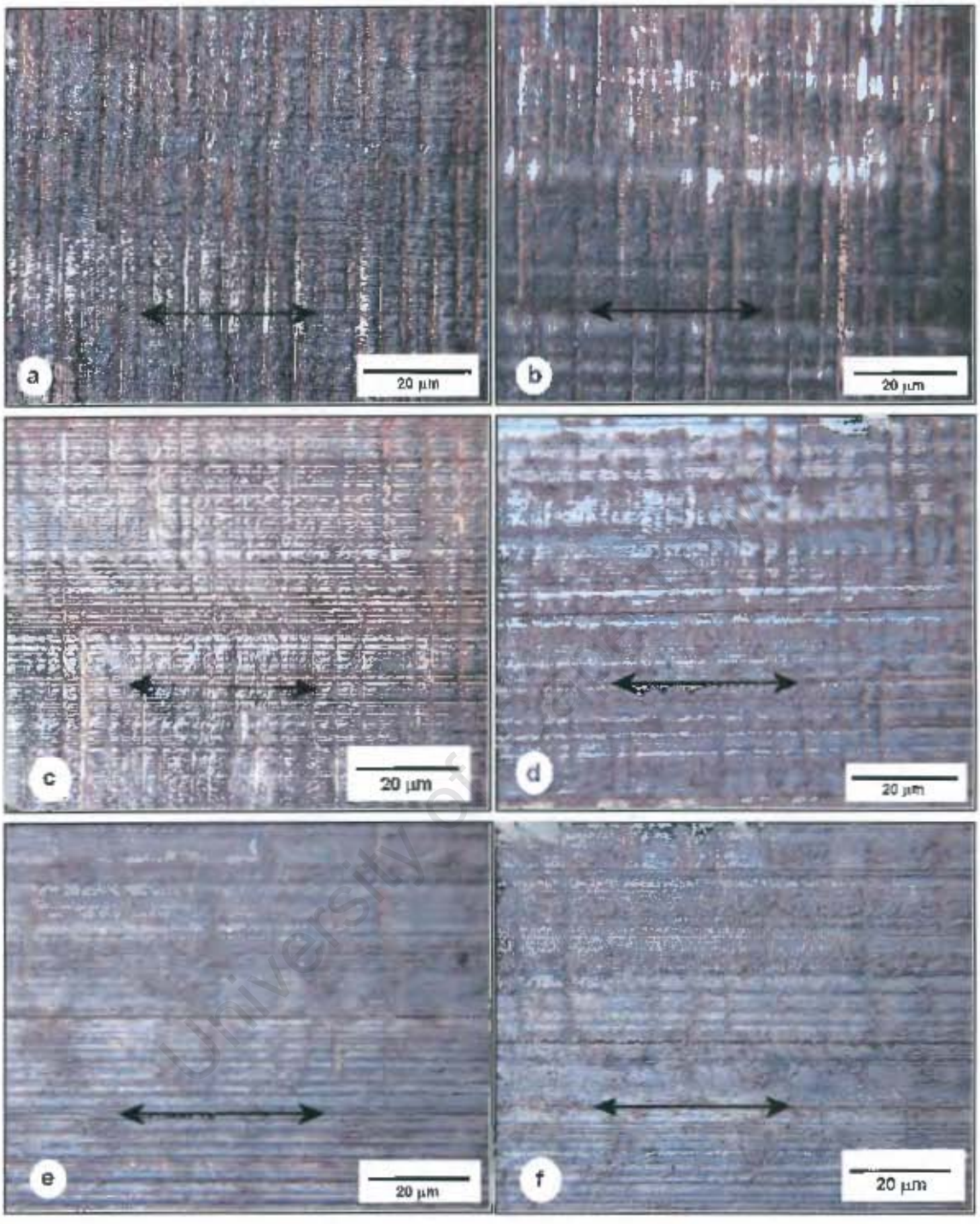

Figure 4.7: **Optical micrographs showing the development and growth of the transfer film on the metal counterface after rubbing (a) 0.2 km, (b) 0.4 km, (c) 1 km, (d) 2 km, (e) 3.5 km and (f) 5 km against PF1125. The arrows indicate the sliding direction.**

4.3.2.3 FRICTION AND WEAR RESULTS AND ANALYSIS

The steady states volumetric wear of the PTFE composites were converted to specific wear rates using their densities and equation 3.2. Table 4.2 lists the steady state friction and wear results of the grades tested at an average sliding speed of 0.2 m/s and a pressure of 2.6 MPa, with the grades showing lowest wear results listed on top of the each group. The unfilled PTFE grade, PV1000 is included in group one for comparison purposes. The wear results of the unfilled PTFE under dry sliding conditions were three orders of magnitude higher than those of the filled PTFE composites. It is also clear from the table that the glass bead filled PTFE grades showed higher wear rates compared with other filled PTFE composites.

The addition of molybdenum disulphide to glass fibres improved the wear resistance of glass fibre filled PTFE, PF1125 IN by 45 % as shown by PF1717 (see table 4.2). Pressure sintering as well the addition of small amounts of carbon improved the wear resistance by the same magnitude as illustrated by PF1125 PS and PF2226, respectively. The steady states friction coefficients of the composites show no discernible trends. The additions of MoS_2, to glass fibre filled PTFE, appears to have an effect of reducing the friction coefficient from 0.23 to 0.18 (see table 4.2). The addition of barium sulphate to the glass fibre filled PTFE seem to have an opposite effect, as the coefficient of friction of PF1125 increased from 0.23 to 0.26 after the addition of this additive.

The surface roughness results showed a steady decrease with sliding distance as can be seen in table 4.2. These results are consistent with the formation of the transfer film on the counterface during the sliding process as well as the polishing effect caused by the glass. The initial surface roughness values were measured before the tests were performed. The surface roughness values were also measured at regular intervals during and on completion of the test. Roughness values were measured perpendicular to the grinding marks on the stainless steel counterfaces.

Table 4.2: The dry sliding friction and wear results of the PTFE grades at 2.6 MPa+.

Material	Wear rate $mm^3/N.m$ $x10^{-6}$	Coefficient of friction (dynamic)	Initial R_a μm	Final R_a μm (After 5km)	Filler
PF1125 PS	0.31	0.23	0.20	0.13	SGF
BP6688 N	0.32	0.19	0.19	0.11	LGF+MoS_2
PF1727	0 44	0.19	0.21	0.12	SGF+ MoS_2
PFR1125	0.45	0.20	0.19	0.15	SGF
PF1125 IN	0.47	0.22	0.20	0 13	LGF
PF1125 BP	0.50	0.25	0.20	0.15	SGF+pigment
PF1125	0.57	0.23	0.21	0.15	SGF
PFR1125+0.5	0.60	0.23	0.19	0 14	SGF+pigment
PV1000	148 8	0.20	0.21	0.13	unfilled
PF1717	0.26	0.18	0.19	0.13	SGF+MoS_2
PF2226	0.32	0.20	0.19	0 15	SGF+pigment
PF2226 B	0.49	0.23	0.20	0.14	SGF+pigment
PFR2226	0 58	0.21	0.19	0.14	SGF+pigment
PF2031	0.58	0.26	0.20	0 14	SGF+$BaSO_4$+pigm.
T103-02	0.59	0.20	0 19	0.13	GFL
T101-02	0 69	0.25	0.20	0.15	SGB
T096/02	0.71	0.24	0.21	0.15	HHGB
T097/02	3.77	0 22	0.21	0.17	SHGB

+ SGF = short glass fibre, LGF = Long glass fibre, GFL = Glass flakes, SGB = solid glass beads, HHGB = hard hollow glass beads and SHGB = soft hollow glass beads.

4.3.2.3.1 Variation of Wear with Load

The variation of volume loss vs. sliding distance curves for the glass filled PTFE at the various loads are given in appendix B. The variation of the specific wear rates of glass filled PTFE composites with pressure are shown in table 4.3. Generally, the wear rates of the PTFE composites seem to increase with the contact pressure increases from 2.6 MPa to 6.4 MPa. The wear rates of the grades under these pressures increased from 0.26 $x10^{-6}$ $mm^3/N.m$ to 2.3 $x10^{-5}$ $mm^3/N.m$, with soft hollow glass bead filled PTFE showing the highest wear rates. The wear results shown in table 4.3 were summarised and plotted in bar charts. Figure 4.8 shows how the specific wear rates of the PTFE composites vary under the afore-mentioned loads. The pressure of 6.4 MPa seemed too

high for the PTFE grades as they all showed high wear rates. All of these grades showed signs of severe deformation under this load. A smaller amount of glass fibres in combination with MoS_2 seemed to have a similar impact in reducing wear as can be seen when PF1717 which has 12 % glass fibre is compared with PF1125 which has 25 % glass fibres. Table 4.3 and figures 4.8 a to c show that the grades that perform well under the tested pressures are those containing MoS_2, carbon and the pressure sintered grades.

Table 4.3: Variation of specific wear rates of PTFE composites with load*.

Material	Pressure (MPa)				Filler
	2.6	3.3	4.5	6.4	
	$mm^3/N.m$ $x10^{-6}$	$mm^3/N.m$ $x10^{-6}$	$mm^3/N.m$ $x10^{-6}$	$mm^3/N.m$ $x10^{-6}$	
PF1125 PS	0.31	0.40	0.59	0.84	SGF
PFR1125	0.45	0.36	0.90	0.88	SGF
PFR1125+0.5	0.60	0.40	0.64	0.90	SGF+pigment
BP6688 N	0.32	0.40	0.41	0.95	LGF+MoS_2
PF1727	0.44	0.45	0.48	1.10	SGF+ MoS_2
PF1125 BP	0.50	0.68	1.23	1.20	SGF+pigment
PF1125 IN	0.47	0.5	0.60	1.24	LGF
PF1125	0.57	0.56	0.50	1.34	SGF
PV1000	148.8	377.1	459.6	854.5	unfilled
PF1717	0.26	0.12	0.40	0.55	SGF+MoS_2
PF2226 B	0.49	0.41	0.63	1.20	SGF+pigment
PF2226	0.32	0.38	0.53	1.30	SGF+pigment
PF2031	0.58	0.66	0.90	1.37	SGF+$BaSO_4$+pigm.
PFR2226	0.58	0.44	0 59	1.44	SGF+pigment
T101-02	0.69	0.65	1.10	1.20	SGB
T096/02	0.71	0.74	0.82	3.80	HHGB
T103-02	0.59	0.76	1.44	4.71	GFL
T097/02	3.77	2.42	3.10	23.0	SHGB

* SGF = short glass fibre, LGF – Long glass fibre, GFL = Glass flakes, SGB – solid glass beads, HHGB = hard hollow glass beads and SHGB = soft hollow glass beads.

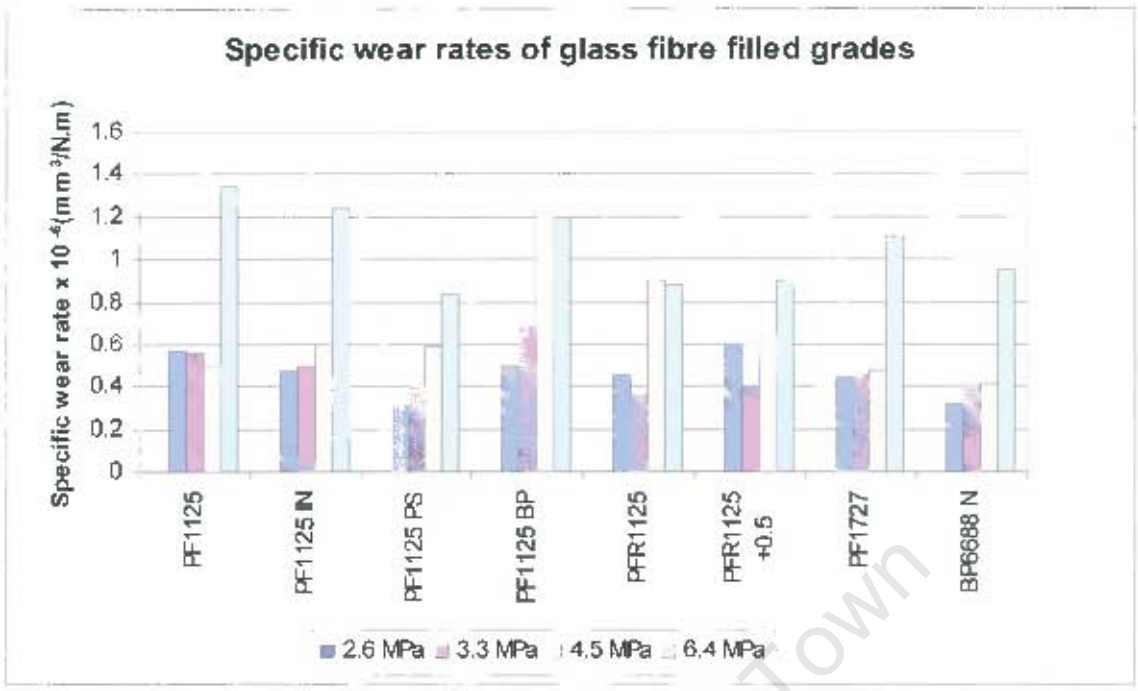

(a)

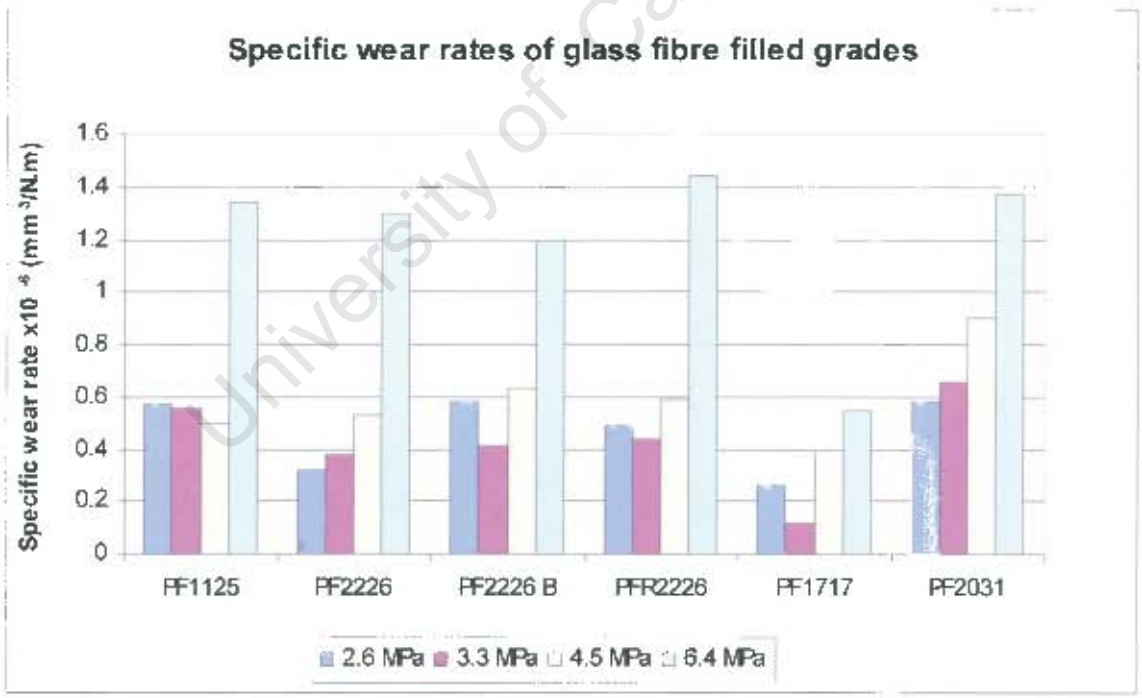

(b)

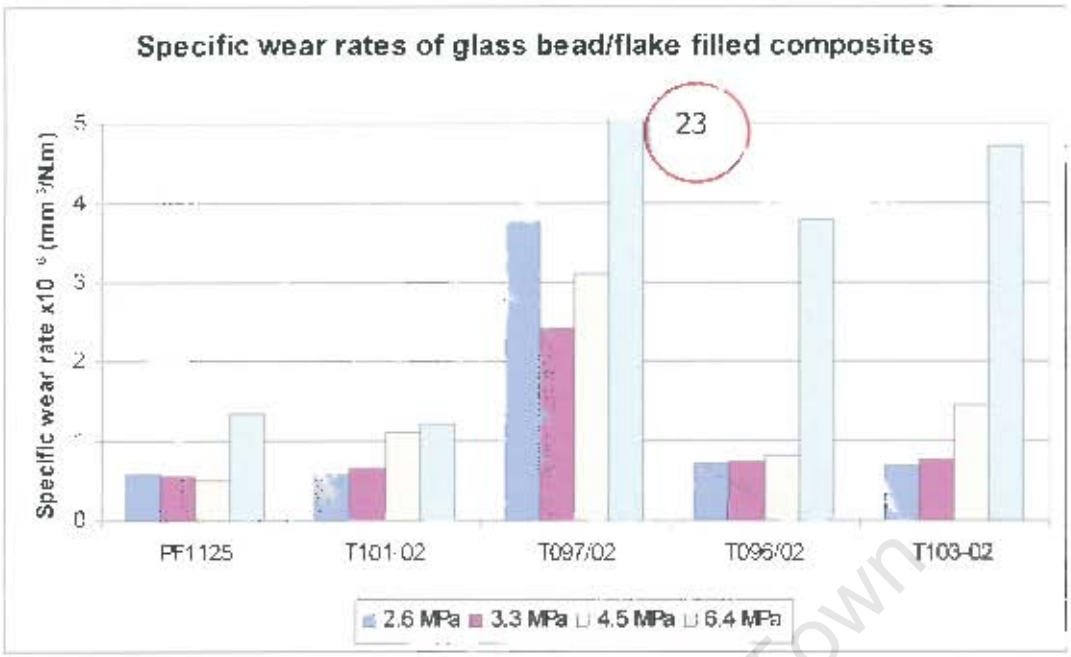

(c)

Figure 4.8: The wear variation with pressure of (a), (b) glass fibre filled PTFE composites and (c) glass bead/flake filled composites. The wear rate of soft hollow glass bead filled PTFE is 23 x10^{-6} mm^3/N.m at 6.4 MPa and shown by the circle.

4.3.2.3.2 Variation of Friction with Load

The steady state dynamic coefficient of friction results obtained during the sliding process are summarised in table 4.4. The friction results for PTFE composites do not show significant variation but seem to decrease slightly with increasing load. All the friction values obtained were below 0.28, and are consistent with the friction values that often quoted in literature for glass fibre filled PTFE. The friction results were summarised and plotted in bar charts. Figure 4.9 shows the variation of friction with load at an average velocity of 0.2 m/s. All the grades containing MoS_2 i.e. BP6688 N, PF1727 and PF1717 show relatively low friction coefficients during steady state wear.

Table 4.4: Variation of the dynamic coefficient of friction with load.

Material	Pressure (MPa)			
	2.6	3.3	4.5	6.4
PF1125	0.23	0.19	0.19	0.17
PF1125 BP	0.25	0.23	0.24	0.21
PF1125 IN	0.22	0.20	0.21	0.19
PF1125 PS	0.23	0.24	0.18	0.20
PF1727	0.19	0.20	0.18	0.16
BP6688 N	0.19	0.17	0.17	0.16
PFR1125	0.20	0.18	0.22	0.19
PFR1125+0.5	0.23	0.21	0.22	0.17
PF2226	0.20	0.18	0.19	0.18
PFR2226	0.21	0.18	0.20	0.18
PF2226 B	0.23	0.20	0.20	0.18
PF1717	0.18	0.16	0.17	0.17
PF2031	0.26	0.24	0.21	0.22
T096/02	0.24	0.22	0.21	0.19
T097/02	0.22	0.20	0.19	0.20
T103-02	0.25	0.22	0.21	0.18
T101-02	0.20	0.19	0.19	0.18

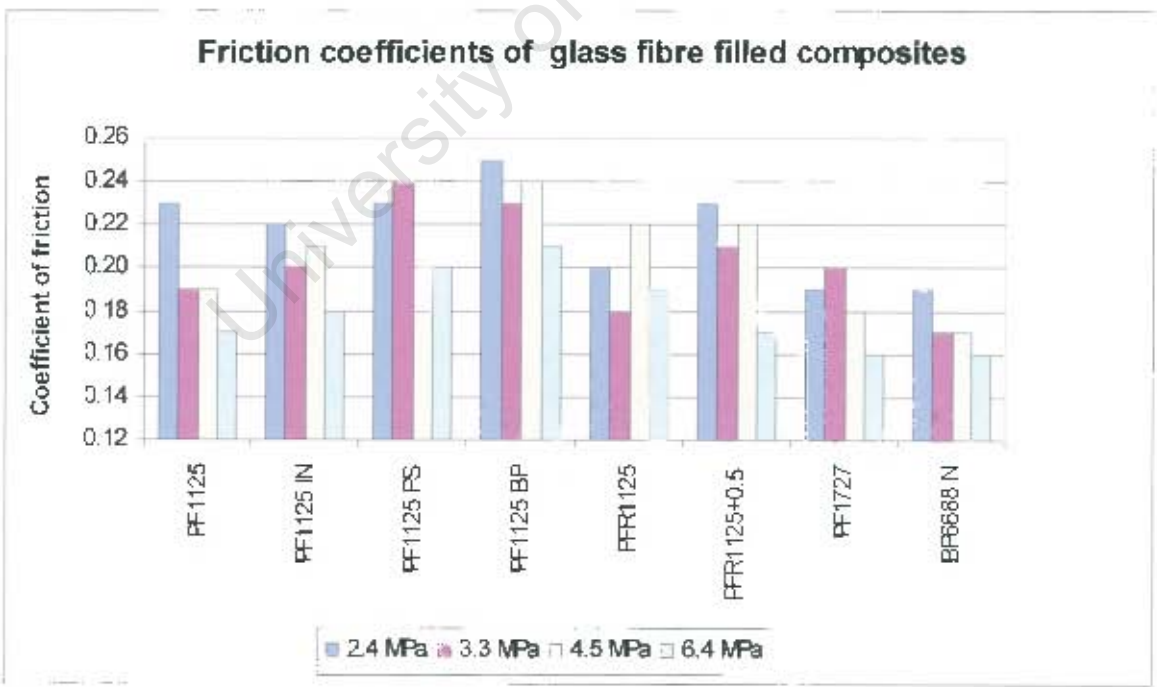

(a)

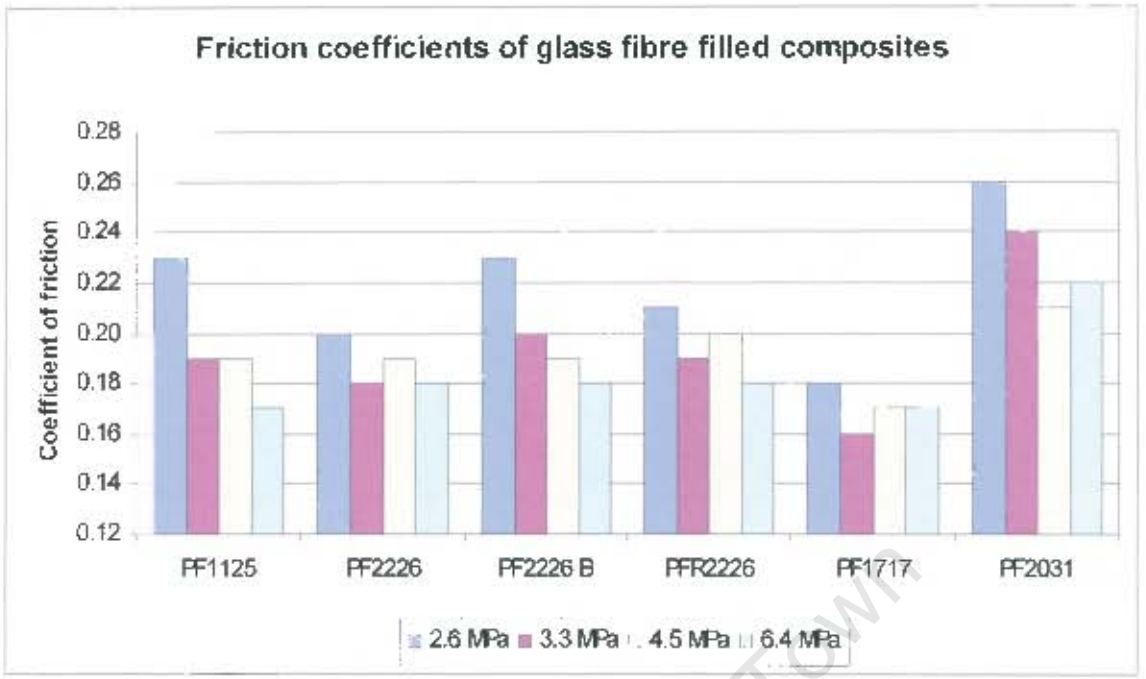

(b)

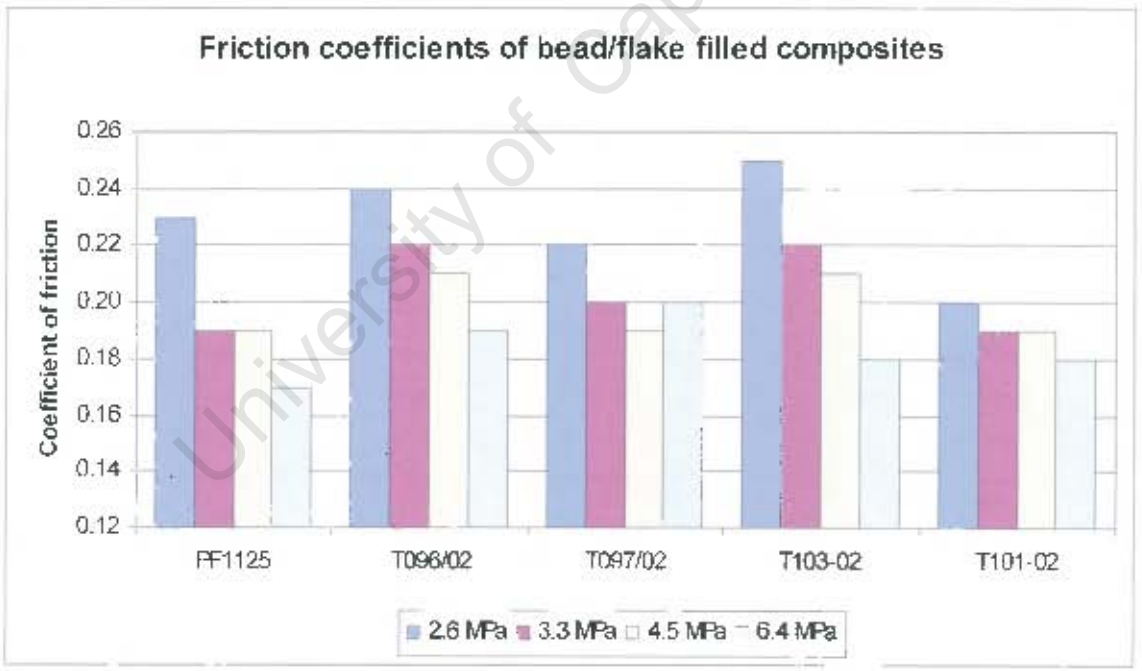

(c)

Figure 4.9: **The variation of the steady state dynamic coefficient of friction with load for (a), (b) glass fibre filled PTFE and (c) glass bead/flake filled PTFE composites.**

4.3.2.4 WORN SURFACE CHARACTERISATION

In order to understand the friction and wear results better, surface analysis techniques such as scanning electron microscopy and optical microscopy were employed. Both the worn composite pins and worn stainless steel counterfaces were analysed. In additions to these, x-ray analysis, x-ray photo-electron spectroscopy as well as surface profile analyses were done to complement microscopy.

4.3.2.4.1 Microscopy

Figures 4.10 (a)–(e) show transfer film on the stainless steel counterfaces after it was worn against PF1125, PF1125 BP, BP6688 N (glass fibre filled-), T096/02 (hard hollow glass bead filled-) and T103-02 (glass flake filled PTFE), respectively. The micrographs show that the transfer films on the counterface are similar in terms of the extent to which they cover the metal surface after 5 km of wear testing. However, figures 4.10 (a) and (b) show that the films appear to be uniform, a typical feature for glass fibre filled PTFE. Figure 4.10 (c) on the other hand, which shows the 2 % molybdenum disulphide glass fibre filled PTFE rubbed against stainless steel, shows a much smoother, coherent and adherent film. The transfer film formed on rubbing glass bead filled PTFE and flake filled PTFE against the metal counterface are shown in figures 4.10 (d) and 4.10 (e), respectively. It is clear from the figures that the transfer film formed on the counterface is less coherent and much thicker in the case of the bead filled PTFE grade. This is due to the broken bead fragments that occur during the sliding process resulting in a much thicker film.

Figure 4.11 shows the high magnification pictures of some of the micrographs shown in figure 4.10. Figure 4.11 (a) clearly shows pieces of glass fibre fragments scattered onto the counterface. At this stage most of the valleys are filled with transfer material. These micrographs show similar scratch marks caused by the abrasion of the glass fragments. The transfer film deposited by the hard hollow bead filled grade (T096/02) appeared to be thicker than that for the other grades.

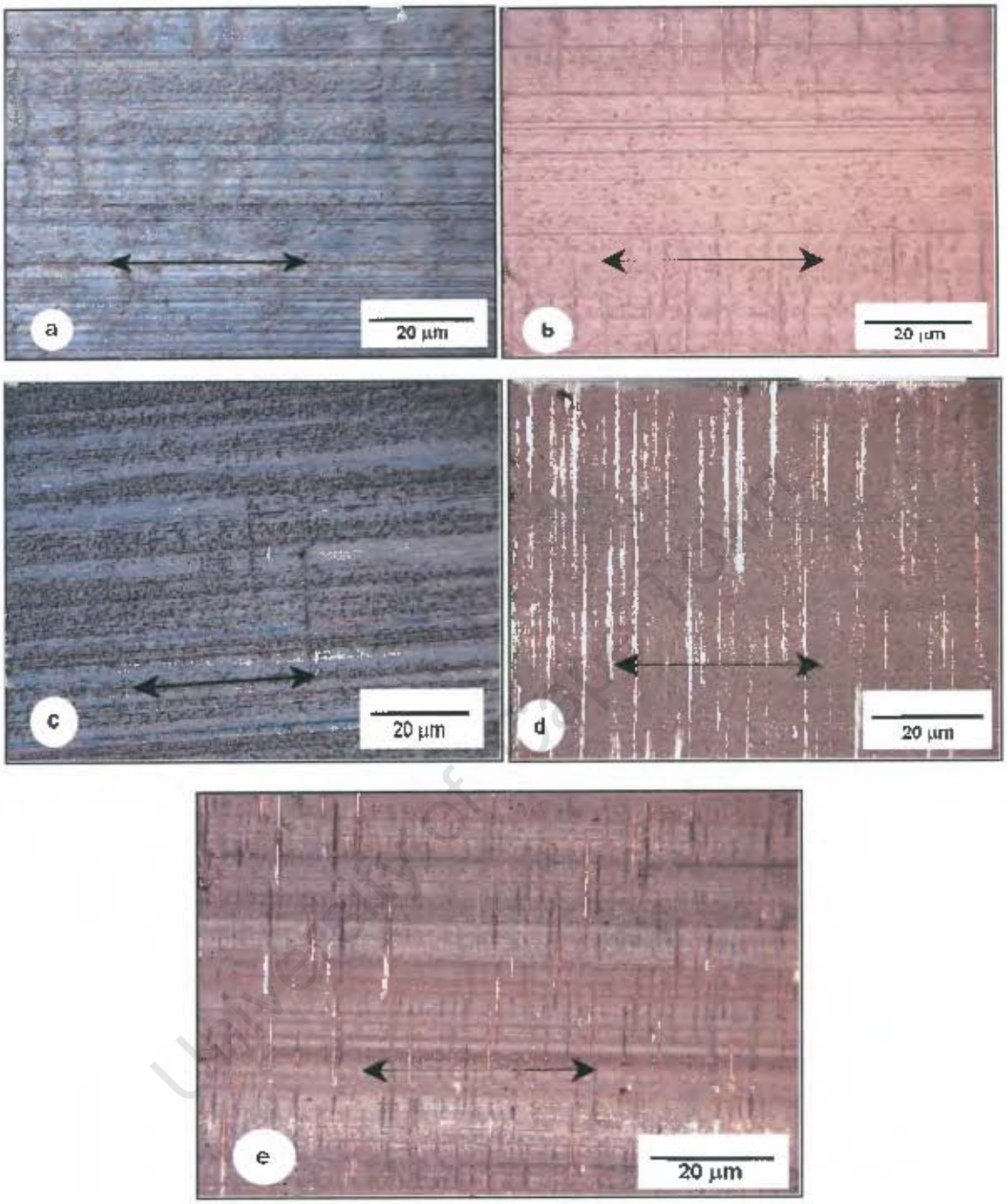

Figure 4.10: **Optical micrographs depicting the nature of transfer film on the stainless steel counterface after being rubbed against (a) PF1125 (b) PF1125 BP, (c) BP6688 N, (d) T096/02 and (e) T103-02, under a load of 4.5 MPa. The arrow indicates the sliding direction.**

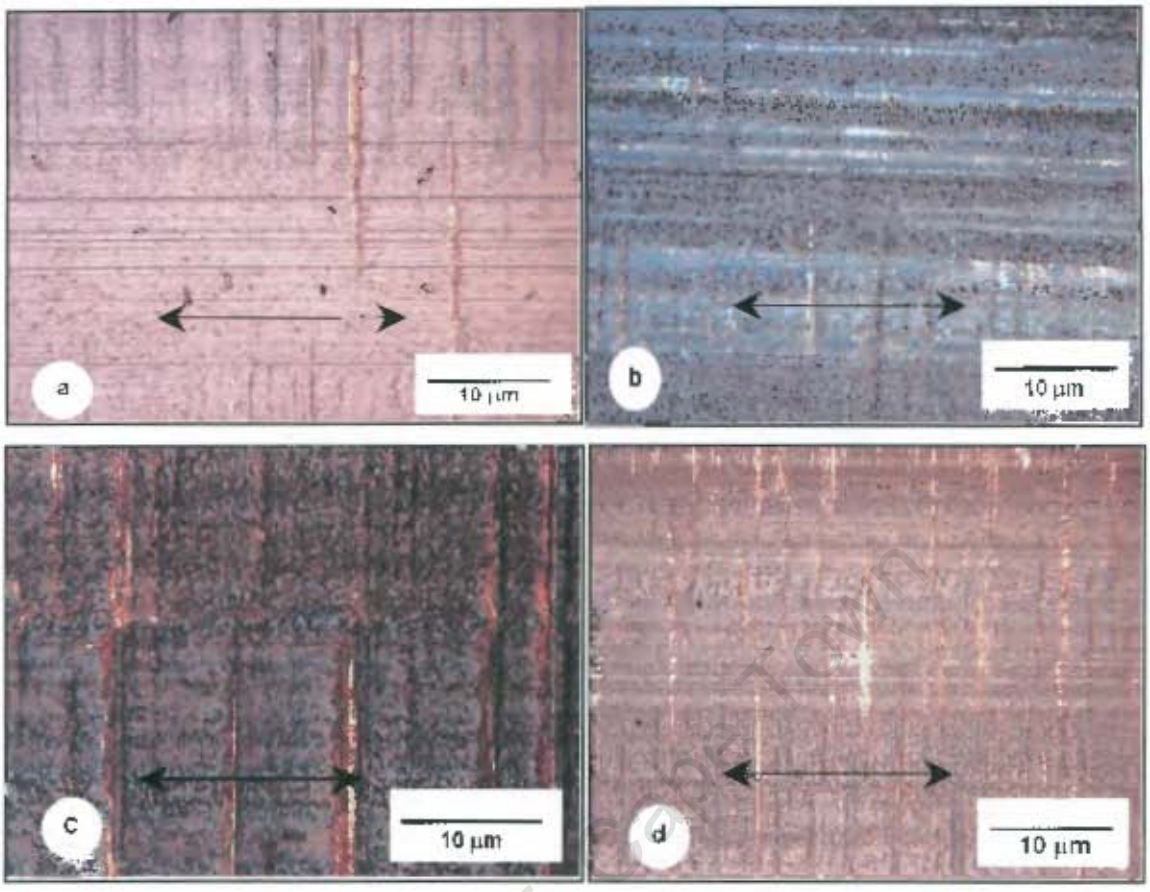

Figure 4.11: The high magnification pictures of the micrograph shown in figure 4.9 for (a) PF1125 BP with glass fibres scattered all over the stainless steel surface, (b) BP6688 N, (c) T096/02 and (d) T103-02. The arrows indicate the sliding direction.

SEM micrographs showing the worn glass fibre filled PTFE composite pins for PFR1125 are shown in figure 4.12. Figures 4.12 (a) and (b) show a broken and loosely bound fibre as well as scars left by glass fibres, respectively. The figure also shows that the fibres are generally broken down into smaller fragments before being detached from the matrix. Figures 4.12 (c) and (d) illustrate pieces of glass fibres detached from the matrix. Figure 4.12 (c) shows that due to continuous sliding the glass fibre pulls out of the adjacent polymer while figure 4.12 (d) shows a fibre that is mobile at the interface.

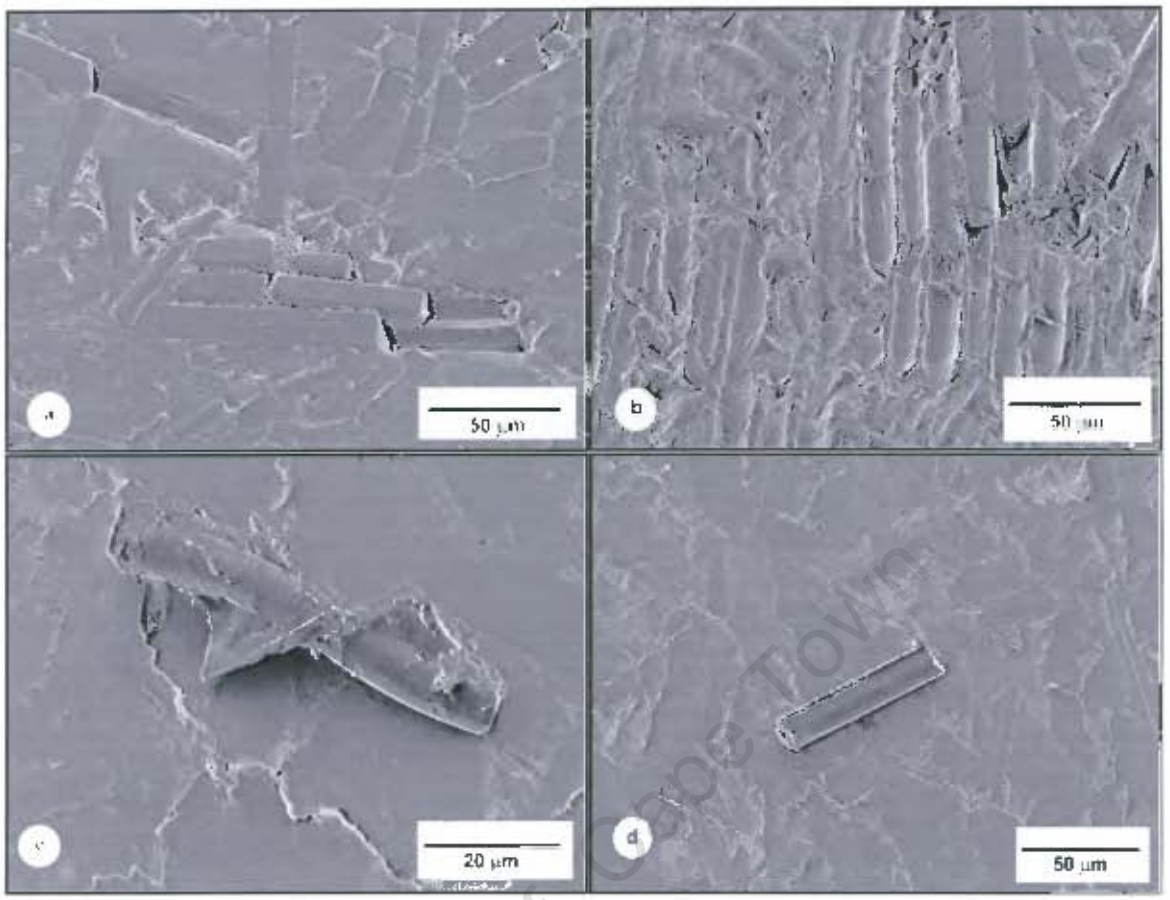

Figure 4.12: SEM micrographs of the PFR1125 worn pin surfaces after sliding 3 km against stainless steel counterfaces showing (a) fibre breakage as well as the polishing effect of glass fibres, (b) scars left by the fibre pull-out, (c), (d) pieces of glass fibres on the polymer pin.

4.3.2.4.2 Profilometric Analysis

After the sliding process, the stainless steel counterfaces were studied by means of the surface profilometer and figures 4.13 and 4.14 show the typical profiles obtained. Figure 4.13 shows how the topography of the counterfaces changes with sliding distance upon rubbing against PF1125. The development of the transfer film is evident in the disappearance of the sharp peaks due to the grinding marks shown in figures 4.13 (a) and (b). Therefore, the uneven but smooth profiles shown figures 4.13 (c) and (d) are due the transfer film on the metal counterface

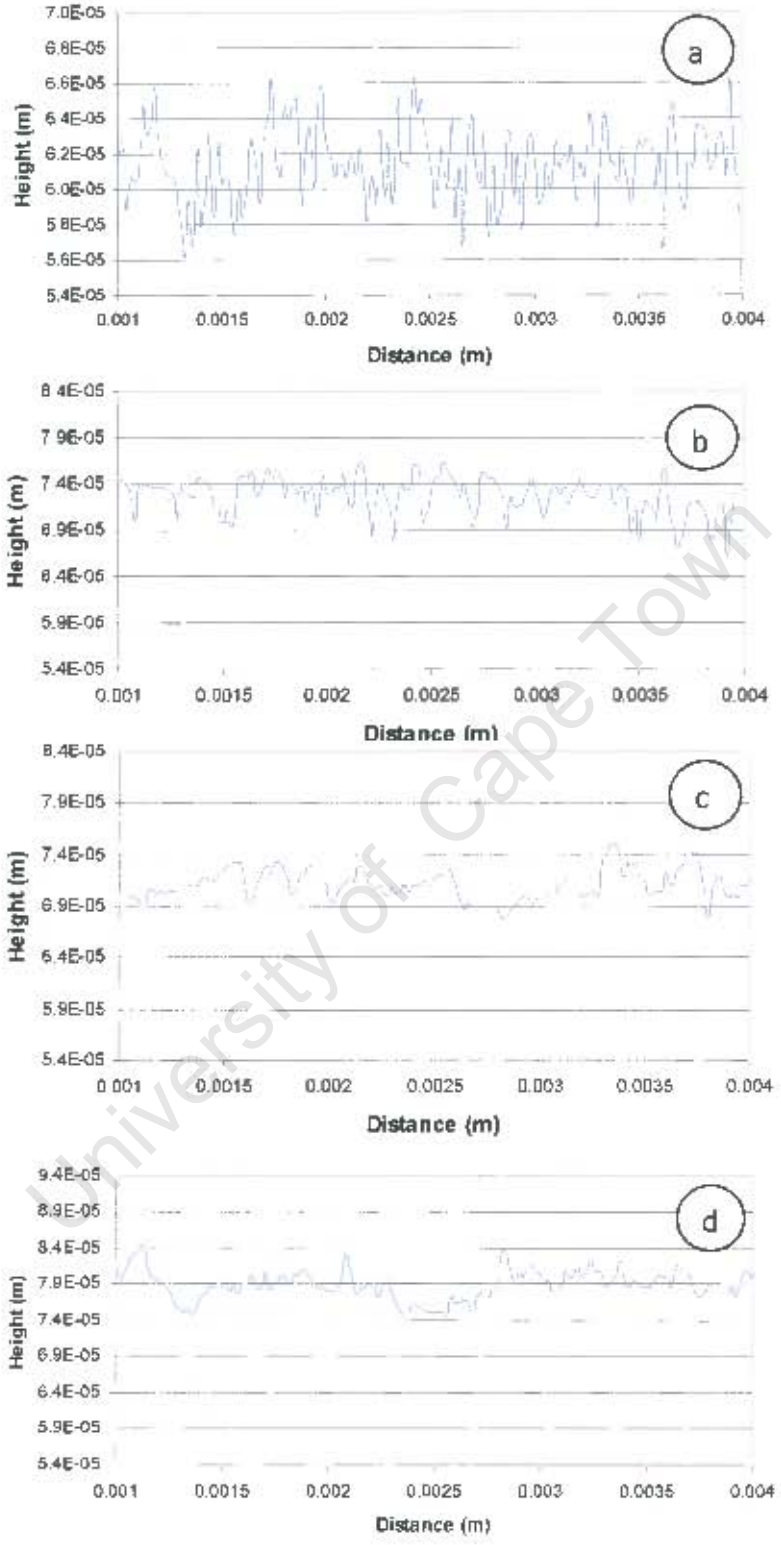

Figure 4.13: Profiles of the (a) unworn counterface, (b), (c), (d) worn counterfaces after sliding 1, 3 and 5 km, respectively against PF1125.

Figure 4.14 shows stainless steel surface profiles obtained after being rubbed for 5 km against different PTFE composites. The surface topography of the counterfaces is modified by the presents of the transfer film. The surface profiles represented by figure 4.14 all seem to be relatively smooth and fairly uniform in the middle of the counterface, where these traces were taken, except the one for the surface worn against hard hollow glass bead filled PTFE (T096/02). The topography of the metal counterfaces show significant smoothing with distance after being rubbed against the glass bead filled PTFE composite, T096/02, and this is consistent with the thick transfer film shown in figure 4.11 (c). Although the profiles due to rubbing against other PTFE composites are fairly similar, the unevenness characterised by deep and shallow troughs on the counterface surface after rubbing against PF1125 is clearly visible. The profiles obtained when the counterfaces were rubbed against molybdenum disulphide filled grade, PF1717, together with glass flake filled PTFE both showed evenness except for sharp troughs that are probably due to the grooves on the counterface.

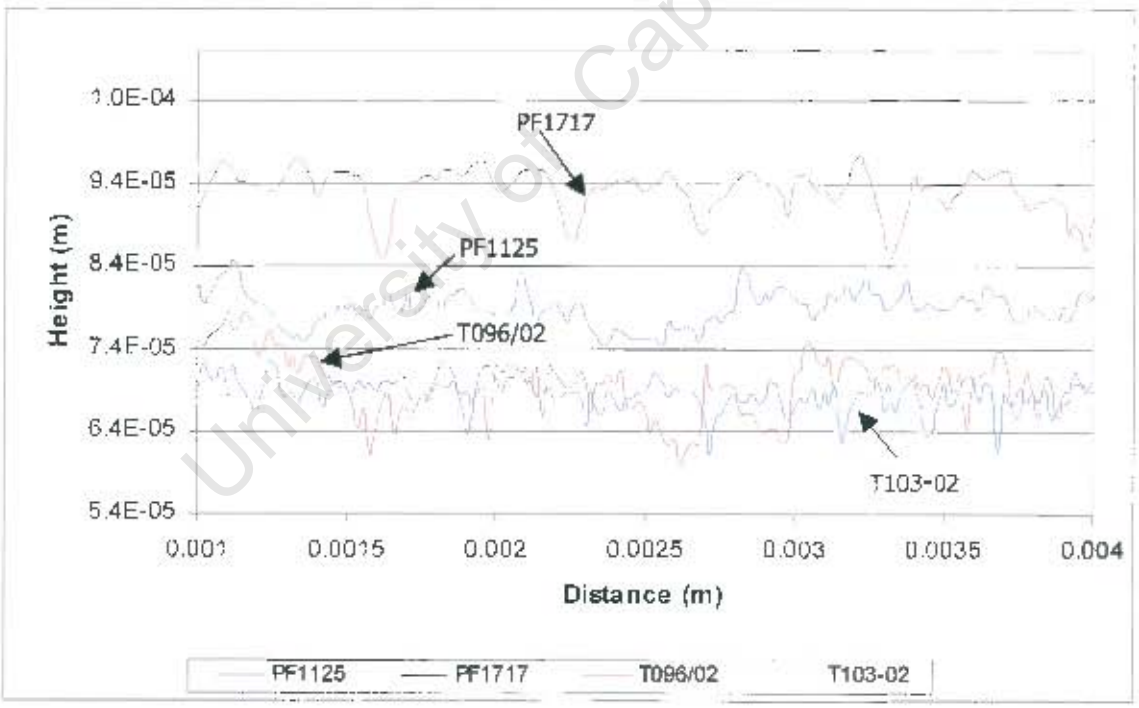

Figure 4.14: The stainless steel surface profile after sliding 5km at 0.2 m/s and 4.5 MPa. The profiles were obtained by means of a surface profilometer.

4.3.2.4.3 X-ray Analysis of the Counterface

Further studies were undertaken to fully understand the effect and influence of molybdenum disulphide on the wear behaviour of glass fibre filled PTFE. X-ray maps of on a section of the BP6688 N pin surface were taken and are presented in figure 4.15. Figure 4.15 (a) shows a SEM micrograph of a section of a BP6688 N pin surface exposing both the matrix as well as the fillers. Figures 4.15 (b), (c) and (d) show the fluorine (white), sulphur (green) and molybdenum (green) x-ray maps of the corresponding coloured areas in figure 4.15 (a), respectively. The element present is represented by the dots in each x-ray map. It would appear from the maps that the MoS_2 filler is not uniformly spread across the pin surface. The transfer film formed by BP6688 N seemed more coherent than that formed by other glass fibre filled PTFE composites. Therefore, further tests using XPS were undertaken to understand the transfer film and bonding mechanisms.

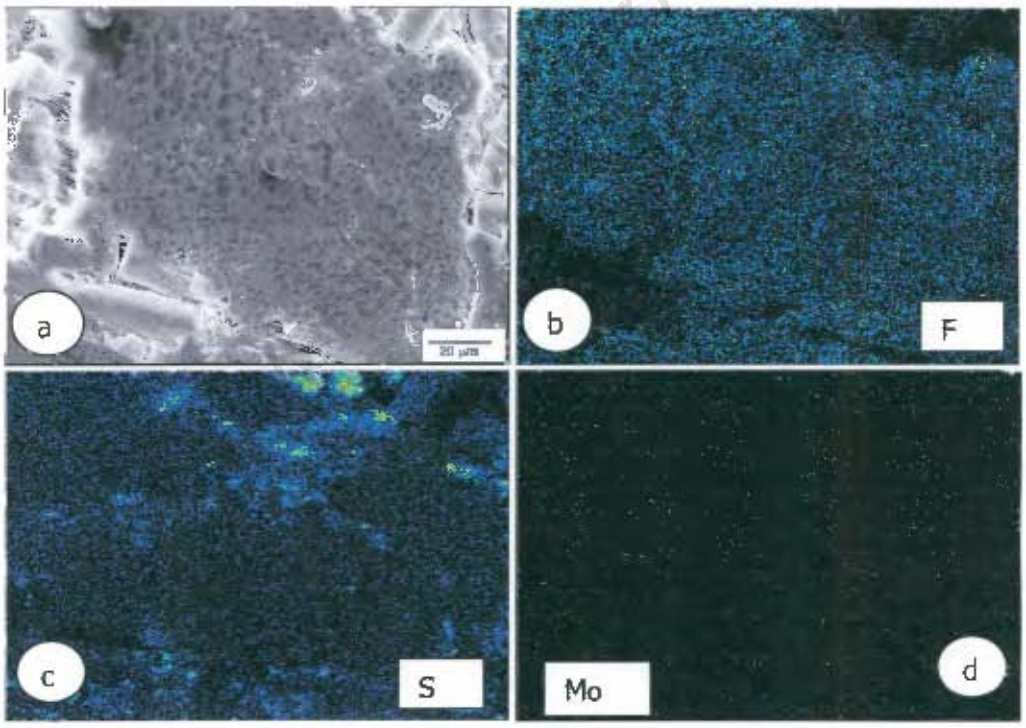

Figure 4.15: (a) SEM of the worn surface of a BP6688 N surface showing an exposed glass fibre; (b), (c) and (d) X-ray maps of the BP6688 N surface, showing the fluorine, sulphur and molybdenum concentrations.

4.3.2.4.4 *XPS Analysis of the Counterface*

The binding energies and the relative atomic concentrations of elements on the stainless steel counterface after rubbing against BP6688 N were analysed by XPS. X ray photo-electron spectra of the worn counterface are shown in figures 4.16 and 4.17 with the peak assignments summarised in table 4.5. The bond energies from these plots were compared with the data listed in the ***Handbook of X-ray Photoelectron Spectroscopy***[97]. Table 4.5 lists the binding energies as well as peak resources of the important elements detected by the instrument. The calcium, silicon, aluminium and magnesium present on the counterface are constituents of glass fibres. Two discrete peaks can be seen from the fluorine, F (1s) spectra in figure 4.17. The peak at a binding energy 689.7 eV in figures 4.16 and 4.17 (a) with a corresponding peak in the C (1s) spectra at 291.1 eV (figure 4.17 (c)) can be attributed to the an unreacted PTFE species. The F (1s) peak at the lower binding energy of 686 eV does not have a corresponding peak in the C (1s) spectra and this suggests that the peak originates from metallic fluoride formed as a result of a chemical reaction. The Fe (2p) peak at 710.6 eV is also present which could suggests the presence of ferric oxide as was found by various researchers[97,93].

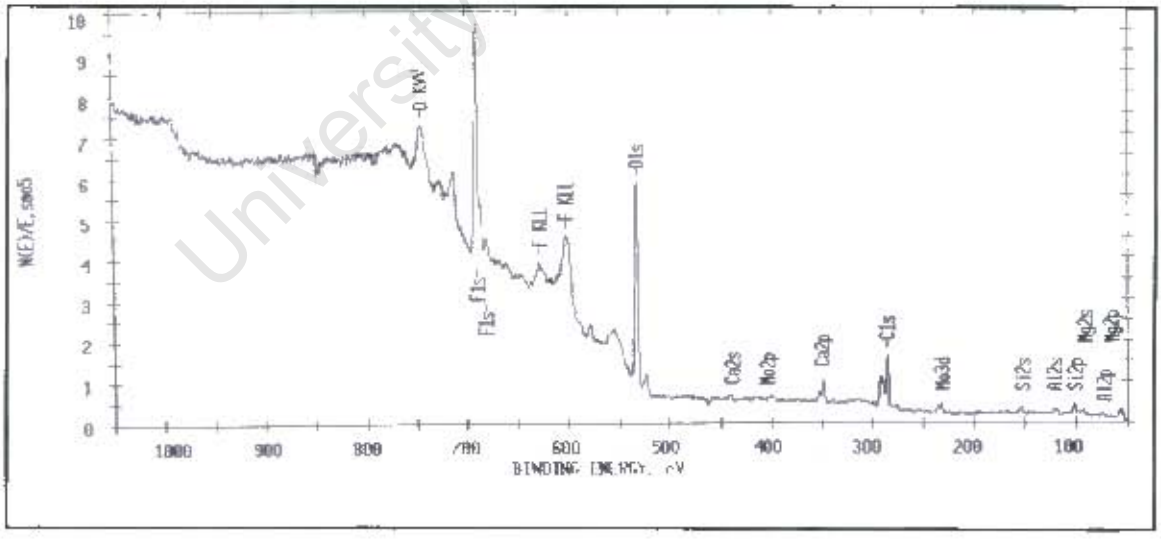

Figure 4.16: XPS spectra of the transfer film of BP6688 N on a stainless steel surface.

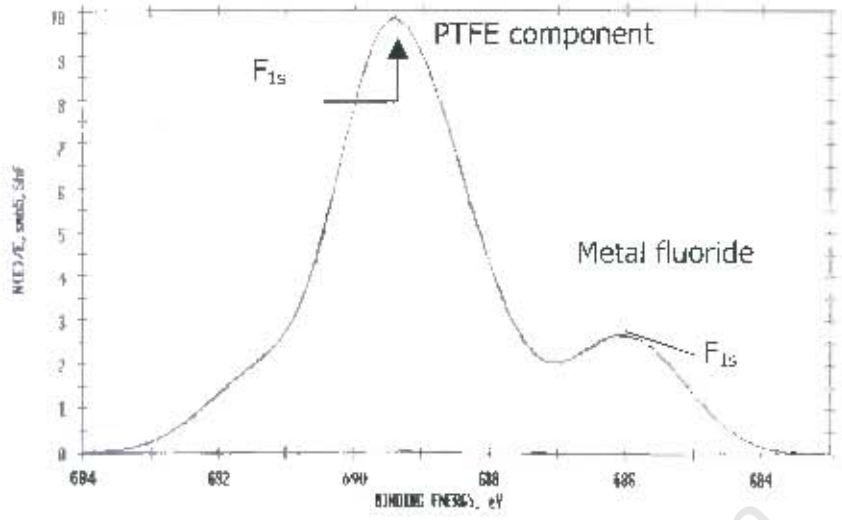

(a)

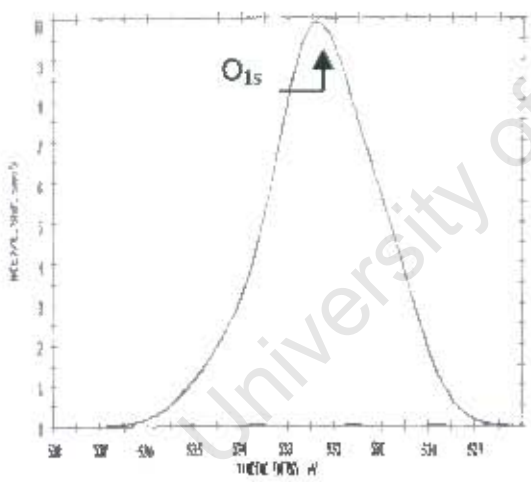

(b)

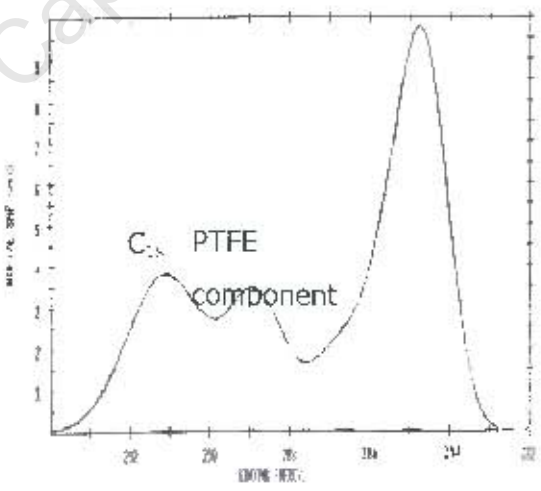

(c)

Figure 4.17: XPS analysis of the transfer film grown on the stainless steel surface after being worn against BP6688 N showing the (a) F 1s, (b) O 1s and (c) C 1s spectra after 5 km of sliding at 0.2 m/s under a load of 4.5 MPa.

Table 4.5: Chemical analysis of the metal counterface after being worn against BP6688N.

Elements	*Binding energy (eV)*	*Peak resourse*	*Relative atomic concentration (%)*
C1s	291.1	PTFE	25.5
	288.8	?	
	284.6	contamination	15.8
O1s	532.5	stainless steel	57.8
F1s	689.7	PTFE	36.1
	686	iron fluoride	17.9
Fe2p	710.6	Fe_2O_3	

The transfer film of the materials was further characterised by using x-ray diffraction. The degree of crystallinity of the bulk material as well as that of the debris formed were analysed in an effort to better understand the transfer of the composites.

4.3.2.4.5 Wide Angle X-Ray Diffraction Analysis

The materials used for x-ray diffraction (XRD) analysis were PV1000, PF1125, PF1125 PS, BP6688 N, PF2226, PFR2226, T097/02 and T103-02. These materials were deemed sufficient and necessary as they include all forms of the glass fillers being studied. The wear debris of these materials were further studied and analysed for significant changes in molecular structure compared with the bulk material. However, the wear debris resulting from sliding tests of glass fibre filled PTFE materials was too little and could not be scratched off the metal counterfaces. Thus, only the wear debris resulting from the wear tests of unfilled PTFE, glass bead filled PTFE and glass flake filled PTFE are reported. Figure 4.18 shows the wide angle x-ray diffraction scans of these materials; other scans are given in appendix D. The degree of crystallinity of each material was calculated using equation 2.2 and the results are tabulated in table 4.6. Figure 4.18 (a) shows an XRD scan of unfilled PTFE, PV1000, with the crystalline and amorphous regions clearly indicated. Figure 4.18 (b) shows that there is no shoulder due to the amorphous phase in the debris and a consequent increase of about 7% as shown in

table 4.6. Figure 4.18 (c) shows an extra peak at an angle of 16° due to the MoS_2 filler. The shoulder for the debris obtained from glass flake filled PTFE is also absent in figure 4.18 (d) with a consequent increase of 8% for the worn material in table 4.6.

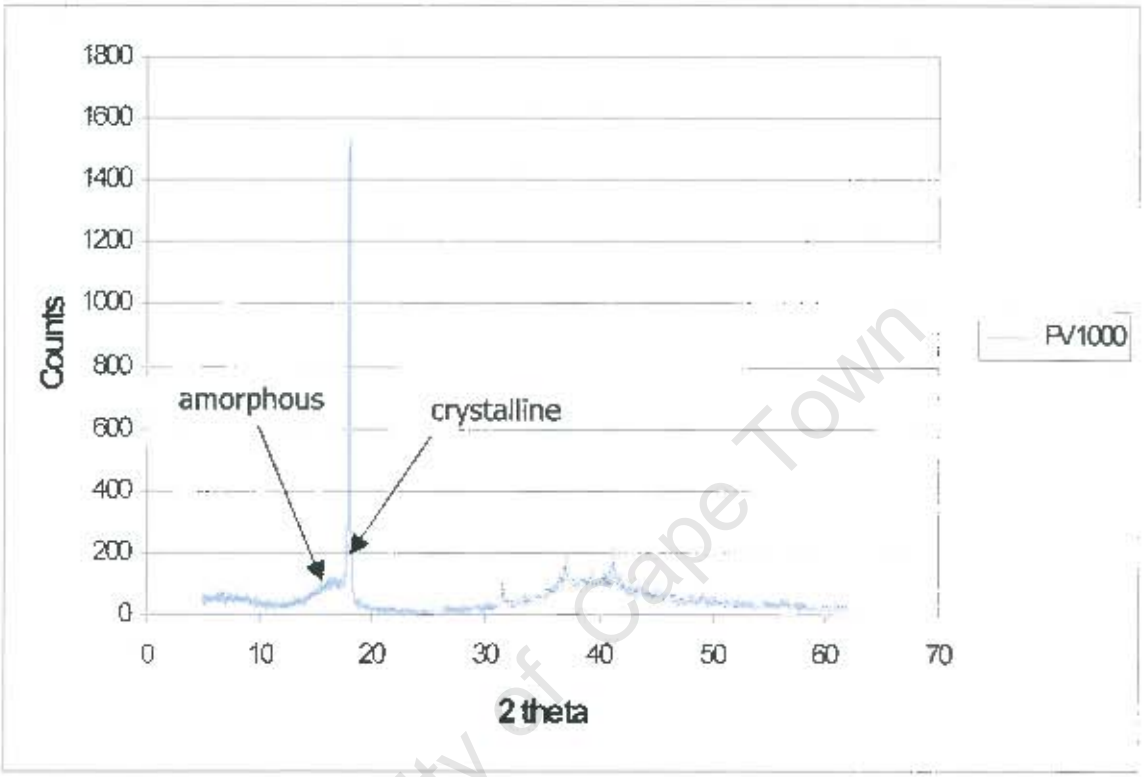

(a)

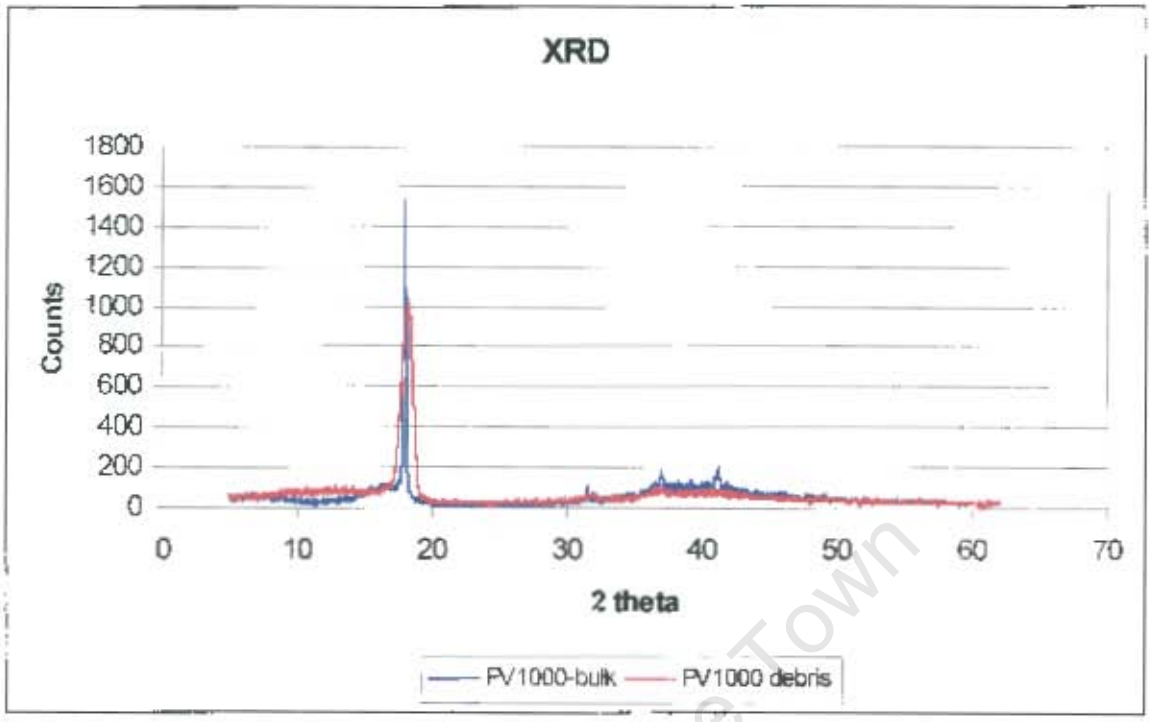

(b)

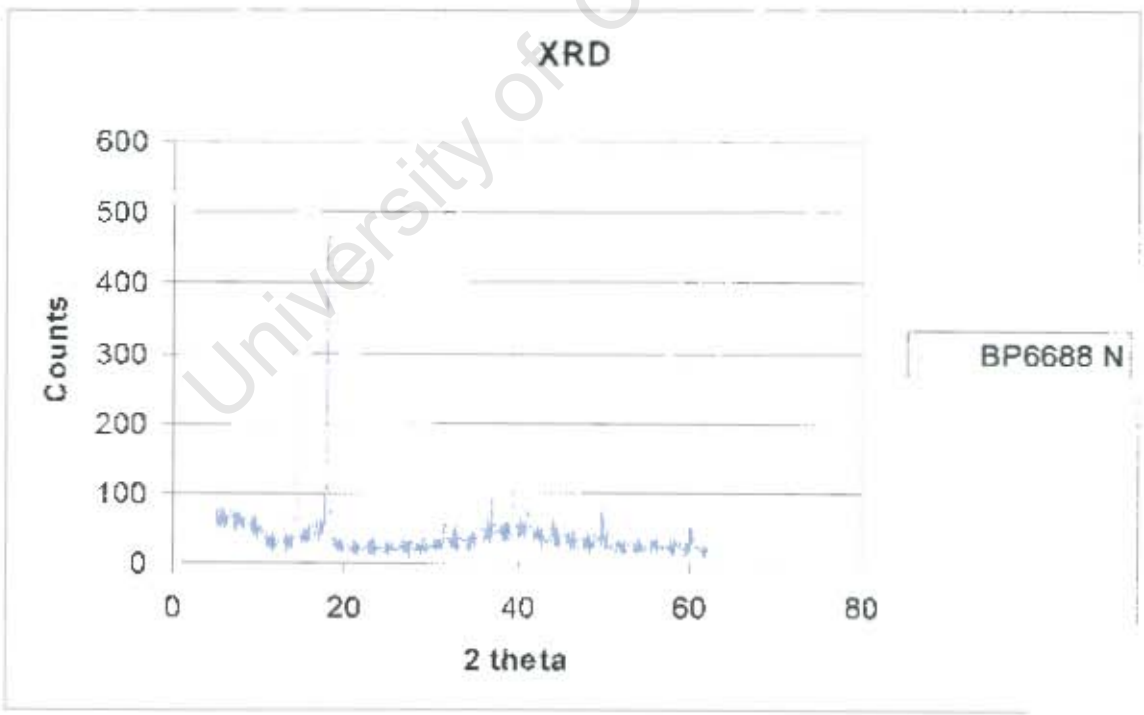

(c)

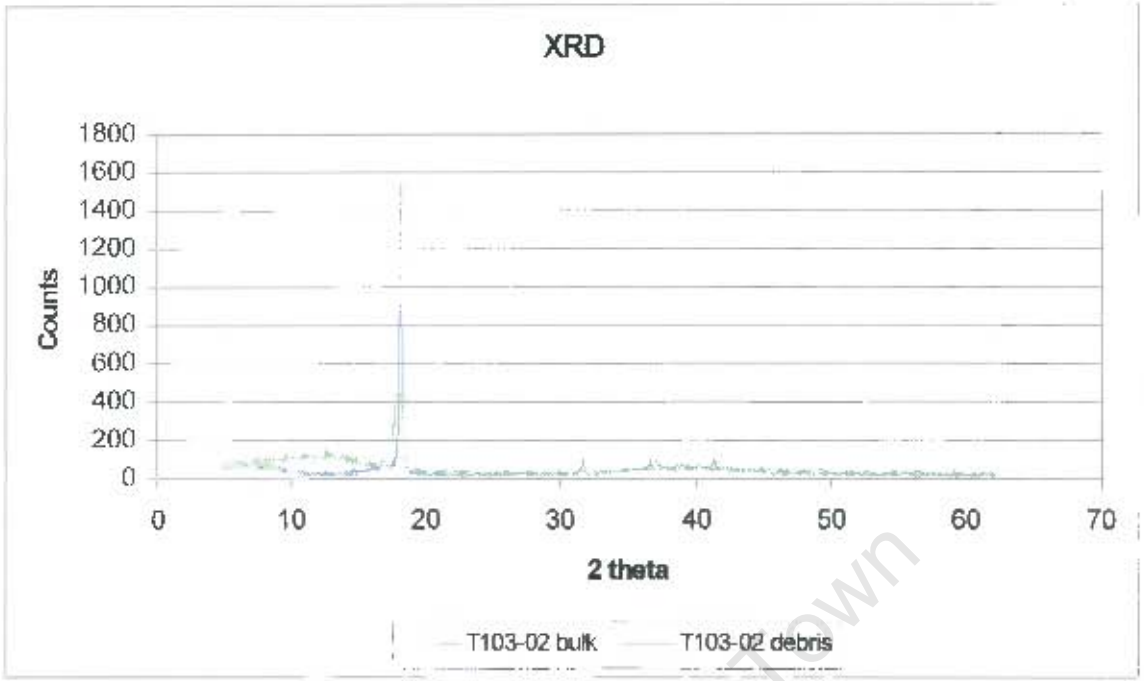

(d)

Figure 4.18: X-ray diffraction scans of different PTFE composites.

Table 4.6: The degree of crystallinity of different PTFE composites[a].

Polymer	*Materials*		*Crystallinity*	*Filler*
	unworn bulk polymer	*debris*		
PV1000	X	X	53, 60	unfilled
PF1125	X		57	SGF
PF1125 PS	X		59	SGF
PFR1125	X		57	SGF
PF2226	X		54	SGF
PFR2226	X		58	SGF
BP6668 N	X		68	LGF
T097/02	X	X	55, 57	SHGB
T103-02	X	X	53	GFL

[a] SGF = short glass fibre, LGF = long glass fibre, SHGB = soft hollow glass beads, GFL = glass flakes.

4.3.2.4.6 Differential Scanning Calorimetry

The differential scanning calorimetry (DSC) results obtained were not conclusive in terms of characterising the debris and bulk materials of glass flake filled PTFE. However, using equation 2.1 and assuming that the heat of fusion of 100 % crystalline PTFE, ΔH_f°, is 61.17 J/g the crystallinity of the bulk material (T103-02) was found to be 30 % whilst that of debris was found to be 22.4 %. The degree of crystallinity of the debris was therefore smaller than that of the bulk composite materials, in sharp contrast to the XRD results. The DSC scans of the bulk T103-02 and the debris are shown in appendix E. The DSC also shows that the onset of melting for glass flake PTFE debris was at 317.1 °C while that of the solid bulk material occurred at 324 °C. The low melting point of the debris could be due to the short molecular chains of the debris resulting from chain scission during the sliding process.

4.3.3 Lubricated Sliding Wear Results

The effect of a lubricant on the wear of the PTFE composites was investigated by performing wear tests for some of the composites in distilled water using the reciprocating sliding wear rig. In addition, Vesconite hilube, a polyester-based material that is commonly used as a bearing in under water systems was used for comparison purposes (refer to section 3.3.1). All tests were conducted under a load of 577 N (6.4 MPa). Figure 4.19 shows the variation of the volumetric wear of Vesconite hilube and glass fibre filled PTFE the sliding distance under water lubricated conditions. In water, all the materials show high wear rates that persisted throughout the tests. This behaviour was attributed to the absence of the film on the counterface, being prevented from forming on the metal surface. The wear behaviour of the other PTFE composites that were studied under identical sliding conditions were similar to that of PF1125 and Vesconite hilube. Figure 4.20 summarises the specific wear rates obtained when the glass fibre filled PTFE and Vesconite hilube were slid against the metal counterface in distilled water. It is clear from the figure that Vesconite hilube shows low wear rates in water whilst the glass flake filled PTFE gave the highest wear results. The wear rate of Vesconite hilube is about twenty times better than that of BP6688 N.

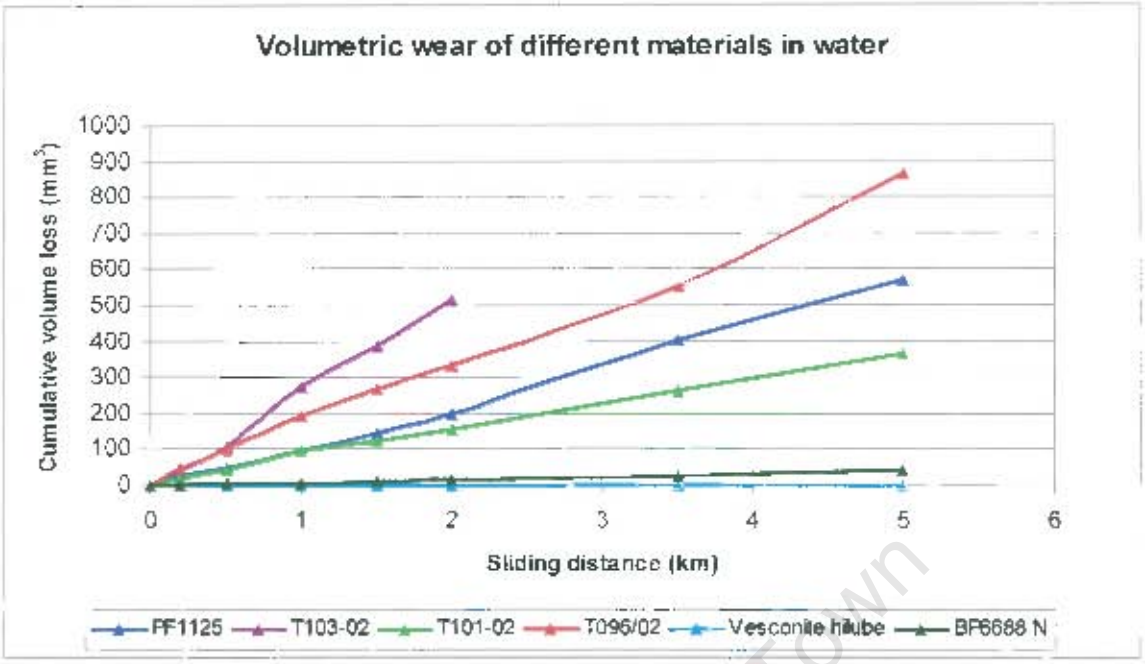

Figure 4.19: The volumetric wear of different materials in distilled water.

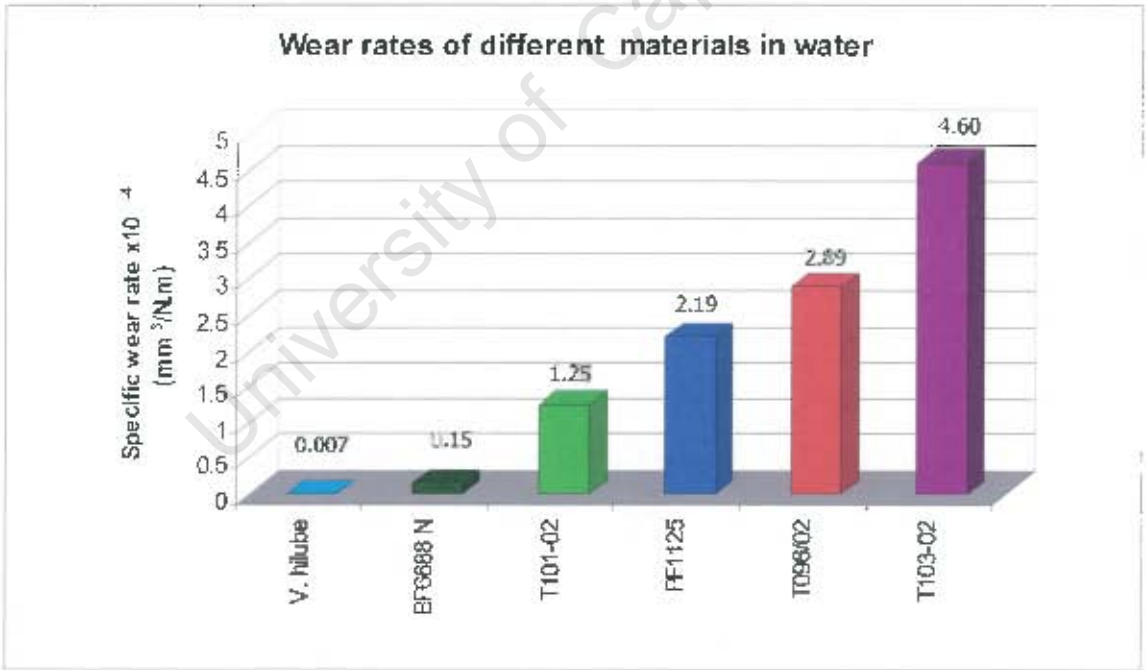

Figure 4.20: The wear results of different materials obtained in distilled water.

Figure 4.21 shows optical micrographs illustrating the effect of lubrication on the metal counterfaces when worn against PTFE composites. No transfer film is observed on the metal counterfaces for the materials tested in distilled water. An inspection of the metal counterfaces showed no transfer film except for composite lumps at the end of the stroke. Figures 4.21 (a) and (b), show scattered glass fragments on the metal surface after being worn against PF1125. Figure 4.21 (b), in particular, illustrates the thick flake like deposits that characterised many of the glass fibre filled grades, resulting in high wear rates. Figures (c) and (d) illustrate the thick polymer transfer at the end stroke and the featureless central section of the metal counterface, respectively, after sliding against BP6688 N. Glass flake filled grades showed high wear rates in water. Figures 4.21 (e) and (f) show optical micrographs of glass flake filled PTFE polymer wear pins after being slid against stainless steel counterface in water. The figure shows that flakes are not effective in reducing wear in water due to their easy separation from the PTFE matrix.

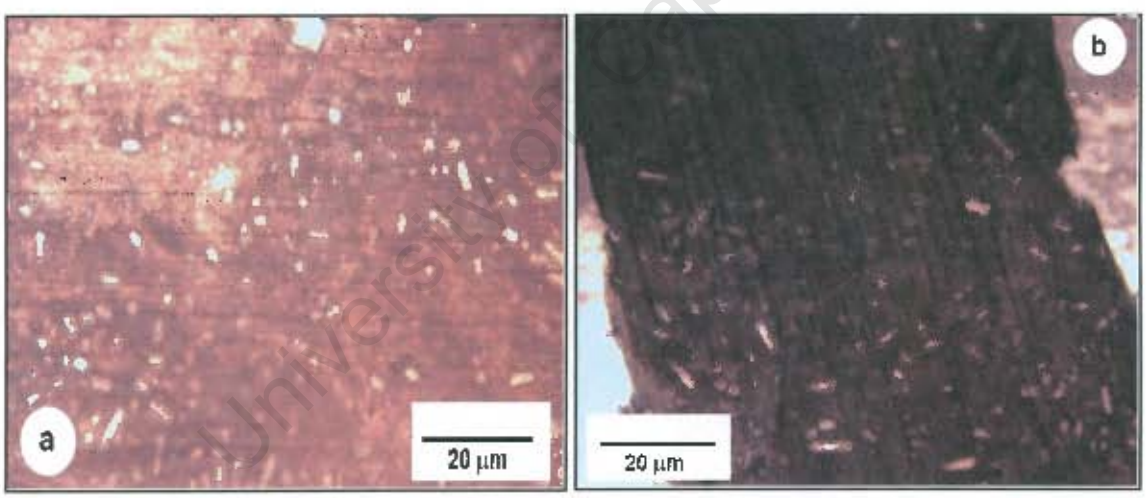

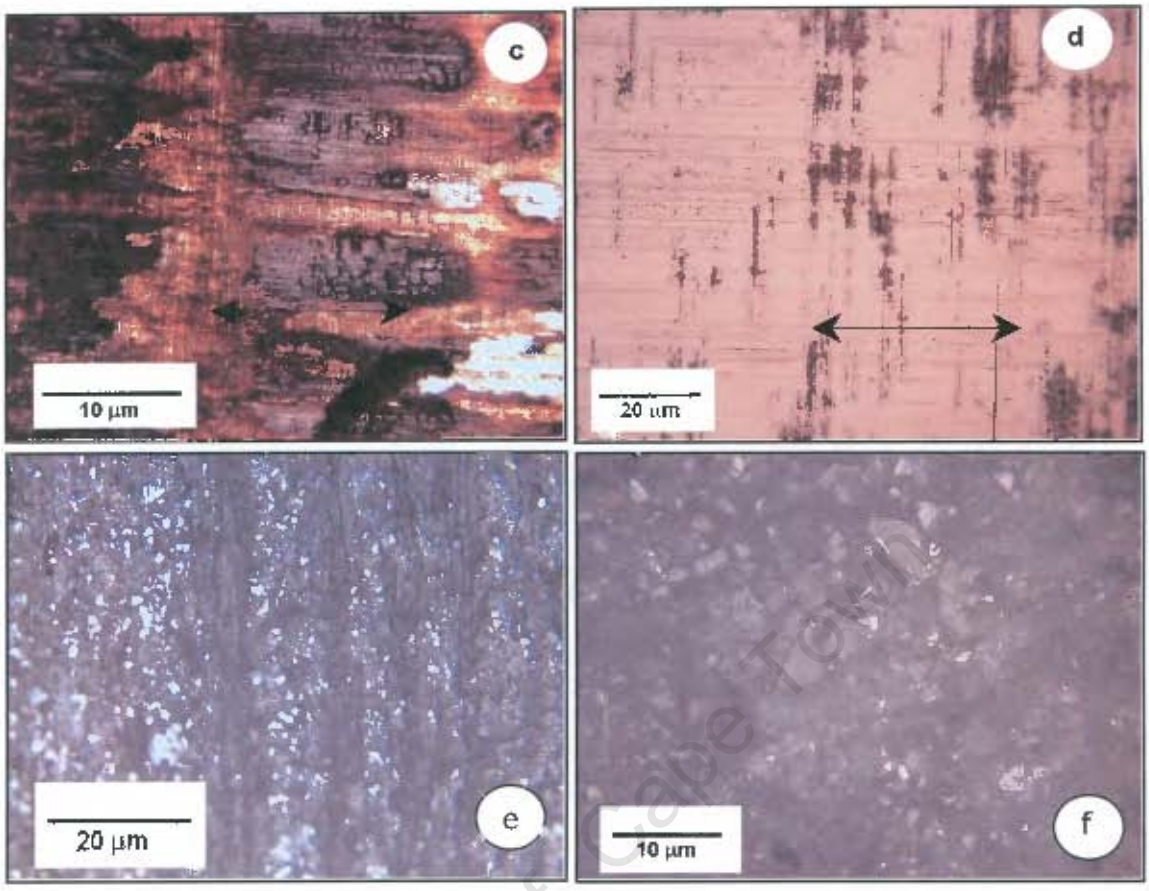

Figure 4.21: Optical micrographs of the worn stainless steel counterfaces after 5 km of sliding against (a), (b) PF1125 and (c), (d) BP6688 N, in distilled water. Figures 4.21 (e) and (f) show the optical micrographs of the glass flake filled PTFE pins after being slid against PTFE in distilled water. The arrows indicate the sliding direction.

4.4 DRY SLIDING PIN-ON-DISK RESULTS

In addition to the reciprocating sliding wear tests, a pin-on-disk was used to investigate the friction and wear behaviour of PTFE composites at constant velocity. Calibration tests were performed on the pin-on-disk using PF1125. Three wear tests were performed on the pin-on-disk for 30 km at a sliding speed of 1.5 m/s and a load of 80 N

(2.6 MPa). The following wear rates were obtained: 0.43 x10^{-6} mm^3/N.m, 0.45 x10^{-6} mm^3/N.m and 0.46 x10^{-6} mm^3/N.m with an average wear of 0.45 x10^{-6} mm^3/N.m. The wear reproducibility was found to be within 7 % and this was deemed to be acceptable. Subsequently, single wear tests were performed on the pin-on-disk for 30 km under different loads and sliding speeds.

4.4.1 Friction and Wear Results

Dry sliding friction and wear tests performed on the pin-on-disk showed specific wear rates of between 0.1 and 1.3 x10^{-6} mm^3/N.m. These tests were carried out at sliding speeds of 1, 1.5 and 2.0 m/s and at different pressures ranging from 1 MPa to 5 MPa. The volume loss vs. sliding distance curves showed a bedding in and steady state wear regime as was found in the reciprocating wear tests. The glass fibre filled composites showed average wear values of about 0.4 x10^{-6} mm^3/N.m with the 25 % glass fibre+5 % $BaSO_4$ filled grade, PF2031, showing the highest wear rate of 1.66 x10^{-6} mm^3/N.m at 2.5 MPa. It would appear from the pin on disk studies that the factors that lead to a lowering in wear rates are the additions MoS_2, and the processing conditions of sintering and reprocessing. From figure 4.22 (b) it would also appear that increasing the MoS_2, content to about 6 % is further beneficial for wear even at the expense of glass fibre content, as grade PF 1717 has 6 % MoS_2, and 12 % short glass fibres. The solid glass bead filled PTFE grades showed wear rates that are comparable with the glass fibre filled PTFE whilst the hollow glass showed comparatively higher wear rates. It is also interesting to note that the hard hollow bead filled grades performs better than the soft hollow glass bead filled PTFE. The wear rates for the hard hollow glass beads, in turn, are very similar to the glass flake filled PTFE.

4.4.1.1 VARIATION OF WEAR RATE WITH LOAD

Table 4.7 shows the wear results performed on the pin-on-disk at a sliding speed of 1.5 m/s and at pressures ranging from 1 MPa to 2.5 MPa. The polymer grades that shows the lowest wear rate at a pressure of 2.5 MPa is listed at the top of each group. It would appear from table 4.7 that in this pressure range the wear rates did not seem to

increase with contact pressure. These results are similar in magnitude to those obtained with the reciprocating wear rig. The glass bead filled PTFE grades showed consistently higher wear rates under the loads used. The soft glass bead filled grade, T097/02, in particular showed a marked increase in wear from 1 MPa to 2.5 MPa. Above a pressure of 2.5 MPa, various composites showed signs of severe deformation and so tests were restricted to loads less than 2.5 MPa. The wear results in table 4.7 are summarised and plotted in bar charts in figure 4.22.

Table 4.7: Specific wear rates of PTFE composites under different loads'.

Material	*Pressure (MPa)*					*Filler*
	1.0	*1.3*	*1.7*	*2.0*	*2.5*	
	$\times 10^{-6}$	$\times 10^{-6}$	$\times 10^{-6}$ ($mm^3/N.m$)	$\times 10^{-6}$	$\times 10^{-6}$	
PFR1125	0.15	0.17	0.27	0.38	0.30	SGF
PFR1125+0.5	0.38	0.28	0.23	0.30	0.35	SGF
PF1125 IN	0.31	0.30	0.28	0.28	0.38	LGF
PF1125 PS	0.15	0.22	0.27	0.21	0.39	SGF
PF1125	0.46	0.29	0.45	0.41	0.46	SGF
BP6688 N	0.30	0.23	0.18	0.19	0.48	LGF
PF1125 BP	0.97	0.79	0.45	0.79	0.60	SGF
PF1727	0.37	0.22	0.22	0.60	0.69	SGF
PF1717	0.15	0.17	0.18	0.22	0.24	SGF
PF2226	0.38	0.23	0.36	0.53	0.42	SGF
PFR2226	0.38	0.46	0.32	0.55	0.55	SGF
PF2226 B	0.38	0.56	0.41	0.53	0.63	SGF
PF2031	0.30	0.45	0.64	0.95	1.66	SGF
T101-02	0.31	0.22	0.18	0.38	0.42	SGB
T103-02	0.38	0.55	0.59	0.73	0.76	GFL
T096/02	0.64	0.55	0.50	0.55	1.00	HHGB
T097/02	0.60	0.91	1.26	1.05	1.28	SHGB

' SGF = short glass fibre, LGF = long glass fibre, HHBG = hard hollow glass beads, SHGB = soft hollow glass beads, SGB = solid glass beads and GFL = glass flakes.

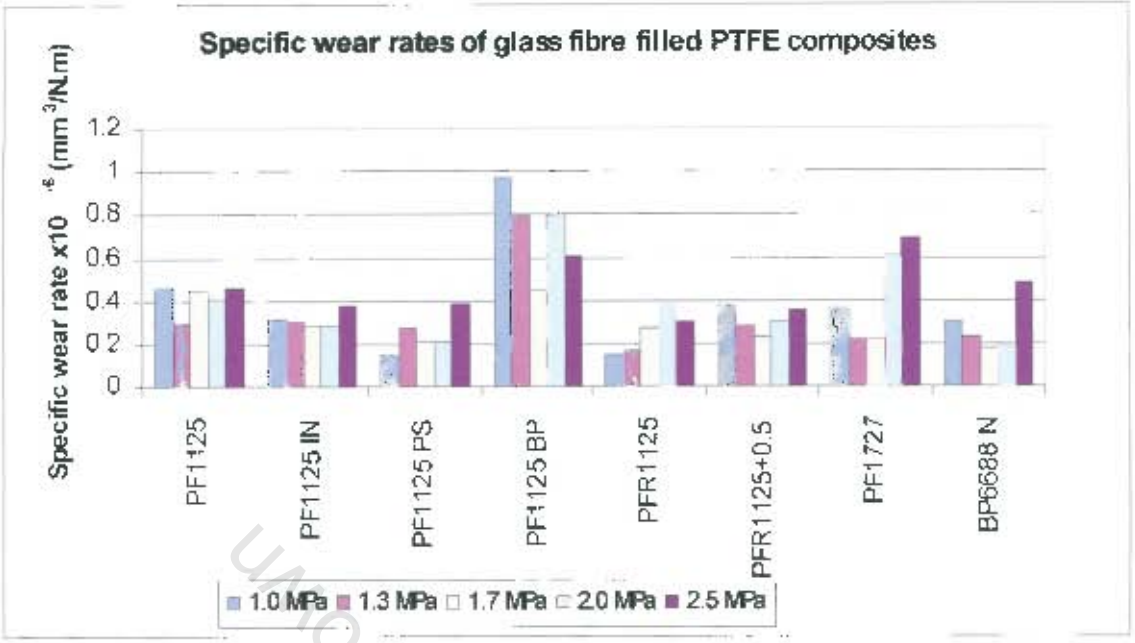

(a)

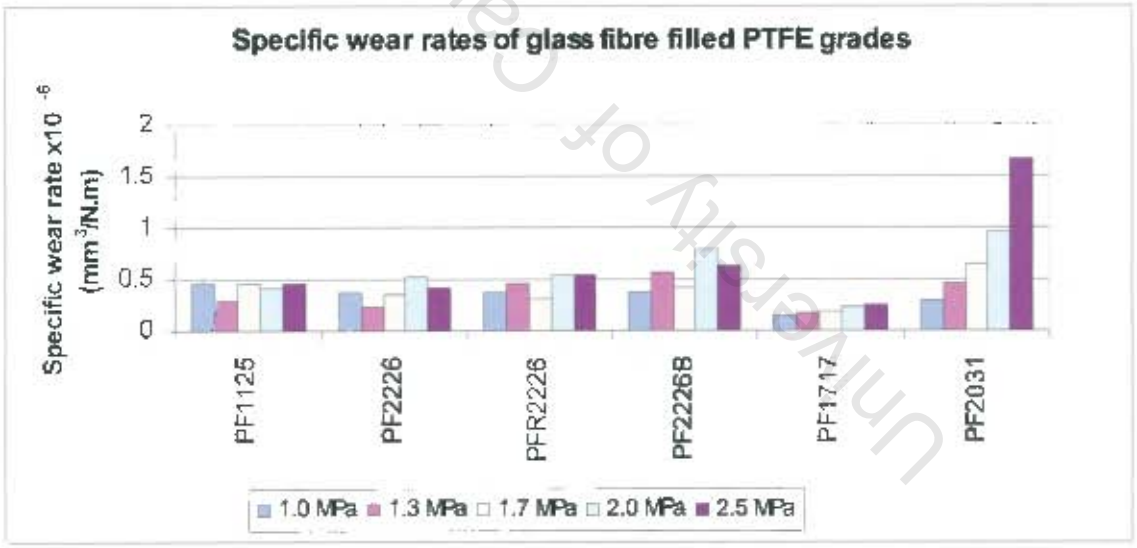

(b)

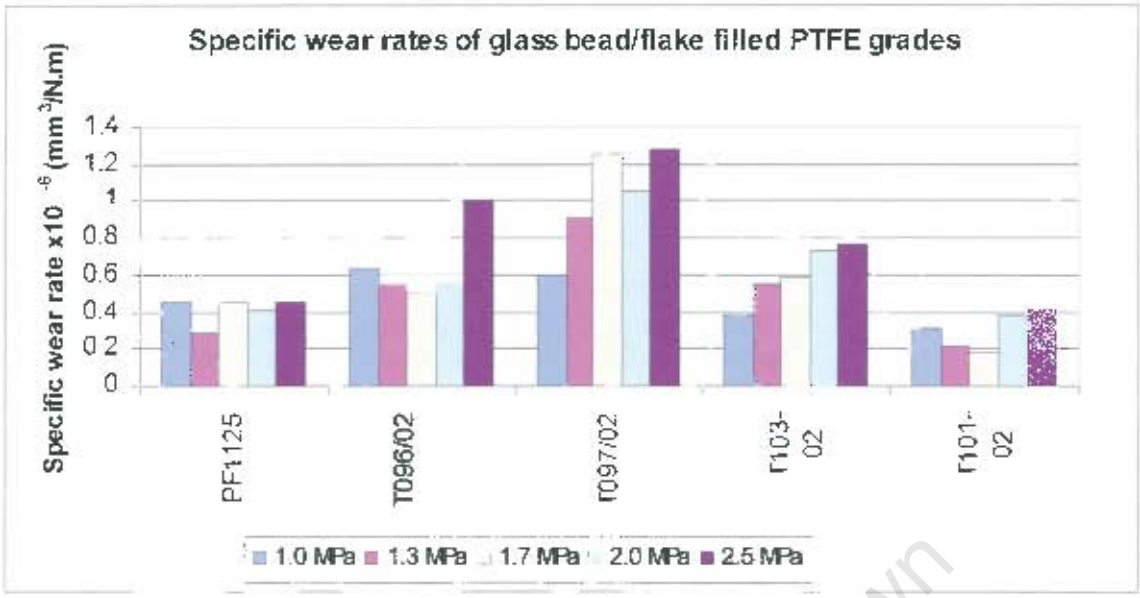

(c)

Figure 4.22: Bar chart representations showing the wear results of (a), (b) glass fibre filled PTFE and (c) glass bead/flake filled PTFE under different pressures.

4.4.1.2 VARIATION OF WEAR RATE WITH SLIDING VELOCITY

The wear rates of selected materials at a pressure of 1.7 MPa (50 N) at three different velocities were investigated and the results are plotted in figure 4.23. The effect of velocity on wear is not clear from these results and that some composites, such as PF1727 showed marginal increases in wear while others showed variable results. PF2031 and PF1125 BP, showed comparatively higher wear rates of up to 0.84×10^{-6} $mm^3/N.m$ compared with other PTFE composites that showed average wear rates of 0.30×10^{-6} $mm^3/N.m$ at 2 m/s. Further tests wear tests were conducted at much higher loads to establish the '***pv*** limits' of reprocessed PTFE grades that are used in this study. The reprocessed grades were first compression moulded and free sintered as described in chapter two. The billets were then pressured sintered.

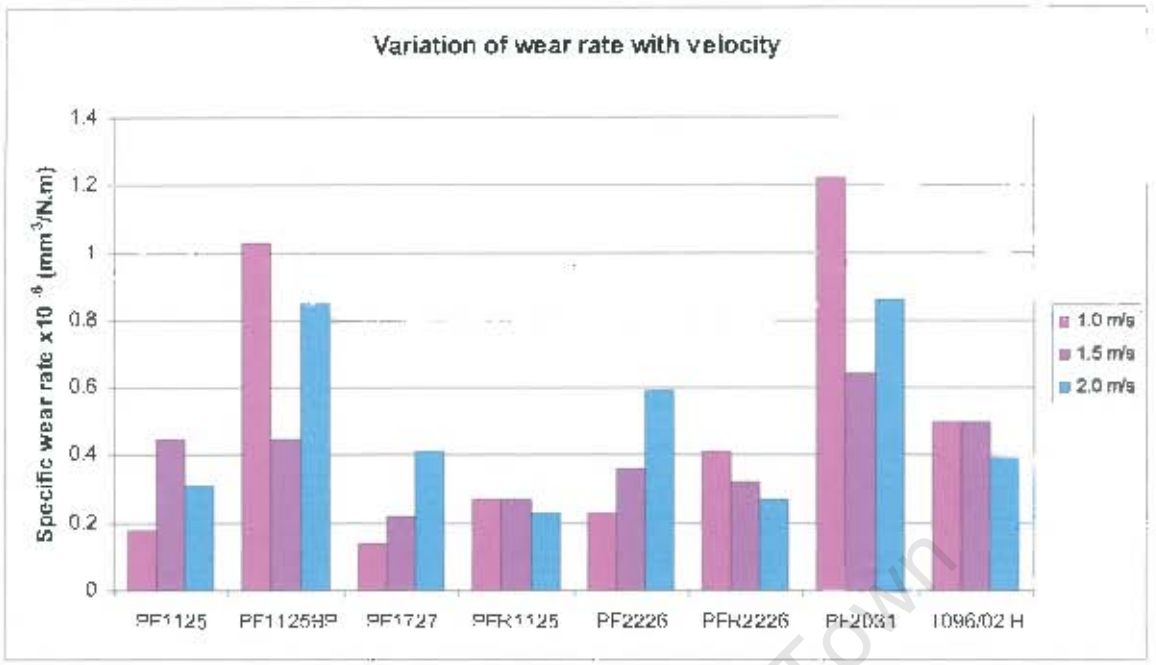

Figure 4.23: The variation of wear rates with sliding velocity for different glass filled PTFE composites.

4.4.1.3 THE PV LIMITS OF REPROCESSED GRADES

Wear tests were undertaken at much higher loads for the reprocessed grades to establish their ***pv*** limits. Since the ***pv*** limit or limiting ***pv*** depends on the sliding velocity and the pressure, the sliding speed was initially held constant at 1.5 m/s and the load was varied between 1 MPa and 5 MPa. The friction and wear results obtained for such tests are shown in table 4.8, with PF1125 grade used only for comparison purposes. These results are plotted in bar charts shown in figures 4.24 and 4.25.

Table 4.8: The wear rates of the reprocessed composites under different pressures.

Material	*Pressure (MPa)*								
	1	*1.3*	*1.7*	*2*	*2.5*	*3*	*3.5*	*4*	*5*
PF1125	0.46	0.29	0.45	0.41	0.46	0.41	0.45	0.54	0.67
PFR1125	0.15	0.17	0.27	0.38	0.30	0.34	0.32	0.33	0 36
PFR1125+0.5	0.38	0 28	0 23	0.30	0.35	0 35	0 32	0.30	0 38
PF2226	0 38	0.23	0.36	0.53	0.42	0.44	0.62	0.58	0.61
PFR2226	0.38	0 46	0.32	0.55	0.55	0.66	0.55	0.50	0.55
Vesconite	3.1	3.55	3.8	3.31	4.65	5.30	6 1	10.6	
Material	Dynamic coefficient of friction								
PF1125	0.24	0.21	0.19	0.17	0 21	0 17	0.19	0 17	0.18
PFR1125	0.14	0.19	0.17	0.18	0.19	0.19	0.19	0.17	0.18
PFR1125+0 5	0.29	0.25	0.24	0.21	0.19	0.2	0.18	0.18	0.2
PF2226	0.19	0.21	0.21	0.24	0.22	0.2	0 2	0.18	0.19
PFR2226	0.24	0.26	0 24	0 23	0.26	0 2	0 19	0.19	0.22
Vesconite	0.26	0.25	0.28	0.30	0.30	0.31	0.34	0.28	

The wear rate of reprocessed PTFE composites showed no rapid increase in wear as the load was steadily increased. Instead, the polymer pins were heavily deformed when a nominal pressure of 4 MPa was used at a sliding speed of 1.5 m/s. However, when the sliding speed was increased to 2 m/s, all the reprocessed PTFE composites showed signs of severe deformation above a nominal pressure of 2.7 MPa. There was, however, no drastic increase in wear above this pressure as can be seen in table 4.9. Vesconite, on the other hand showed higher wear rates compared with PTFE grades at all values of load used. Figure 4.26 shows the variation of wear rate of this material with an increase in load or ***pv***. This figure shows that Vesconite could usefully be used below 3 MPa x m/s. Above this value, the wear rate of Vesconite seems to increase very rapidly.

Table 4.9: **The dry sliding wear results of the reprocessed PTFE composites slid against the stainless steel counterface on a pin-on-disk at a sliding speed of 2 m/s[*].**

Reprocessed grades	*Pressure (MPa)*			*Filler*
	2.3	*2.6*	*3.5*	
	$mm^3/N.m$ $x10^{-6}$	$mm^3/N.m$ $x10^{-6}$	$mm^3/N.m$ $x10^{-6}$	
PFR1125	0.36	0.46	0.50	SGF
PFR1125+0.5	0.33	0.31	0.42	SGF
PF2226	0.59	0.67	0.55	SGF
PFR2226	0.80	0.51	1.02	SGF

[*] SGF = short glass fibre.

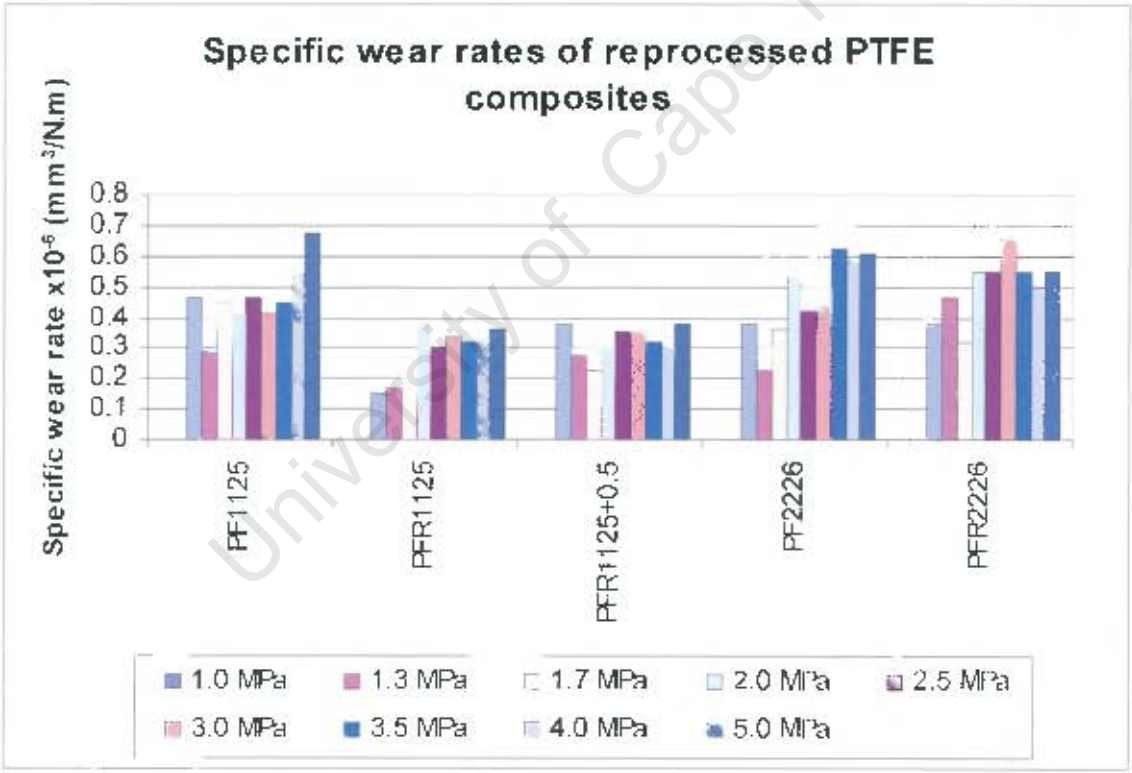

Figure 4.24: **The variation of wear rates of reprocessed PTFE composites with load.**

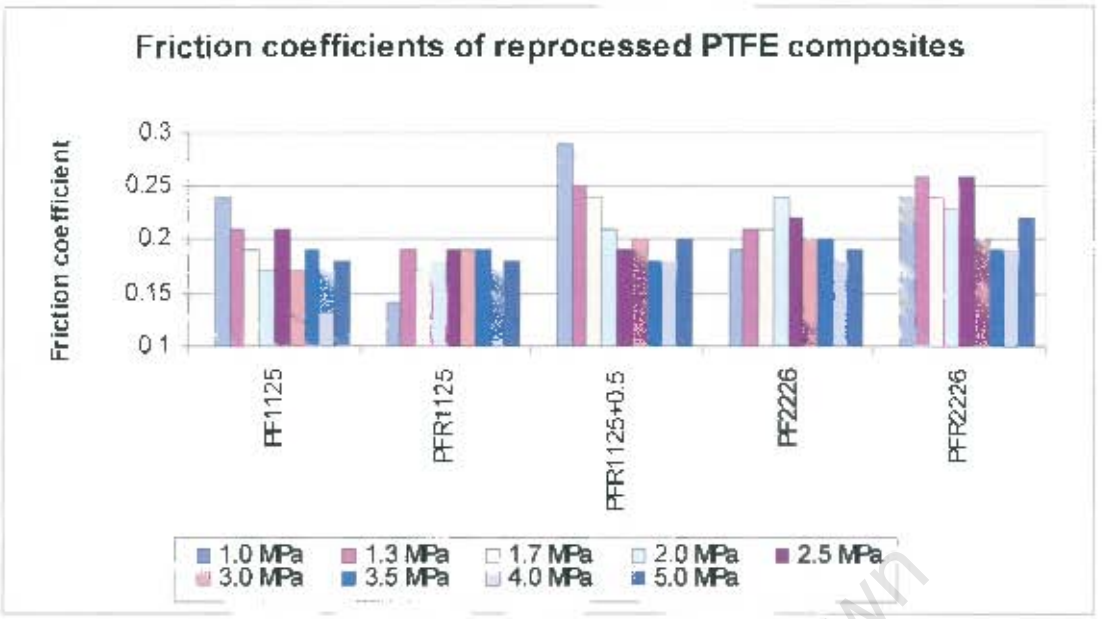

Figure 4.25: The variation of friction coefficients with applied load.

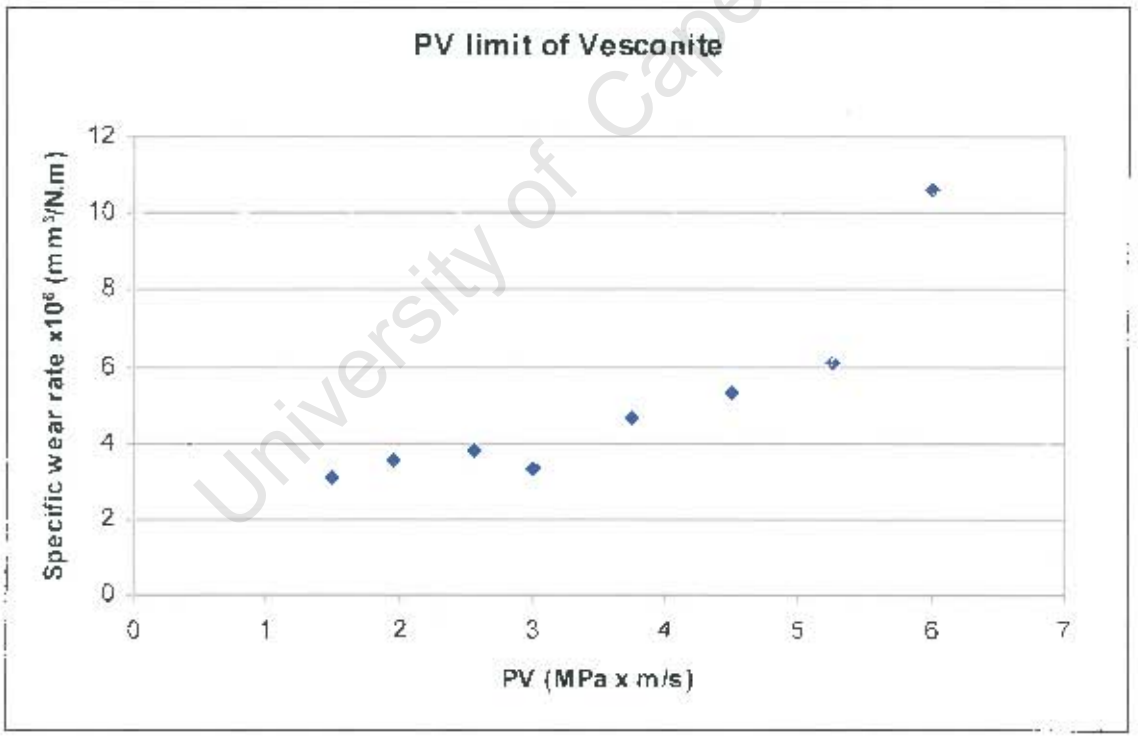

Figure 4.26: Illustration of the *pv* limit of Vesconite.

4.4.1.4 MICROSCOPY

Scanning electron microscopy was further used to characterise the worn composite pins. Figure 4.27 shows the SEM micrographs of different PTFE composites after the sliding. The figure again shows that during sliding, the glass fibres break prior to debonding and pull out. Figure 4.27 (c) and (d) clearly shows that the interfacial bond between the glass beads and the polymer matrix is weak and therefore leads to bead debonding. During the sliding process the glass flakes get exposed to the metal counterface as the relatively soft polymer matrix is worn away. Figures 4.27 (e) and (f) show the SEM micrographs of the unworn glass flake filled PTFE composite and a micrograph after the sliding process, respectively. Figure (g) and (h) show the SEM micrographs of unworn PTFE pin surface and a worn BP6688 N after sliding, respectively.

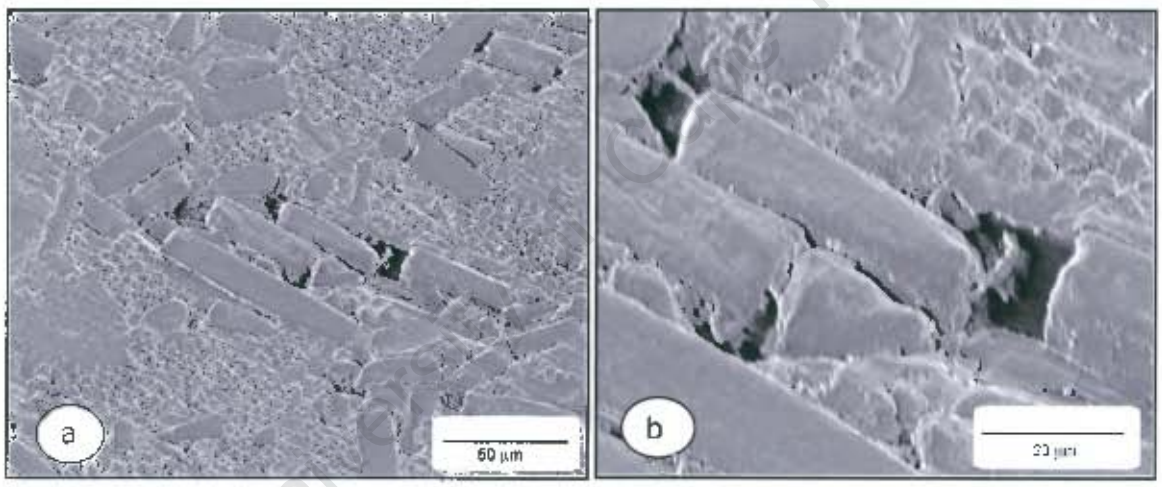

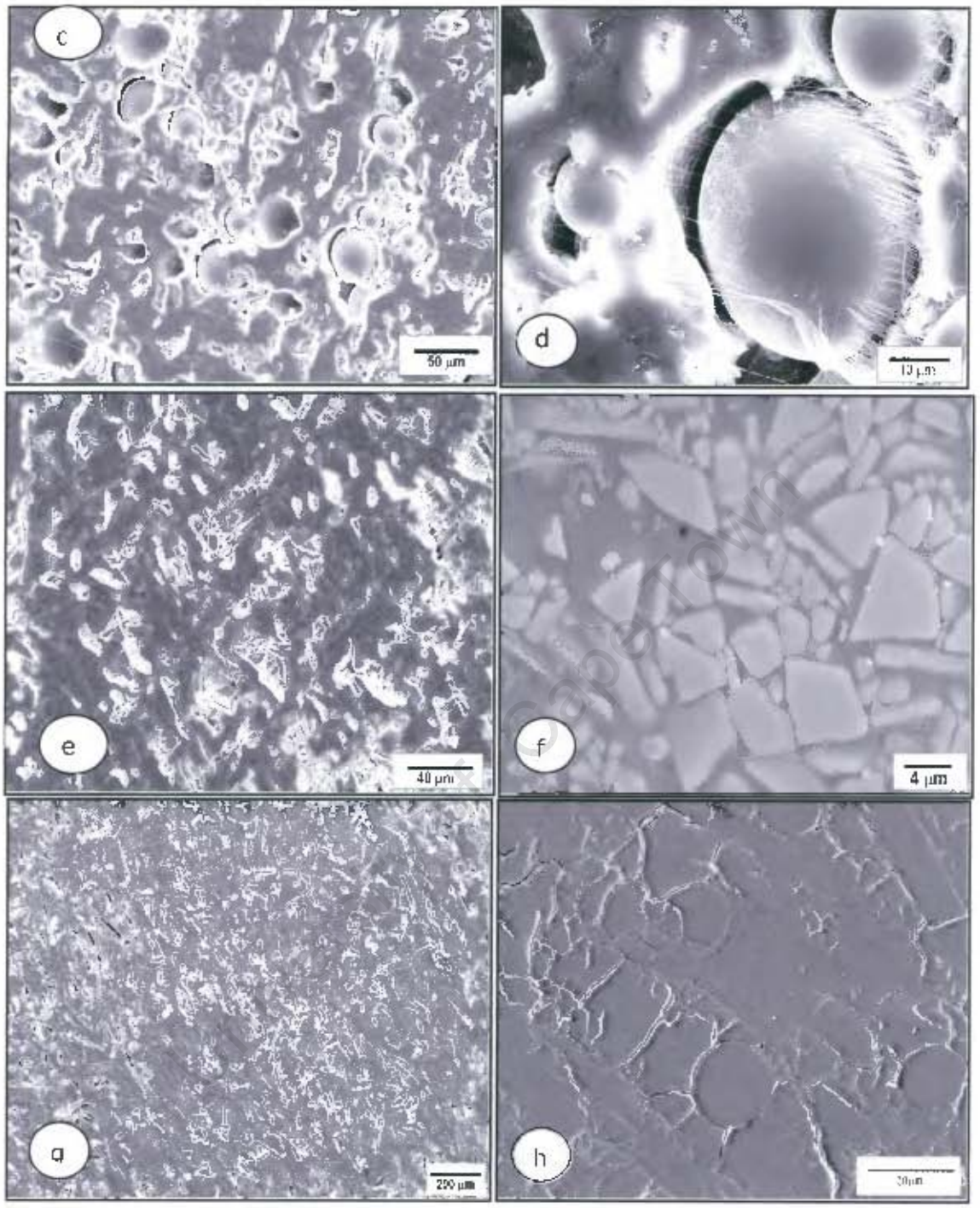

Figure 4.27: **SEM micrographs showing (a) PF2226 after sliding 30 km, (b) the surface image at higher magnification, (c) and (d) solid glass beads in T101-02, (e) T103-02 (bulk) and (f) T013 after sliding 30 km at 1.5 m/s and 2 MPa, (g) and (h) are micrographs of BP6688 N before and after the sliding process, respectively.**

4.5 LUBRICATED SLIDING WEAR TESTS

Sliding wear results for tests performed in distilled water are shown in table 4.10. The table illustrates the dry sliding wear results represented in table 4.7 for comparison purposes. The tests also show that the wear results of Vesconite and Vesconite hilube are very low in water. The transfer film formation was inhibited by the distilled water, and an inspection of the counterfaces after the sliding process revealed featureless surfaces. Figure 4.28 shows the optical micrographs of the metal counterface after sliding against glass fibre filled PTFE and Vesconite.

Table 4.10: Lubricated sliding wear results of selected materials.

Material	*Pressure (MPa)*							*Test condition*
	1.3	1.7	2	2.5	3	3.5	4	
			$x10^{-5}$ $mm^3/N.m$					
BP6688 N	0.23	0.18	0.19	0.48				dry
			7.78					water
BP6688 N PS	0.24	0.25	0.20	0.26				dry
PF1125	0.29	0.45	0.41	0.46	0.41	0.45	0.54	dry
			9.00					water
Vesconite	3.55	3.80	3.31	4.65	5.30	6.10	10.60	dry
			1.06					water
Vesconite hilube	0.07	0.31	0.48	0.41	0.80	0.73	0.83	dry
			0.57					water

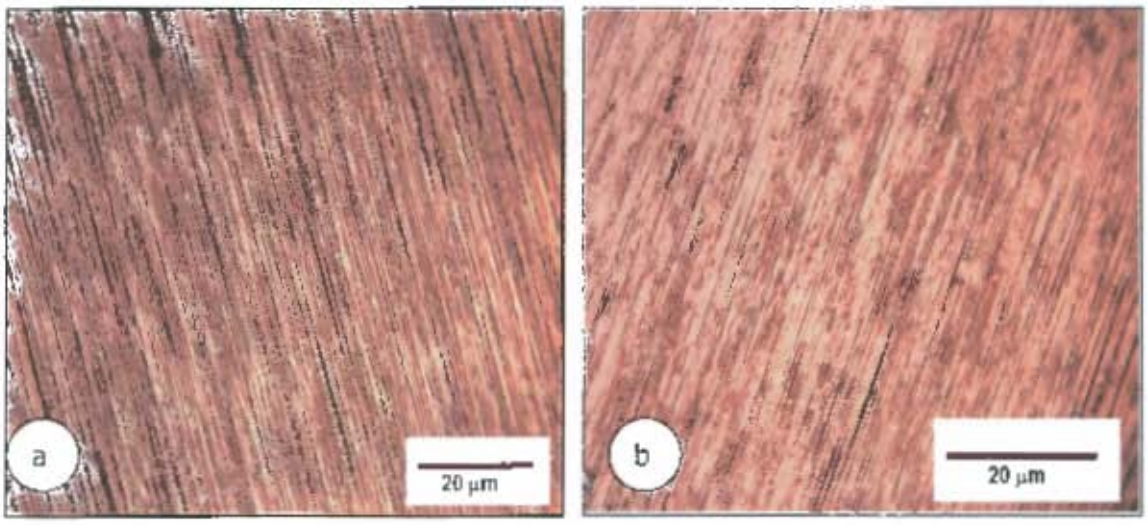

Figure 4.28: **The optical micrographs of the stainless steel counterface after being worn in distilled water against (a) PF1125, (b) Vesconite.**

CHAPTER 5

DISCUSSION

FRICTION AND WEAR

5.1 INTRODUCTION

Due to an increasing demand to design and select materials that will perform better under constantly changing industrial conditions, an understanding of the properties that influence material behaviour is critical. In particular, rapid advances in technology enables the use of new materials to replace traditional materials in applications such as bearings and seals. The performance of these tribological components in service is governed by friction and wear. Thus, understanding the factors that govern the wear process may be useful not only in material selection but also in the consideration of modifying the existing materials so as to enhance their service lives. Therefore, this chapter describes systematically how the salient tribological parameters such as bearing pressure, sliding velocity, counterface roughness, lubrication and filler influence the friction and wear of a glass filled PTFE/stainless steel sliding couple. Details on the morphological changes that occur in the polymer surface layers and the modifications of the stainless steel counterface by the transfer film are also discussed.

5.2 PRIMARY WEAR MECHANISMS

5.2.1 DRY SLIDING WEAR

The variation in volume loss of the PTFE composite materials with sliding distance in dry sliding showed two distinct regimes, a high initial wear regime and a steady state wear regime. The wear regimes were clearly visible from the volume loss versus sliding distance curves for composites slid against a metal counterface with a roughness of 0.2 μm R_a. The high initial wear regime or the bedding-in stage was characterised by abrasive and adhesive wear. The polymer that is worn from the composite pin is either removed from the pin/metal interface as wear debris or adheres onto the counterface as a transfer film. The transfer film is postulated to form through high contact pressures between the initial and relatively clean metal counterface and the polymer composite pin. The initial transfer film is caused by a shearing process which is aided by the orientation of polymer molecules in the surface layers in the sliding direction. As more and more polymer is sheared, the metal counterface is modified by polymer fragments that fill the metal asperity valleys.

As the polymer fragments fill the asperity valleys of the metal counterface, the area of contact increases. The shearing process continues for several traversals, and in the process forms a much thicker non-uniform and patchy transfer film (refer to figure 4.6). However, as more polymer is sheared and deposited onto the metal counterface, the fillers are exposed to the stainless steel surface that is rapidly being transformed. Fillers are broken down during this stage of the sliding process forming small fragments that aid and enhance the formation of an adherent transfer film. During the steady state regime of wear, shearing of material by adhesion still continues but the transfer film is much more uniform and coherent. Thus, sliding wear takes place between the polymer pin and the transfer film that is covering the metal counterface. Using a transmission electron microscope (TEM), Marcus showed that ductile deformation accompanies the adhesive wear process[50]. Two main processes, viz. adhesion and deformation, govern the friction process.

$$F = F_{adhesion} + F_{deformation} \quad [5.1]$$

However, the contribution of each component is difficult to ascertain. The adhesion component of friction is due to the formation and rupture of interfacial adhesion bonds. When the transfer film is formed on the metal counterface the adhesion component of friction drops. The deformation component of friction occurs due to the deformation that occurs during the sliding process with the mechanical energy dissipated through plastic deformation effects. Friction plots showed a similar behaviour to those of volume loss versus sliding distance. The drop in the coefficient of friction therefore seems to be concomitant with a decrease in wear during the steady state region of wear (see figure 4.4).

5.2.2 Water-Lubricated Sliding Wear

The wear results obtained under water lubrication show no adherent transfer of polymer material onto the metal counterface except for polymer lumps deposited at the end of the stroke due to a decrease in the sliding speed and increase in static coefficient of friction. The transfer of polymer onto the counterface is characterized by the shearing of thin films off the polymer pin. Abrasive wear however, seems to be the dominant wear mode throughout. The hard metal asperities that are exposed by the water lubricant plough shallow grooves into the soft polymer pin surface. The abrasive glass fibres that are loosely bound to the PTFE matrix, debond and pull out of the matrix. As sliding progresses, the fibres are further broken down into smaller fragments that act as a third body between the polymer composite pin and the metal surface. The solid glass fragments therefore initiate third-body abrasion which results into even high wear (see figure 4.21). Tanaka argues that the high wear rate for glass fibre filled PTFE in water is due to the easy separation of glass from the polymer matrix[11]. He also claims that water molecules permeate to the interface between the filler in the surface layer of the composite and the PTFE matrix. The hydrophobic nature of glass aids in the separation of the glass from the PTFE matrix resulting in high wear rates.

5.3 Factors Affecting the Friction and Wear of PTFE

5.3.1 The Transfer Film

The formation of a thin, adherent and coherent transfer film was shown to be essential in reducing the wear of PTFE-based composites. The unfilled PTFE showed a coherent but non-adherent transfer onto the stainless steel counterface. The transfer of unfilled PTFE onto the metal counterface has often been thought to be due to destruction of the banded structure since the thickness of a transfer film formed by PTFE is about 20 nm which corresponds to the thickness of the crystalline slices. In his studies on friction and wear of PTFE, Tanaka surmised that the film formation occur via slip between these slices[11]. According to Tanaka the addition of fillers in the PTFE matrix therefore prevents the destruction of the banded structure and reduce wear. However, this unique banded structure of PTFE has been called into question by some researchers[87]. Researchers seem to agree that the low shear strength PTFE transfer film occur via orientation of individual molecules. It has been shown in this study that the glass fillers get exposed during the sliding process due to the preferential transfer of PTFE on the stainless counterface.

5.3.2 The Effect of Fillers on Wear and Friction of PTFE

The specific wear rate of unfilled PTFE obtained from the reciprocating sliding wear rig was found to be of the order of 10^{-3} $mm^3/N.m$. The low coefficient of PTFE is also reported by various researchers and is attributed to the ability of the extended chain linear structure of PTFE to form on a mating counterface during sliding[13,15,21,26]. The repetitive formation and destruction of the film results in high wear rates as shown by Lancaster[53]. The addition of glass fillers improved the wear rate of PTFE three fold and also significantly enhanced the hardness (27 % increase) as well. The hardness values obtained for these polymer grades are listed in figure 3.1. Wear values of the order of 10^{-6} were therefore obtained in dry sliding. The friction of PTFE on the other hand does not seem to be much affected by the filler addition. It is well documented in literature

that fillers improve the wear of PTFE as described in section 5.3.1[94]. The exposure of the glass fillers on the metal counterface does not seem to affect the transfer film formation but modify it. Blanchet and Kennedy have shown that the transfer film is the sole wear reducing mechanism of PTFE and PTFE composites. They further proposed that the filler materials embedded in the PTFE matrix reduce the subsurface deformation and interrupt crack propagation. The transfer film forms that forms on counterface exposed glass fillers across the counterface and provide a low coefficient of friction.

5.3.3 The Effect of Glass Form

The results show that the glass fibres are more effective in reducing the wear of PTFE than the hollow beads and glass flakes. Long glass fibres, in particular show excellent wear results. This could be due to the fact that because of their length, long fibres are tightly bound to the matrix so it is not easy for them to debond and pull out. In other words, the energy required to debond the long fibres and pull them out of the PTFE matrix is high.

During the sliding process, the glass fibres break and form small glass fragments that aid in the mechanical interlocking process by forcing the polymer into the asperity valleys of the metal surface. As sliding continues the glass fibres seem to abrade the counterface as illustrated in figure 4.6 (c) until the polished surface is smooth. The solid glass beads bead filled composites showed good wear rates which are comparable to those of glass fibre filled PTFE in magnitude. The hollow glass beads seem to crumble and crush during the sliding process forming a dense film on the stainless steel counterface. If the applied load is low, the beads may debond from the PTFE matrix and the loose beads plough grooves in the soft PTFE matrix as illustrated in figure 5.1. Figure 5.1 shows a SEM micrograph of hard hollow glass bead filled PTFE after the sliding process. However, solid glass beads filled PTFE composites resulted in thin transfer films which is much similar to that formed by glass fibre filled PTFE materials.

The wear mechanism of glass bead filled PTFE is described by Briscoe and Steward as resulting from the high stresses that develop between the beads and the metal

counterface which could provide suitable mechanical and chemical interactions and allow the polymer to adhere strongly to the metal counterface[95]. The glass flakes that have an aspect ratio of between that of glass beads and glass fibres also showed excellent wear results especially at low sliding speeds and low loads. It is not clear from the experiments undertaken why and how the flake form of glass behave this way. Lancaster proposed that the addition of high aspect ratio inorganic fillers such as glass fibres to PTFE reduce the wear by preferentially supporting the load[96]. Low aspect aspect ratio fillers should therefore produce poor wear resistance since they are ineffective in carrying the load. The work carried out by other researchers however shows otherwise. Particulate and lamellar fillers such as MoS_2 and graphite have been shown to produce good wear results[13,73,97].

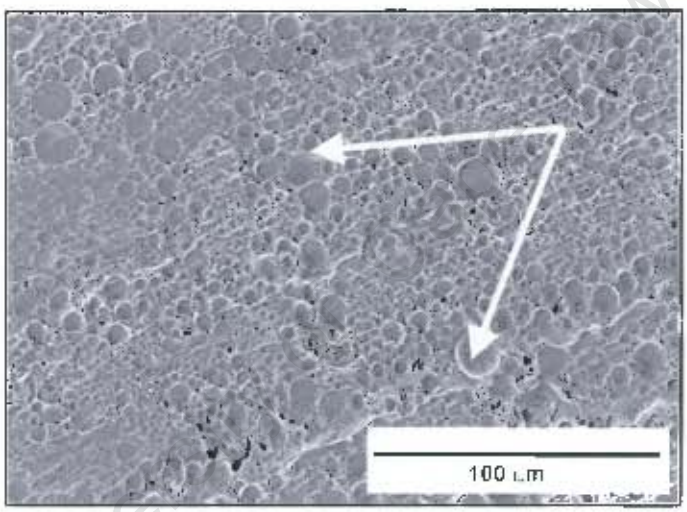

Figure 5.1: SEM micrograph of T096/02 (hard hollow glass bead filled PTFE) after being rubbed against the stainless steel counterface. The arrows show the space left by beads and the shallow grooves they left on the polymer pin.

5.3.4 The Effect of Additives

The addition of additives to glass filled PTFE showed mixed results. Of the two additives used, MoS_2 seems to be effective in reducing both wear and friction of glass fibre filled PTFE whilst $BaSO_4$ does not show any improvement. MoS_2 seems to reduce the wear of

PTFE by deposition on the counterface effectively reducing the abrasive action of glass fibres and maintaining a low friction film. X-ray photoelectron spectroscopy, which was carried out to correlate the tribological behaviours with the tribo-chemical characteristics, show that MoS_2 actively interact with the metal counterface in the process forming chemical bonds (refer to figure 4.16). Therefore, in addition to the mechanical interlocking of polymer fragments into the asperity valleys of the metal, chemical bonds aid in the formation of an adherent polymer film.

5.3.5 The Effect of Pigments

Three different types of pigments were used in this study, namely, cobalt zinc aluminate, cobalt chromium aluminate and carbon. Pigments are generally added to the polymeric materials to give aesthetic appeal but may impart other properties as well. The experimental results, however, show that the addition of a pigment can either slightly improve or worsen the wear behaviour of glass fibre filled PTFE. The addition of cobalt zinc aluminate to the short glass fibres filled PTFE (represented by PF1125) gives a new grade with the code PF1125 BP. The cobalt chromium aluminate is used for PF2031 while carbon is used for PFR1125+0.5, PF2226, PF2226 B, and PFR2226 as shown in figure 3.1. PF1125 BP showed high wear rates under low and high pressures on the pin-on-disk. At low sliding speeds illustrated by the reciprocating rig, the wear of PF1125 BP was still high but comparable in magnitude to that of PF1125. This is probably due to the way the pigment coats the glass fibres. Figure 5.2 shows the difference in microstructure between PF1125 and PF1125 BP. The glass fibres shown on PF1125 seem to be firmly attached to the matrix while in PF1125 BP loose glass fragments on the polymer pin surface are represented by the arrows. In addition, fibre pull-out is clearly illustrated by the space left by the glass fibres.

Cobalt chromium aluminate seems to affect the wear of glass filled PTFE in a similar fashion. Thus, both PF1125 BP and PF2031 showed high wear rates with correspondingly high coefficient of friction values. Carbon does not seem to improve or reduce the wear rate of PTFE grades. No discernible trends were observed in terms of how friction or wear rate vary with load for grades that had this pigment. Although

rate vary with load for grades that had this pigment. Although cobalt zinc aluminate coats the glass fibres, it appears as if it also further weakens the interfacial bond between the glass fibres and the PTFE matrix. As a result, during the sliding process the glass fibres are easily debonded from the polymer matrix. Therefore, fibre pull-out is the main mechanism of wear resulting in high wear rates. Figure 4.11(a) and figure 5.2(b) clearly illustrate this. The arrows in figure 5.2 show loose and debonded glass fibres ready to pull-out of the matrix.

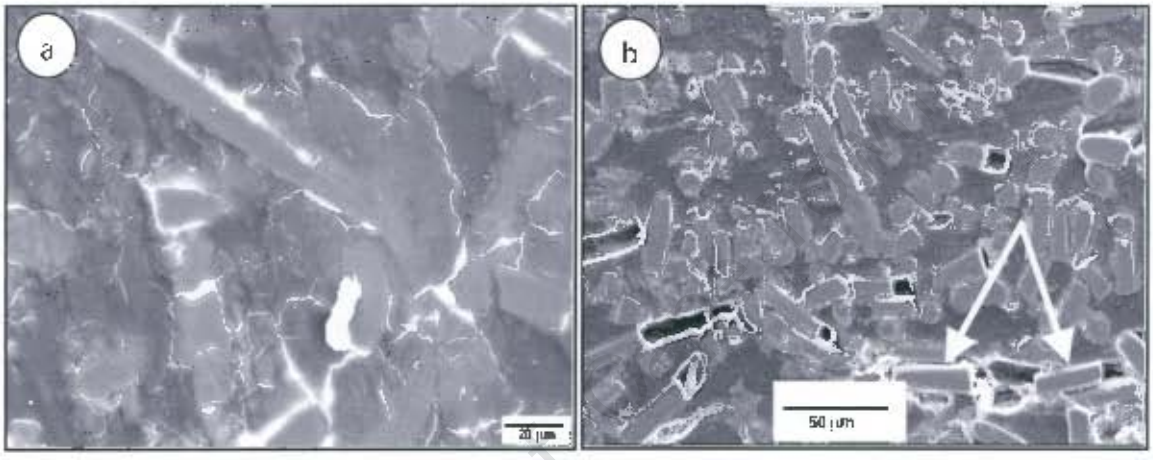

Figure 5.2: SEM micrograph depicting the difference between PF1125 and PF1125 BP. In (b) for PF 1125 BP the fibre pull out mechanism is more evident.

5.3.6 The Effect of Contact Pressure

The specific wear rate of glass filled PTFE composites were found to increase with an increase in nominal pressure under dry and water lubrication. The increase in wear for PTFE composites in water is thought to be due to the ineffectiveness of water film in supporting the load at load lower pressures. Under dry sliding conditions, the wear of PTFE composites increased by more than 50 % between 2.6 MPa and 6.4 MPa. The friction coefficient on the other hand, decreased slightly under the identical sliding conditions. This decrease in friction coefficient could be explained by the viscoelastic

nature of PTFE. Since the deformation is partly elastic, and for an elastic contact the real area $A_r \alpha W^n$ where $n < 1$, then the friction coefficient μ, is proportional to W^{-n}.

5.3.7 The Effect of Sliding Speed and Temperature

Since the thermal conductivities of polymers are low, frictional heat that arises during the sliding process may not be readily dissipated leading to high flash temperatures and subsequently deformation of the polymer surface pin. The sliding speeds employed in this study were fairly low and comparable to those that encountered in industry for polymer bearings. Since the effect of sliding speed is interrelated to the temperature generation at the interface, it is difficult to isolate its effect on wear. Therefore, speeds of between 0.2 m/s and 2 m/s were used in the current study. Although the wear tests were carried out at room temperature, the temperature rise due to frictional heating at the polymer / stainless steel interface was constantly monitored. The maximum surface temperature that was measured was 39 °C. The total surface are at the interface is the combination of this temperature and the flash temperature at the asperity tips. However, the flash temperatures cannot be measured directly but can only be estimated by making prior assumptions. Therefore, different researchers have come up with different ways of measuring these temperatures but the Lancaster equation for calculating flash temperatures for the case of a polymer sliding against steel were used in this study. A simplified mathematical model put forward by Lancaster can be presented as follows:

$$\theta = 2.86x10^{-2}\mu_d P^{0.5}{}_m W^{0.5} V \qquad [5.2]$$

where

θ is the flash temperature

μ_d is the dry friction coefficient

W is the normal load

V is the sliding speed and

P_m is the indentation hardness

The above equation assumes that the load is supported by a single plastically deformed asperity. However, this does not happen in practice as a number of asperities are known to carry the load thereby increasing the real area of contact. The equation further assumes that the indentation hardness is independent of temperature but experimental results show the contrary. Lancaster, for example has shown that hardness decreases with temperature, and thus affecting the real area of contact causing it to decrease with temperature.

5.3.8 The Effect of Processing

The pressure sintered PTFE composites that were used in this study seem to show better wear results than the compression moulded specimens. Thus processing appears to have an effect on the wear behaviour of PTFE composites. The pressure sintered PTFE grade PF1125 PS showed the lowest wear rates for pressures between 1 MPa to 6.4 MPa, and did not seem to increase much with pressure in this range. The reciprocating wear rate of PF1125 PS was 37 % better than that of PF1125 under a contact pressure of 6.4 MPa. The low wear rates exhibited by this grade at low sliding speed (0.2 m/s) and a moderate speed (1.5 m/s) prompted a further study on a similar grade, BP6688 N PS. This grade showed low wear rates but not as low as that shown by BP6688 N and PF1125 PS.

The effect of processing seemed to be less significant at high pressure greater than 4 MPa as the pressure sintered PTFE grades showed similar and high wear rates at pressures above this. Reprocessing seemed to have no significant effect on the wear behaviour of glass fibre filled PTFE. The reasonably low wear rates and coefficient of friction exhibited by these grades under low pressures (< 3 MPa) diminished at higher pressures probably due to the polymer material start losing shape. It was also noted that the addition of the carbon pigment to the glass fibres before sintering had a positive effect on the wear rate of PFR1125+0.5.

5.4 Friction and Wear Behaviour of PTFE

The coefficient of friction of unfilled PTFE is slightly lower than when glass fillers were incorporated. The average steady state coefficient of friction of 0.18 was recorded for the pin-on-disk as well as the reciprocating wear rigs. This low coefficient of friction is in agreement with that in the literature. The wear rate of PTFE, on the other hand drastically decreased when the glass fillers were used. The XPS showed the presence of elements such as molybdenum on the stainless steel counterface rubbed against BP6688 N, indicating that in addition to the mechanical interlocking of polymer fragments into the counterface, chemical reactions between the filler/additive and the counterface occurs. This aids in the adherence of the transfer film to the metal counterface. However recent studies carried out by various researchers on the wear of PTFE against steel, show extremely complex chemical reactions occurring at the polymer / metal interface[64,65]. Apart from the chemical shifts of F1s, C1s and O1s peaks they found unknown oxygen-containing compounds on the metal counterface. Jintang proposed that during the sliding process, the PTFE chains break and form active radicals that can lead to a series of chain reactions[62]. Figure 5.3 shows the wear rates of different materials conducted on the pin-on-disk at 1.5 m/s and 1.7 MPa under dry sliding conditions. The figure clearly shows that the wear rate of bronze filled PTFE (PF1260) is much higher than that of other materials. Vesconite hilube shows the lowest wear rates under these conditions

The wear studies carried out in distilled water reveal high wear rates for glass filled PTFE. This could be explained by appreciating that during sintering the filler is bonded to the PTFE matrix only by means of mechanical bonds. This coupled with the fact that PTFE does not really melt means that the filler is loosely bound to the PTFE matrix. Therefore, in water the water molecules easily separate the glass fillers from the matrix resulting in high wear rates. Marked increases in wear was particularly noted for PF1125 in water compared with dry sliding. Vesconite and Vesconite hilube, on the other hand show excellent wear results compared with glass filled PTFE in water.

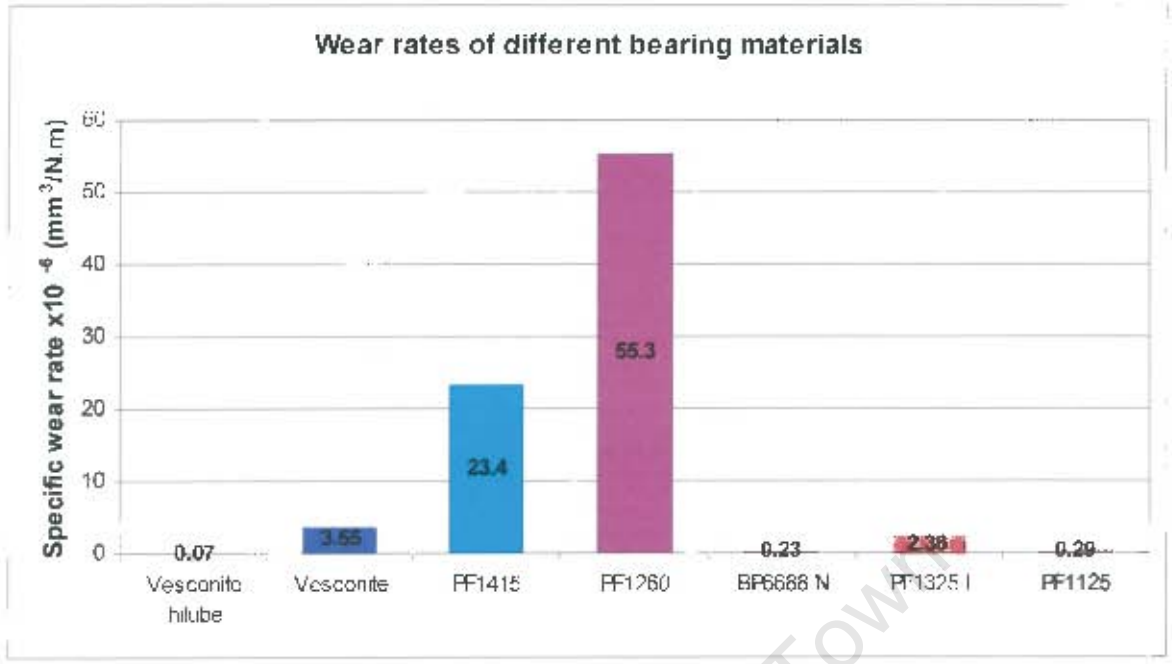

Figure 5.3: **A comparison between the wear of glass fibre filled PTFE and materials with other bearing materials.**

5.4.1 THE *PV* LIMITS

The ***pv*** limit of glass fibre filled PTFE at 1.5 m/s seemed to be about 6 MPa.m/s under dry sliding conditions. This means that components made from the glass filled PTFE could be used up to 4 MPa at 1.5 and this should not be exceeded as heavy deformation of the grades were observed above this pressure. However, when the sliding speed was increased to 2 m/s the reprocessed grades tested deformed heavily above a pressure of 2.6 MPa. Thus the ***pv*** limit is reduced to 5.2 MPa.m/s. This could be due to thermal softening at the interface. The stress level played a key role in terms of limiting the sliding performance of the PTFE grades in that no drastic increase in wear was observed at the velocities employed. It is difficult to assess the effect of temperature and pressure alone, as temperature (due to an increase in sliding velocity) affects the load at which the material creeps. This work agrees, however, that the ***pv*** limit must be specified in terms of velocity. Vesconite on the other hand, showed high wear rates at a sliding speed of 1.5 m/s and deformed above a pressure of 2 MPa. The wear rate of

Vesconite increased drastically above 3 MPa x m/s prior to heavy deformation. Thus, the ***pv*** limit of Vesconite was estimated to be about 3 MPa.m/s at 1.5 m/s.

5.4.2 Worn Surface Analysis

Optical microscopy and scanning electron microscopy revealed that the transfer film plays a critical role in the friction and wear of glass fibre filled PTFE. The dry sliding wear tests performed on both wear rigs showed that due to the crushing and crumbling of hollow glass beads a much thicker film is formed on the stainless steel counterface. This film resulted in equally high friction as well as high wear rates for both grades of hollow glass beads (see figure 4.11 (c)). The wear rate was more pronounced for the soft hollow glass beads filled PTFE grade, T097.02. Since the soft hollow beads do not impart much strength and hardness to the polymer matrix, it is postulated that even though shearing of large sheets of polymer are prevented, the lack of the afore-mentioned properties cannot prevent the shearing of significant amount of polymer from the pin surface during the sliding process.

The long glass fibres seems to be more efficient in reducing wear of PTFE than the short fibres even though the difference is marginal. It is thought that the long fibres achieve this by effectively rubbing and polishing the counterface thereby forming a much uniform and thinner film on the metal counterface (see figure 5.4). The short glass fibres, on the other hand tend to break, scratch and abrade the metal counterface resulting in higher wear rates. XRD results have shown that the crystallinity of the glass bead filled PTFE composites debris is more than that of the original bulk polymer. The analysis of the XRD results show that the difference in the degree of crystallinity can be as high as 15 % (refer to table 4.6). The DSC results of the wear debris and unworn material were not conclusive, and showed a slight decrease in crystallinity of the debris. Although more tests would need to be carried out to understand the structural changes on the polymer pin surface during the sliding process, it is plausible that the increase in the degree of crystallinity is due to the structural alignment of the molecules.

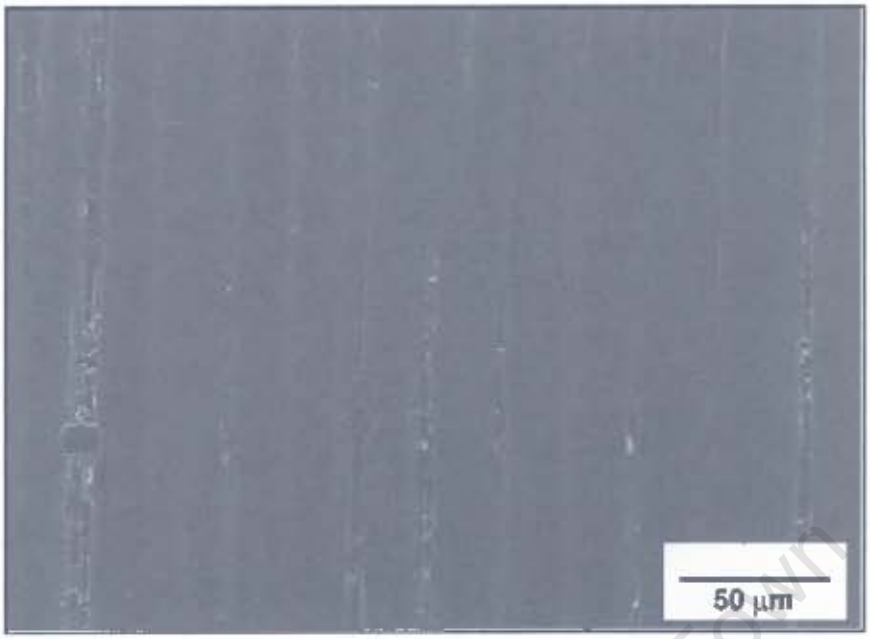

Figure 5.4: An SEM micrograph depicting the transfer film formed for glass fibre filled PTFE on the stainless steel counterface at the end of a dry sliding wear test.

Some researchers have found that the alignment in the transfer film is also responsible for the high adhesion to the metal counterface due to an increase in the number of Van der Waals secondary bonding[50,98]. XRD tests carried out by Marcus on the change in crystallinity with sliding distance of ultra high molecular weight polyethylene (UHMWPE) sliding perpendicular to the to the grinding marks on a stainless steel revealed that the crystallinity of the debris increased with sliding distance. He showed that the degree of crystallinity of UHMWPE wear debris increased up 75 % during the early stages of the sliding process. He surmised that the changes in the crystallinity of the polymer debris was due to the substantial amount of deformation that occurs at the polymer pin surface which led to the significant orientation of the UHMWPE molecules. Therefore, it can be deduced that due to the perpendicular sliding, more polymer can be accommodated in the asperity valleys of the counterface and so deformation can occur easily. The increase in crystallinity at the interface is more probably due to the structural breakdown of the polymer during the sliding process. The original; banded structure of PTFE is

sheared and destroyed giving rise to an oriented transfer film, the adhesion to the metal counterface depending profoundly on the surface roughness, the nature and type of filler and the presence or absence of an external lubricant.

CHAPTER 6

CONCLUSIONS

Based on the study undertaken the following conclusions can be drawn:

- The sliding wear behaviour of polytetrafluoroethylene is complex and difficult to measure using a single index. The wear performance of PTFE depends on a number of factors such as the sliding parameters, processing, type and level of filler. A change in one of these parameters often leads to a change in other parameters, thus making the wear performance determination difficult. However, general trends in friction and wear variations were observed in this study.

- The specific wear rates of unfilled PTFE were three orders of magnitude higher than that of glass filled PTFE and increased steadily with an increase in contact pressure. The specific wear rates of glass filled PTFE composites also increased with an increase in contact pressure from 1 MPa to 6.4 MPa above which they heavily deformed. The wear results obtained on the reciprocating sliding wear rig when the pressure was varied from 2.6 to 6.4 MPa ranged from 2.6 $x10^{-6}$ $mm^3/N.m$ to 2.3 $x10^{-5}$ $mm^3/N.m$ at an average sliding speed of 0.2 m/s. The wear results obtained on the pin-on-disk at a sliding speed of 1.5 m/s also increased from 0.15 $x10^{-6}$ $mm^3/N.m$ to 1.28 $x10^{-6}$ $mm^3/N.m$ between the pressure ranges 1 MPa to 2.5 MPa. Thus, the rate of wear can be considered to be independent of the type of motion under the conditions of the sliding parameters used.

- Glass fibre filled PTFE composites showed the lowest wear rates while the soft hollow glass bead filled PTFE grades showed the highest wear rates on both wear rigs used. The high wear rates exhibited by the hollow glass beads was

thought to be a direct result of glass beads crumbling and crushing during the sliding process, thereby forming a thicker transfer film on the metal counterface. The sliding wear rates shown by hard hollow glass bead filled PTFE were similar in magnitude to those of glass flake filled PTFE. The solid glass bead filled PTFE showed low wear rates that were also comparable in magnitude to those of glass fibre filled PTFE.

- An adherent transfer film onto the metal counterface is crucial for low wear under dry sliding conditions. Factors such as a 'rough' counterface helps to mechanically lock polymer fragments into the valleys between the asperities. The adherence of the transfer film is aided by chemical reactions between the polymer and the metal counterface and high contact pressures caused by the glass fillers.

- The addition of MoS_2 to glass fibre filled PTFE reduced the wear rate at pressures lower than 3 MPa but as the pressure was increased further, the wear rates did not improve much except for PF1717 (12 % wt short glass fibres+6 % wt MoS_2). PF1717 showed low wear rates at low sliding speed (0.2 m/s) and medium speed (1.5 m/s) at which the tests were conducted. It would therefore seem that the level of glass in the polymer matrix (25 % wt) is less important than the level of MoS_2. The addition of cobalt zinc aluminate pigment to glass fibre filled PTFE increased the wear whilst carbon pigment did not affect the wear rate.

- The PTFE composites processed by pressure sintering showed lower wear rates compared to the compression moulded grades under low pressures (less than 3.3 MPa), but at much higher pressures the wear rates of pressure sintered grades were similar in magnitude to those of compression moulded grades. Reprocessed PTFE composites showed low and stable wear results up to 4 MPa above which they deformed.

- The wear tests conducted in distilled water revealed that the glass filled PTFE had high wear rates, two orders of magnitude higher than dry sliding wear rates.

This was attributed to the easy separation of glass fillers from the PTFE matrix in water.

- The ***pv*** limit is the product of the pressure and velocity and does not indicate the relative importance on wear of the individual parameters. It was found that PTFE is very sensitive to deformation at particular velocities and hence the instance of dramatic increases in wear must be specified at a particular velocity. The glass fibre filled PTFE, for instance, showed ***pv*** limits of 6 MPa x m/s at 1.5 m/s and 5 MPa x m/s at 2 m/s under dry sliding conditions. Vesconite on the other hand, showed a ***pv*** limit of 3 MPa x m/s at 1.5 m/s.

- Vesconite hilube showed lower wear rates in water compared with the glass filled composites. Under dry sliding conditions, however, the wear behaviour of Vesconite hilube and glass fibre filled PTFE are similar in magnitude.

REFERENCES

1. Tevruz T.,Tribological Behaviours of Bronze-filled Polytetrafluoroethylene, Wear, Vol. 230, 1999, pp. 61-69.
2. Reay C., The South African Mechanical Engineer, Vol. 53, May 2003.
3. General Guide to the Choice of Journal Bearing Type, Tribology, ©Engineering Science Data Unit Ltd, Vol. 1, Item No. 65007, 1965.
4. Kim M. L., Kirk-Orthmer, Encyclopedia of Chemical Technology, Bearing Materials to Carbon, 4 th edition, Vol. 4, Howe-Grant M.(ed.), John Wiley and Sons Publishers, New York, pp. 1-22.
5. American Hoechst Corporation, "Hostaflon" Information 21 New: Hostaflon TFM, PTFE for Special Tasks, 1983.
6. Hoechst Aktiengesellschaft, "Hoechst Plastics-Hostaflon", 1984.
7. Hall C., Polymer Materials: An Introduction for Technologists and Scientists, MacMillan Publishers Inc., 1981.
8. McNicol A., Dowson D and Davies M., The Effect of Humidity and Electrical Fields Upon The Wear of High Density Polyethylene and Polytetrafluoroethylene, Wear, Vol.181, 1995, pp. 603-612.
9. Gangal S.V., Kirk-Othmer, Encyclopedia of Chemical Technology, 3rd edition, Vol.11, Kroschwitz J.I. (ed.), John Wiley and Sons Publishers, New York, 1994, pp. 1-24.
10. Teflon® PTFE Fluoropolmer Resins, Start with Du Pont Properties Handbook.
11. Birley A., W., Plastics Materials, Leonard Hill, USA: Chapman and Hall, 1982.
12. Briscoe B. J and Stolarski T. A., Transfer Wear of Polymers During Combined Linear Motion and Load Axis Spin, Wear, Vol. 104, 1985, pp. 121-137.
13. Tanaka K., Effect of Various Fillers on the Friction and Wear of PTFE-Based Composites, in K. Friedrich (ed.), Friction and Wear of Polymer Composites, Elsevier, New York, 1986, pp. 137-174.
14. Speerschneider C. J., and Li C. H., Some Observations on the Structure of Polytetrafluoroethylene, Journal of Applied Physics, 1962, pp. 25-187.
15. Geil P. H., Polymer Single Crystals, Interscience, New York, 1963, p. 183.
16. Bunn C. W., Cobbold A. J., and Palmer R. P., Journal of Polymer Science, Vol.38, 1958, p. 38.
17. Makinson K. R., and Tabor D., Proceedings of the Royal Society London Series A., Vol. 281, 1964, p. 49.

18. Biswas S. K., Friction and Wear of PTFE, Wear, Vol.158, 1992, pp. 193-211.
19. Ariawan A. B., Ebnesajjad S. and Hatzikiriakos S. G., Preforming Behaviour of Polytetrafluoroethylene Paste, Powder Technology, Vol. 121, 2001, pp. 249-258.
20. Ebnesajjab S., Fluoroplastics: Non-Melt Processible Fluoroplastics, Plastic Design Library, Vol.1, William Andrew, New York, 2000.
21. Clark E. S., The Molecular Comformation of Polytetrafluoroethylene: Forms II and IV Polymer, Vol. 40, 1999.
22. Osswald T. and Menge G., Material Science of Polymers for Engineers, Hanser/Gardner Publications Inc., 1995.
23. Hohl M., W., The Wear Behaviour of UHMWPE and Ion Implanted UHMWPE Against Different Counterfaces, MSc Thesis, University of Cape Town, 1998.
24. Chawla K.K., Composite Materials, Material Research and Engineering, Ilshner B. and Grant N.J. (eds.), Springer-Verlag Publishers, 1989, pp. 60-200.
25. Birley A.W., Haworth B. and Batchelor J., Processing, Properties and Materials Engineering, Physics of Plastics, Hanser Publishers, Barcelona, 1992.
26. Moore G.R. and Kline D.E., Properties and Processing of Polymers for Engineers, Soc. Plastic Engnrs. Inc., Prentice Hall, London, 1984.
27. Physical Properties of Unfilled and Filled Polytetrafluoroethylene, Fluon, ICI Petrochemicals and Plastic Division Technical Service Note F12/13, Imperial Chemical Industries, 1981.
28. Kline D.E., Thermal Conductivity Studies of Polymers, Journal of Polymer Science, Vol. 50, 1961.
29. Eiermann K. C., and Hellwege H. K., Thermal Conductivity of High Polymers from –180 to + 90°C, Journal of Polymer Science, Vol. 57, 1962, pp. 100-105.
30. Evans D. G. and Lancaster J. K., The Wear of Polymers, Treatise on Materials Science and Technology, Scott D. (ed.), Vol. 13, Academic Press Inc., 1979, pp. 85-139.
31. Price D. M., Thermal Conductivity of PTFE and PTFE Composites, Proceedings of the Twenty-eighth Conference of the North American Thermal Analysis Society, October 4-6, 2000, Florida, pp. 579-583.
32. Sangeeta H. and Jog J. P., Sintering of Ultra High Molecular weight Polyethylene, Bulletin of Material Science, Vol. 23, No.3, June 2000, pp. 221-226.
33. Hambir S. and Jog J. P., Sintering of Ultrahigh Molecular Weight Polyethylene, Bulletin of Material Science, Vol. 23, No.3, Indian Academy of Sciences, June 2000, pp. 221-226.
34. Filled Compounds of Teflon® PTFE, Du Pont pamphlet.
35. Hoechst High Chem , Polymer materials, Processing of the Suspension Polymers Hostaflon TF and Hostaflon TFM.

36. Anderson J. C., Wear of Commercially Available Plastic Materials, Tribology International, Vol. 15, No. 5, 1982, pp. 255-263.
37. Halling J., Principles of Tribology, the Macmillan Ltd, 1978, pp. 72-90.
38. Harsha A. P. and Tewari U. S., Tribo Performance of Polyaryletherketone Composites, Polymer Testing, Vol. 21, 2002, pp. 697-705.
39. Czichos H., Introduction to Friction and Wear in K. Friedrich (ed.), Friction and Wear of Polymer Composites, Elsevier, New York, 1986, pp. 1-19.
40. Hutchings I.M., Tribology, Friction and Wear of Engineering Materials, Macmillan, 1992.
41. Zhang Z., Xue Q., Liu W. and Shen W., Friction and Wear of Metal Powder Filled PTFE Composites Under Oil Lubricated Conditions, Wear, Vol. 210, 1997, pp. 151-156.
42. Bowden F. P. and Tabor D., "Friction", An Introduction to Tribology, Doubleday & Company, Inc., 1973, pp. 4-24.
43. Czichos H., Tribology, A Systems Approach to the Science And Technology of Friction, Lubrication and Wear, Tribology Series 1, Elsevier, Amsterdam, 1978, pp. 52-53.
44. Tabor D., Tribology – The Last 25 Years, A Personal View, Tribology International, Vol. 28, No.1, February 1995, pp. 7-10.
45. Greenwood J. A. and Williamson J. B. P., Contact of Nominally Flat Surfaces, Proceedings of the Royal Society, London, Vol. A 295, 1966, pp. 300-318.
46. Moore D. F., The Friction and Lubrication of Elastomers, Pergamon Press Ltd, 1975, p. 21.
47. Briscoe B. J., Wear of Polymers: An Essay on Fundamental Aspects, Tribology International, Vol. 14, No.4, 1981, pp. 231-240.
48. Bely V. A., Sviridyonok A. I., Petrokovets M. I. and Savkin V. G., Friction and Wear in Polymer-Based Materials, Pergamon Press Ltd., 1982, pp. 109-123.
49. Stachowiak G. W. and Batchelor A. W., Engineering Tribology, Tribology Series, 24, Elsevier, Amsterdam, 1993, pp. 612-765.
50. Marcus K., Micromechanisms of Polymer Sliding Wear, PhD Thesis, University of Cape Town, 1992.
51. Lancaster J. K., Abrasive Wear of Polymers, Wear, Vol. 14, 1969, pp. 223-235.
52. Ratner S. B., Farbevora I. I., Randyukevich O. V. and Lure E. G., Connection Between the Wear Resistance of Plastics and Other Mechanical Properties, Soviet Plastics, Vol. 7, 1964, pp. 37-45.
53. Lancaster J. K., Friction and Wear, Polymer Science, Jenkins A. D. (ed.), a Materials Science Handbook, Ch. 14, North Holland Publ. Co., Elsevier, N.Y., 1972.
54. Friedrich K., Friction and Wear of Polymer Composites, Wear of Reinforced Polymers by Different Abrasive Counterparts, Elsevier, New York, 1986, pp. 233-285.

55. Cirino M., Pipes R. B. and Friedrich K., The Abrasive Wear Beahaviour of Continuous Fiber Polymer Composites, Journal of Material Science, Vol. 22, 1987, pp. 233-287.
56. Buckley D. H., Surface Effects in Adhesion, Friction, Lubrication and Wear; Tribology Series 5, Elsevier Scientific Publishing Company, Amsterdam, 1981, pp. 473-500.
57. Pooley C. M. and Tabor D., Friction and Molecular Structure: The Behaviour of Some Thermoplastics, Proceedings of the Royal Society, Series A, Vol. 329, 1972, pp. 251-272.
58. Tanaka K. and Miyata T., Studies on the Friction and Transfer of Semicrystalline Polymers, Wear, Vol. 41, No. 2, 1977, pp. 383-398.
59. Tabor D., The Role of Surface and Intermolecular Forces in Thin Film Lubrication, Microscopic Aspects of Adhesion and Lubrication, Georges J. M. (ed.), Amsterdam, Elsevier, Tribology Series, Vol. 7, 1982, pp. 651-670.
60. Lancaster J. K., Lubrication of Carbon Fibre-Reinforced Polymers Part 1 – Water and Aqueous Solutions, Wear, Vol. 20, 1972, pp. 335-351.
61. Sviridyonok A.I., Self-lubrication Mechanisms in Polymer Composites, Tribology International, Vol. 24, No. 1, 1991, pp. 37-42.
62. Jintang G., Tribochemical Effects in Formation of Polymer Transfer Film, Wear, Vol. 245, 2000, pp. 100-106.
63. Jintang G., Shaolan M., Jinzhu L. and Dupeng F., Tribochemical Effects of Some Polymers/Stainless, Wear, Vol. 212, 1997, pp. 238-243.
64. Gong D., Zhang B., Xue Q. and Wang H., Investigation of Adhesion Wear of Filled Polytetrafluoroethylene by ESCA, AES and XRD, Wear, Vol. 57, 1990, pp. 25-39.
65. Van Voort J. and Bahadur S., The Growth and Bonding of Transfer Film and the Role of CuS and PTFE in the Tribological Behaviour of PEEK, Wear, Vol. 181, pp. 212-221.
66. Gong., D., Zhang B., Xue Q. and Wang H., Effect of Tribological Reaction of Polytetrafluoro-ethylene Transferred Film with Substrates on Its Wear Behaviour, Wear, Vol. 137, 1990, pp. 267-273.
67. Theiler G., Hubner W., Gradt T., Klein P. and Friedrich K., Friction and Wear of PTFE Composites at Cryogenic Temperatures, Tribology International, Vol. 35, 2002, pp. 449-458.
68. Lancaster J. K., Introduction to Bearing Materials, Non-Metallic Bearings in Engineering, NCT Notes, 1989, pp. 1-38.
69. Clauss F.J., Solid Lubricants and Self-lubricating Solids, Academic Press Inc., New York, 1972.
70. Filled Compounds of Teflon PTFE, Du Pont Brochure, pp.18-19.
71. Tervoort T. A., Visjager J. F. and Smith P., Melt Processable Polytetrafluoroethylene-

Compounding, Fillers and Dyes, Journal of Fluorine Chemistry, Vol. 114, 2002, pp. 133-137.

72. Arkles B., Gerakaris S. and Goodhue R., Wear Characteristics of Fluoropolymer Composites in Advances in Polymer Friction and Wear, Lee H. (ed.), Plenum Press., 1974, pp. 663-688.
73. Bijwe J., Logani C. M., and Tewari U. S., Influence of Fillers and Fibre Reinforcement on Abrasive Wear Resistance of Some Polymeric Composites, Wear, Vol. 138, 1990, pp. 77-90.
74. Tewari U. S., Bijwe J., On the Abrasive Wear of Some Polyimides and Their Composites, Tribology International, Vol. 24, 1991, pp. 247-254.
75. Allen C., Ball A., A Review of The Performance of Engineering Materials Under Prevalent Tribological and Wear Situations in South African Industries, Tribology International, Vol. 29, No. 2, 1996, pp. 105-116.
76. Briscoe B. J., Stolarski T. A. and Davies G. J., Boundary Lubrication of Polymers in Model Fluids, Tribology International, Vol. 17, 1984, p. 129.
77. Watanabe M., Wear Mechanism of Composites in Aqueous Environments, Wear, Vol. 158 1992, pp. 79-86.
78. Tanaka K. and Ueda S., The Mechanism of Wear of Polytetrafluoroethylene Above its Melting Point, Wear, Vol. 39, 1976, pp. 323-334.
79. O'Rourke J. T., Fundamentals of Friction, PV and Wear of Fluorocarbon Resins, Modern Plastics, Vol. 43, September 1965, pp. 161-169.
80. Tabor D. and Shooter K. V., The Frictional Properties of Plastics, Proceedings of Royal Society, Vol. 65, Series B, 1952, p. 671.
81. Tabor D. and Pascoe M. W., The Friction and Deformation of Polymers, Proceedings of the Royal Society of London, Vol. 235, Series A, 1956, pp. 210-224.
82. Milz W. C. and Sargent L. B., Friction Characteristics of Plastics, Lubrication Engineering, 1955.
83. Crease A.B., The Wear Performance of Rubbing Bearings-Improved Data For Design, The Wear of Non-Metallic Materials, Dowson D., Godet M. and Taylor C.M. (eds.), September 1976, p. 249.
84. Tanaka K., Uchiyama Y. and Toyooka S., The Mechanisms of Wear of Polytetrafluoroethylene, Wear, Vol. 23, 1973, pp.153-172.
85. Praat G. C., Plastics-based Bearings, Braithewaite E.R. (ed.), Lubrication and Lubricants, Elsevier, Chapter 7, 1967.
86. Lancaster J. K., Dry Rubbing Bearings, Neale M. J. (ed.), Tribology Handbook, Butterworths, Section A4, 1973.

87. Tanaka K. and Yamada Y., Influence of Counterface Roughness on the Friction and Wear of Polytetrafluoroethylene and Polyacetal-based Composites, Proceedings of the Institution of Mechanical Engineers International Conference, Vol. 1, 1987, pp. 219-223.
88. Tanaka K., Some Interesting Problems That Remain Unsolved in My Work on Polymer Tribology, Tribology International, Butterworth Heinemann, Vol. 28, No.1, 1995, p. 19-22.
89. Neale M.J., Tribology Handbook, Butterworth & Co. (Publishers) Ltd., A4, 1989.
90. Moore D. F., Principles and Applications of Tribology, Pergamon Press, Oxford, 1975.
91. Wagner C. D., Riggs W. M., Davies L.E.,Moulder J. F. and Muillenberg G.E, Handbook of X-ray Photoelectron Spectroscopy, Perkin-Elmer, Eden Prairie, 1978.
92. Cadmamn P. and Gossedge G.M., The Chemical Nature of Metal-Polytetrafluoroethylene Tribological Interactions Studied by X-ray Photoelectron Spectroscopy, Wear, Vol. 54 1979, pp. 211-215.
93. Gao J., Mao S., Liu J. and Feng D., Tribological Effects of Some Polymers/Stainless steel, Wear, Vol. 212, 1997, pp. 238-243.
94. Blanchet T.A. and Kennedy F.E., Sliding Wear Mechanism of Polytetrafluoroethylene (PTFE) and PTFE Composites, Wear, Vol.153, 1992, pp. 229-243.
95. Briscoe B.J and Steward M.D., The Effect of Carbon and Glass Fillers on the Transfer Film Behaviour of PTFE Composites, Tribology 1978, Material Performance and Conservation, ImechE Conf. Publications, 1978, pp. 17-20.
96. Lancaster J.K. The Effect of Carbon Fibre Reinforcement on the Friction and Wear of Polymers, Journal of Physics D: Applied Physics, Vol.1, No. 5, 1968, pp. 549-559.
97. Bahadur S. and Tabor D., The Wear of Polytetrafluoroethylene, Wear, Vol. 98, 1984, pp. 1-13.
98. Shen C. and Dumbleton J. H., The Friction and Wear Behaviour of Irradiated Very High Molecular Weight Polyethylene, Wear, Vol. 30, 1974, pp. 349-364.

APPENDIX A: PROPERTIES OF PTFE COMPOSITES AND VESCONITE

A 1:

Physical properties of PTFE compared to other fluorine-containing thermoplastics.

Material				PTFE	FEP	PFA	PCTFE	PVDF
Properties		Testing method	Unit					
Density	23 °C	DIN 53479	g/cm^3	2.15-2.19	2.12-2.17	2.12-2.17	2.10-2.20	1.76-1.78
Tensile strength at break	23 °C	DIN 53455	N/mm^2	22-40	18-25	27-29	30-38	38-50
Percentage elongation at break	23 °C	DIN 53455	%	250-500	250-350	300	80-200	30-40
Ball indentation hardness	23 °C	DIN 53456	N/mm^2	23-32	23-28	25-30	30	65
Proof resilience	23 °C	DIN 53455	N/mm^2	10	12	14	40	46
Modulus in tension	23 °C	DIN 53457	N/mm^2	400-800	350-700	650	1000-2000	800-1800
Modulus in flexure	23 °C	DIN 53457	N/mm^2	600-800	660-680	650-700	1200-1500	1200-1400
Shore hardness D	23 °C	DIN 53505		55-72	55-60	60-65	70-80	73-85
Melting temperature		ASTM 2116	°C	327	253-282	300-310	185-210	165-178
Cont. service temp. without load			°C	260	205	260	150	150
Coefficient of thermal exp. 10^{-5}		DIN 52328	K^{-1}	10-16	8-14	10-16	4-8	8-12
Thermal conductivity	23 °C	DIN 52612	W/K .m	0.25	0.2	0.22	0.19	0.17
Specific heat	23 °C		KJ/kg.K	1.01	1.17	1.09	0.92	1.38
Oxygen index			%	> 95	> 95	> 95	> 95	> 43
Water absorption		DIN 53495	%	< 0.01	< 0.01	< 0.03	< 0.01	< 0.03

The addition of fillers on PTFE does not affect its coefficient by much as shown in the table below.

Coefficient of friction of PTFE/steel under dry sliding condition (Literature)

PTFE type	Rubbing speed m/s	
	0.5	1.0
unfilled PTFE	0.25	0.27
PTFE + 15 % glass fibre	0.15	0.15
PTFE + 25 % glass fibre	0.15	0.15
PTFE + 15 % graphite	0.14	0.14
PTFE +25 % carbon	0.22	0.21
PTFE + 60 % bronze	0.20	0.22

A 2

Vesconite and Vesconite hilube typical properties

Vesconite physical properties	Value & unit
Density	1.38 g/cm^3
Melting point	260 °C
Hardness Shore (D)	84
Tensile strength at yield (ASTM D-638)	65 MPa
Tensile strength at break	62 MPa
Flexural yield strength	120 MPa
Deflection temperature at 1.85 MPa	93 °C
Modulus of elasticity under compression	2290 MPa
Compression strength at yield	92 MPa
Shear strength	49 MPa
Heat conductivity	0.3 W.K^{-1}.m^{-1}
Coefficient of linear thermal expansion	6x10^{-5} mm.mm^{-1}.°C^{-1}
Maximum moisture absorption in water at 20°C	0.50 %
Dynamic unlubricated friction coefficient on steel	0.12-0.20

Vesconite hilube physical properties	Value & unit
Density	1.38 g/cm^3
Melting point	260 °C
Hardness Shore (D)	82
Tensile strength at yield (ASTM D-638)	66 MPa
Tensile strength at break	65 MPa
Flexural yield strength	113 MPa
Deflection temperature at 1.85 MPa	117 °C
Modulus of elasticity under compression	2206 MPa
Compression strength at yield	99 MPa
Shear strength	49.4 MPa
Heat conductivity	0.3 W.K^{-1}.m^{-1}
Coefficient of linear thermal expansion	6x10^{-5} mm.mm^{-1}.°C^{-1}
Maximum moisture absorption in water at 20°C	0.50 %
Dynamic unlubricated friction coefficient on steel	0.10

APPENDIX B: The calibration wear data for the recirpocating sliding wear rig.

B 1.

The reciprocating sliding wear rig was calibrated using 25 % short glass fibre filled PTFE, PF1125. Four tests were performed at an average sliding speed of 0.2 m/s under dry sliding conditions. The speecific wear rates obtained for such tests are shown shown in the calibration chart below. The volumetric wear obtained is shown in B 2.

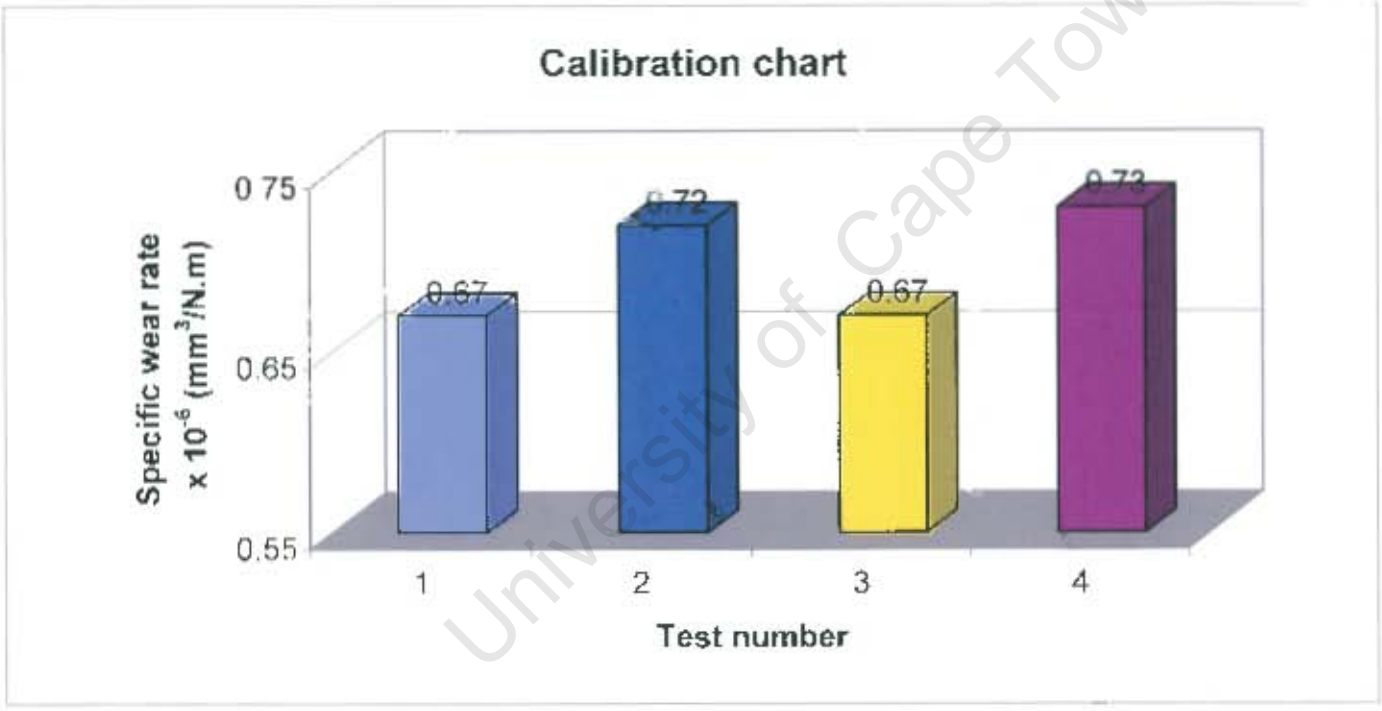

L_1		L_2		R_1		R_2		Average	Sliding distance
Mass loss mg	Volume mm^3	Mass loss mg	Volume loss mm^3	Mass loss mg	Volume loss mm^3	Mass loss mg	Volume loss mm^3	mm^3	km
0	0	0	0	0	0	0	0	0	0
1.1	0.51	1.2	0.55	1.3	0.60	1.2	0.55	0.55	0.2
1.4	0.65	1.3	0.60	1.7	0.78	1.5	0.69	0.68	0.5
2.1	0.97	2.0	0.92	2.3	1.06	2.1	0.97	0.98	1
2.5	1.15	2.4	1.11	2.7	1.24	2.6	1.20	1.18	1.5
2.8	1.29	2.7	1.24	3	1.38	2.9	1.34	1.31	2
3.8	1.75	3.4	1.57	4.1	1.89	3.9	1.80	1.75	3.5
4.5	2.07	4.3	1.98	4.9	2.26	4.8	2.21	2.13	5
6.2	2.86	6	2.76	6.5	3.00	6.4	2.95	2.89	8
7.1	3.27	7.0	3.23	7.4	3.41	7.6	3.50	3.35	10

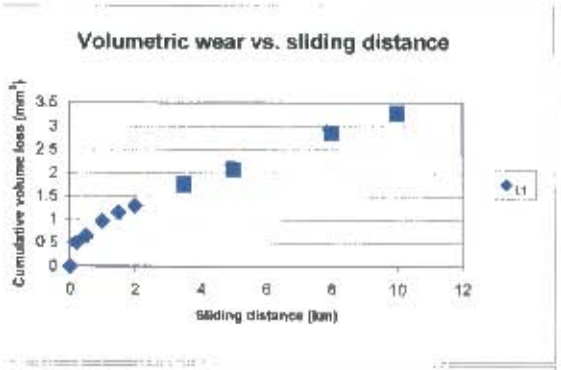

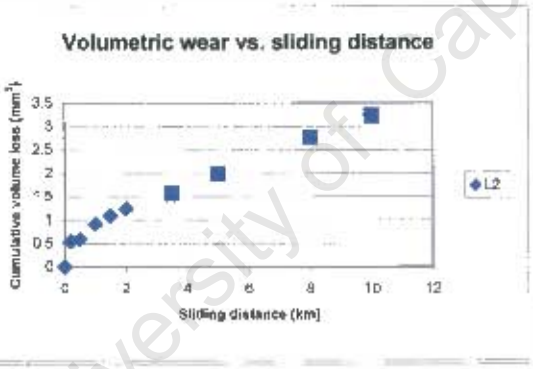

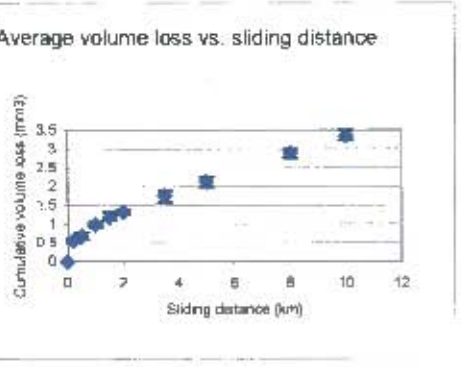

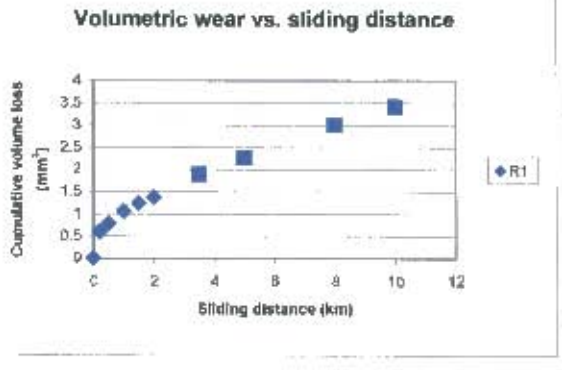

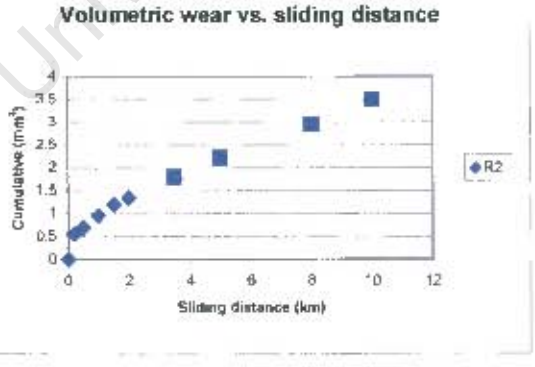

B 2:

Reproducibility wear results

Material: PF1125

L_1, L_2, R_1 and R_2 represent four tests undertaken

C 1 Reciprocating dry sliding wear data

Load N	Pressure MPa	Velocity m/s	Mass loss mg	Sliding distance km	Coeff. of friction μ_k	Volume loss mm^3	Roughness μm R_a
				0		0	0.2
405	4.50	0.2	2.1	0.2	0.15	0.95	0.2
405	4.50	0.2	2.3	0.5	0.14	1.04	0.18
405	4.50	0.2	2.5	1	0.15	1.13	0.18
405	4.50	0.2	2.7	1.5	0.16	1.22	0.16
405	4.50	0.2	3.0	2	0.16	1.36	0.15
405	4.50	0.2	3.6	3.5	0.17	1.63	0.15
405	4.50	0.2	4.6	5	0.17	2.08	0.14

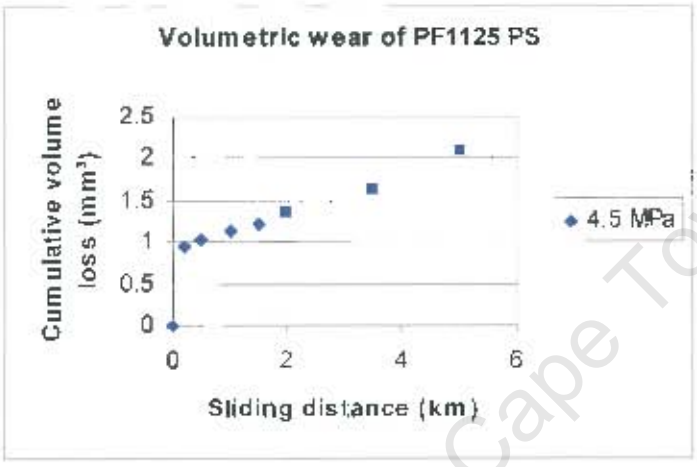

Load N	Pressure MPa	Velocity m/s	Mass loss mg	Sliding distance km	Coeff. of friction μ_k	Volume loss mm^3	Roughness μm R_a
				0		0	0.19
577	6.40	0.2	3.2	0.2	0.13	2.9	0.19
577	6.40	0.2	3.5	0.5	0.14	2.9	0.18
577	6.40	0.2	3.8	1	0.15	2.9	0.17
577	6.40	0.2	4.2	1.5	0.16	2.9	0.16
577	6.40	0.2	4.7	2	0.17	2.9	0.14
577	6.40	0.2	6.0	3.5	0.18	2.9	0.12
577	6.40	0.2	7.9	5	0.17	2.9	0.10

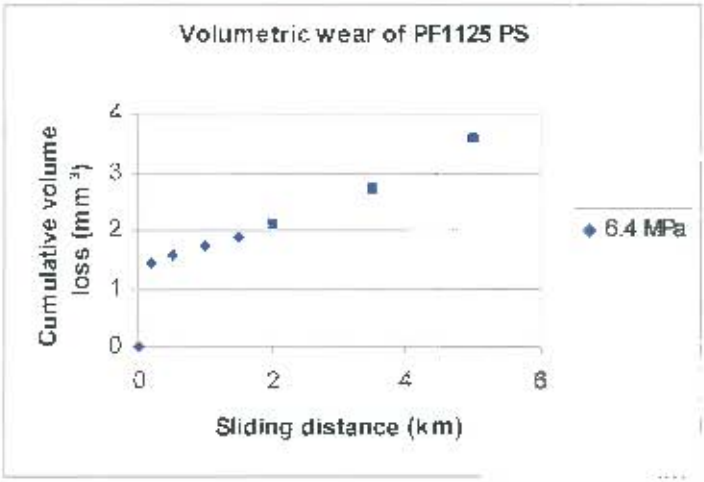

Load N	Pressure MPa	Velocity m/s	Mass loss mg	Sliding distance km	Coeff. of friction μ_k	Volume loss mm^3	Roughness μm R_a
				0		0	0.2
405	4.50	0.2	2.8	0.2	0.15	1.24	0.2
405	4.50	0.2	3.3	0.5	0.14	1.47	0.18
405	4.50	0.2	3.5	1	0.15	1.56	0.18
405	4.50	0.2	3.7	1.5	0.16	1.64	0.16
405	4.50	0.2	3.8	2	0.16	1.69	0.15
405	4.50	0.2	4.0	3.5	0.17	1.78	0.15
405	4.50	0.2	4.3	5	0.17	1.91	0.14

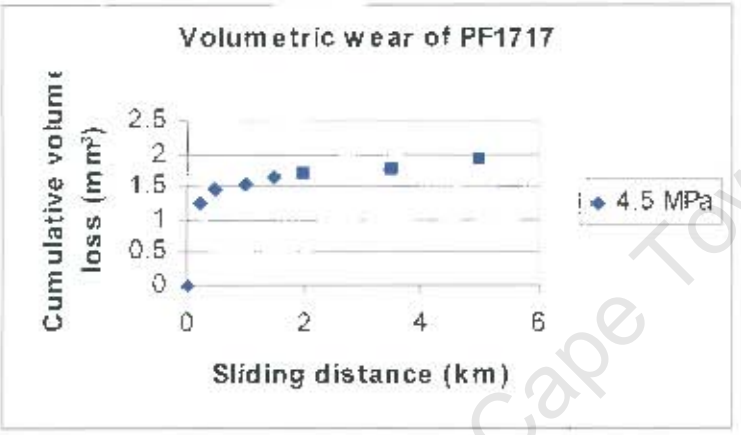

Load N	Pressure MPa	Velocity m/s	Mass loss mg	Sliding distance km	Coeff. of friction μ_k	Volume loss mm^3	Roughness μm R_a
				0		0	0.2
577	6.40	0.2	4.6	0.2	0.13	2.0	0.19
577	6.40	0.2	4.9	0.5	0.14	2.2	0.18
577	6.40	0.2	5.2	1	0.15	2.3	0.19
577	6.40	0.2	5.2	1.5	0.17	2.3	0.16
577	6.40	0.2	5.6	2	0.16	2.5	0.13
577	6.40	0.2	6.6	3.5	0.16	2.9	0.1
577	6.40	0.2	7.5	5	0.17	3.3	0.09

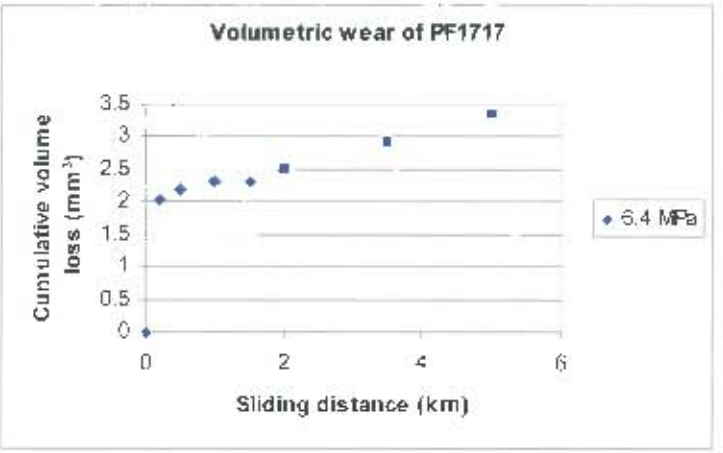

Load N	Pressure MPa	Velocity m/s	Mass loss mg	Sliding distance km	Coeff. of friction μ_k	Volume loss mm^3	Roughness $\mu m\ R_a$
			0	0		0	0.20
450	4.50	0 2	0.1	0.2	0.15	0 05	0 20
450	4.50	0 2	0.3	0.5	0.17	0.14	0.17
450	4.50	0.2	0.3	1	0.18	0.14	0.16
450	4.50	0.2	0.5	1.5	0.18	0.23	0.18
450	4.50	0.2	0.7	2	0 20	0.32	0.18
450	4.50	0.2	2.2	3.5	0.21	1.00	0.19
450	4 50	0.2	4.0	5	0 23	1.81	0.19

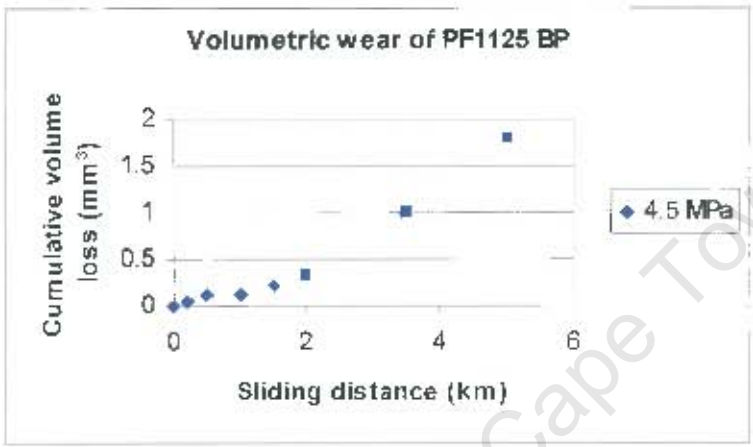

Load N	Pressure MPa	Velocity m/s	Mass loss mg	Sliding distance km	Coeff. of friction μ_k	Volume loss mm^3	Roughness $\mu m\ R_a$
			0	0		0	0.20
577	6.40	0.2	1.0	0.2	0 14	0.45	0.20
577	6.40	0.2	1.4	0 5	0 15	0.63	0.16
577	6.40	0.2	2 1	1	0.17	0.95	0 17
577	6.40	0.2	2.7	1.5	0.17	1.22	0.15
577	6.40	0.2	3.0	2	0.19	1.36	0.17
577	6.40	0.2	5.5	3.5	0.21	2.49	0.14
577	6.40	0.2	8 1	5	0.22	3.67	0.16

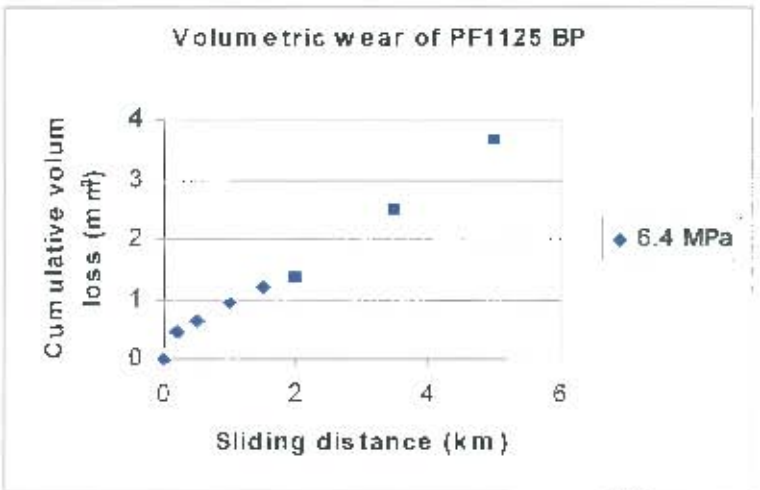

Load N	Pressure MPa	Velocity m/s	Mass loss mg	Sliding distance km	Coeff. of friction μ_k	Volume loss mm^3	Roughness $\mu m\ R_a$
			0	0		0	0.20
405	4.50	0.2	2.0	0.2	0.15	0.92	0.19
405	4.50	0.2	2.7	0.5	0.15	1.24	0.18
405	4.50	0.2	3.0	1	0.17	1.38	0.17
405	4.50	0.2	3.3	1.5	0.18	1.52	0.16
405	4.50	0.2	3.5	2	0.18	1.61	0.17
405	4.50	0.2	4.0	3.5	0.19	1.84	0.15
405	4.50	0.2	4.8	5	0.21	2.21	0.13

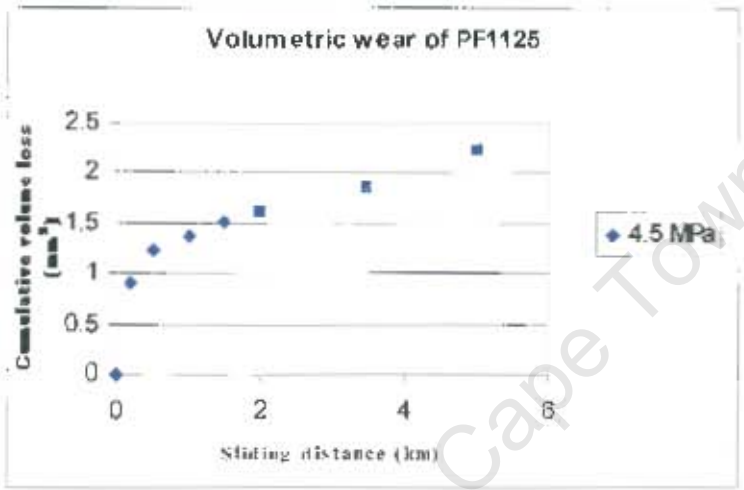

Load N	Pressure MPa	Velocity m/s	Mass loss mg	Sliding distance km	Coeff. of friction μ_k	Volume loss mm^3	Roughness $\mu m\ R_a$
			0	0		0	0.20
577	6.40	0.2	1.9	0.2	0.14	0.9	0.20
577	6.40	0.2	2.2	0.5	0.15	1.0	0.18
577	6.40	0.2	2.8	1	0.18	1.3	0.16
577	6.40	0.2	3.7	1.5	0.18	1.7	0.16
577	6.40	0.2	4.3	2	0.19	2.0	0.15
577	6.40	0.2	7.3	3.5	0.20	3.4	0.14
577	6.40	0.2	9.3	5	0.21	4.3	0.13

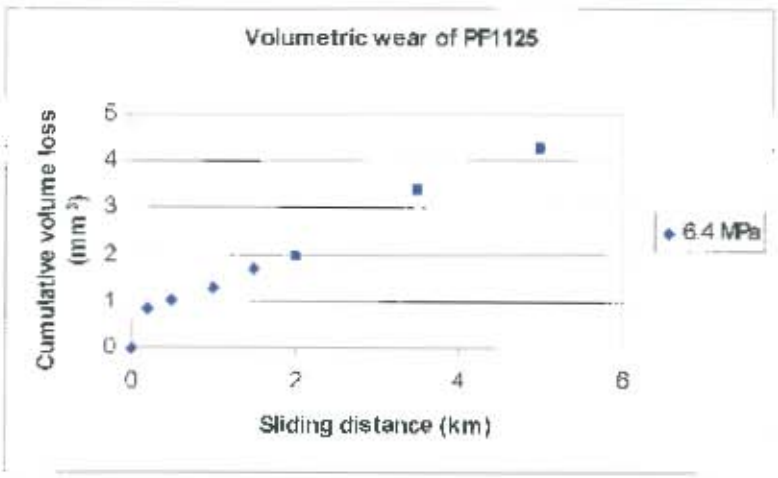

Load N	Pressure MPa	Velocity m/s	Mass loss mg	Sliding distance km	Coeff. of friction μ_k	Volume loss mm^3	Roughness $\mu m\ R_a$
				0		0	0.20
405	4.50	0.2	4.3	0.2	0.15	2.61	0.19
405	4.50	0.2	6.4	0.5	0.17	3.88	0.19
405	4.50	0.2	8.3	1	0.17	5.03	0.17
405	4.50	0.2	8.9	1.5	0.18	5.39	0.17
405	4.50	0.2	9.1	2	0.19	5.52	0.18
405	4.50	0.2	11.4	3.5	0.19	6.91	0.19
405	4.50	0.2	15.3	5	0.20	9.27	0.18

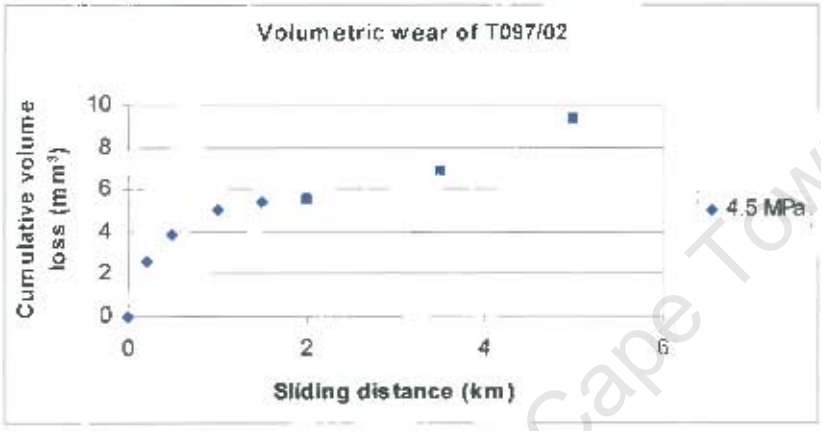

Load N	Pressure MPa	Velocity m/s	Mass loss mg	Sliding distance km	Coeff. of friction μ_k	Volume loss mm^3	Roughness $\mu m\ R_a$
				0		0	0.19
577	6.40	0.2	15.2	0.2	0.15	9.21	0.19
577	6.40	0.2	28.4	0.5	0.17	17.21	0.17
577	6.40	0.2	44.9	1	0.17	27.21	0.16
577	6.40	0.2	56.9	1.5	0.18	34.48	0.19
577	6.40	0.2	67.6	2	0.19	40.97	0.19
577	6.40	0.2	104.9	3.5	0.19	63.58	0.2
577	6.40	0.2	133.4	5	0.20	80.85	0.17

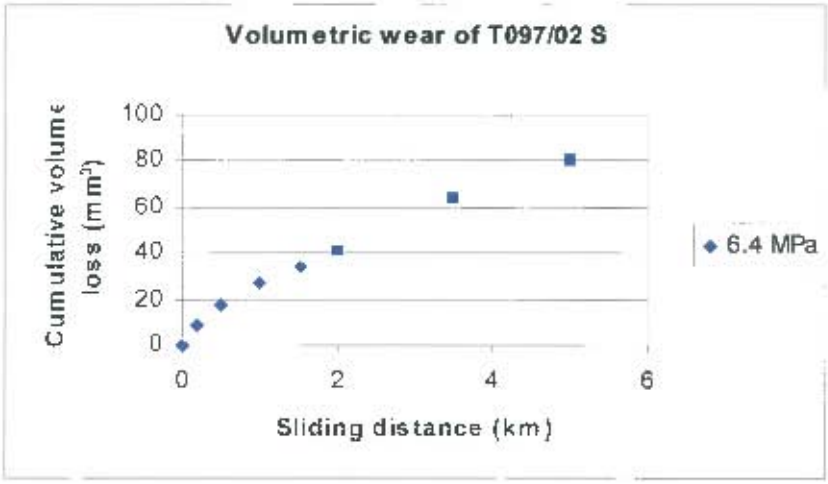

C 2 Pin-on-disk dry sliding wear data

Wear data for PF1717

Load N	Pressure MPa	Velocity m/s	Mass loss mg	Density g/cm^3	Sliding distance km	Coeff. of friction	Volume loss mm^3
			0		0		0
40.2	1.33	1.5	0.7	2.25	0.5	0.13	0.31
40.2	1.33	1.5	0.9	2.25	2	0.13	0.40
40.2	1.33	1.5	1.1	2.25	5	0.13	0.49
40.2	1.33	1.5	1.2	2.25	10	0.14	0.53
40.2	1.33	1.5	1.3	2.25	20	0.14	0.58
40.2	1.33	1.5	1.5	2.25	30	0.14	0.67

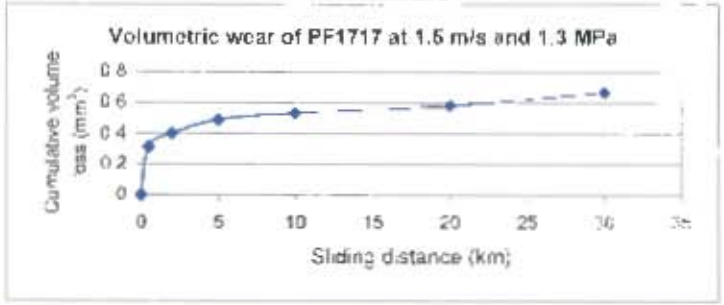

Load N	Pressure MPa	Velocity m/s	Mass loss mg	Density g/cm^3	Sliding distance km	Coeff. of friction	Volume loss mm^3
			0		0		0
60.4	2.00	1.5	0.7	2.25	0.5	0.13	0.31
60.4	2.00	1.5	0.8	2.25	2	0.14	0.36
60.4	2.00	1.5	0.9	2.25	5	0.16	0.40
60.4	2.00	1.5	1.1	2.25	10	0.16	0.49
60.4	2.00	1.5	1.4	2.25	20	0.17	0.62
60.4	2.00	1.5	1.7	2.25	30	0.19	0.76

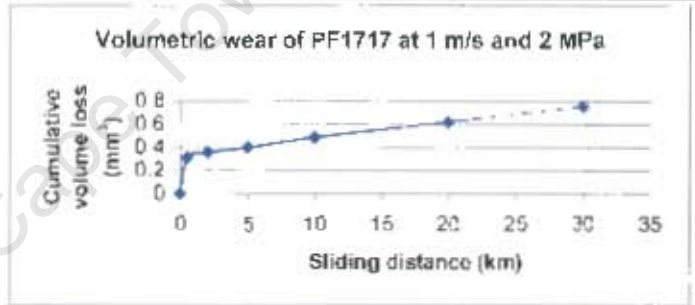

Load N	Pressure MPa	Velocity m/s	Mass loss mg	Density g/cm^3	Sliding distance km	Coeff. of friction	Volume loss mm^3
			0		0		0
50.3	1.67	1.5	0.5	2.25	0.5	0.13	0.22
50.3	1.67	1.5	0.9	2.25	2	0.14	0.40
50.3	1.67	1.5	0.9	2.25	5	0.15	0.40
50.3	1.67	1.5	1.2	2.25	10	0.16	0.53
50.3	1.67	1.5	1.4	2.25	20	0.16	0.62
50.3	1.67	1.5	1.6	2.25	30	0.18	0.71

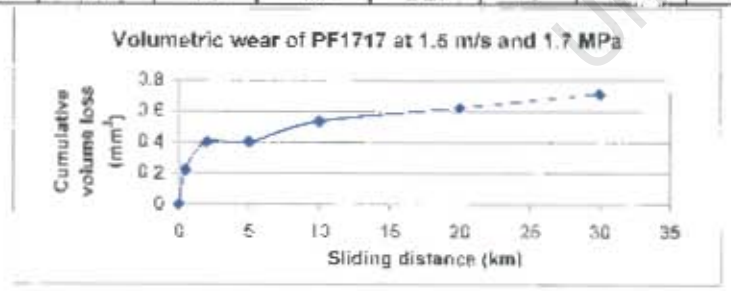

Load N	Pressure MPa	Velocity m/s	Mass loss mg	Density g/cm^3	Sliding distance km	Coeff. of friction	Volume loss mm^3
			0		0		0
75.6	2.50	1.5	0.5	2.25	0.5	0.12	0.22
75.6	2.50	1.5	0.6	2.25	2	0.13	0.27
75.6	2.50	1.5	0.8	2.25	5	0.13	0.36
75.6	2.50	1.5	0.9	2.25	10	0.13	0.40
75.6	2.50	1.5	1.2	2.25	20	0.17	0.53
75.6	2.50	1.5	1.7	2.25	30	0.19	0.76

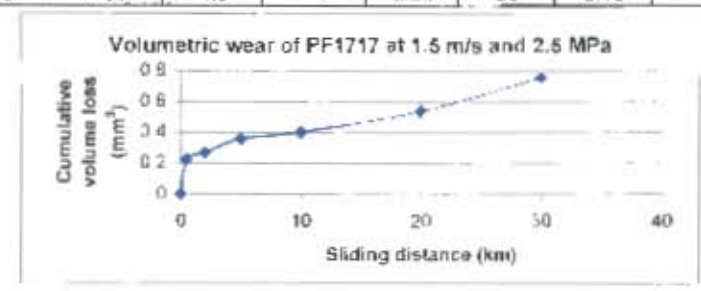

Wear data for PF1125 PS

Load N	Pressure MPa	Velocity m/s	Mass loss mg	Density g/cm^3	Sliding distance km	Coeff. of friction	Volume loss mm^3
			0		0		0
40.2	1.33	1.5	0.7	2.21	0.5	0.13	0.32
40.2	1.33	1.5	1.2	2.21	2	0.13	0.54
40.2	1.33	1.5	1.3	2.21	5	0.14	0.59
40.2	1.33	1.5	1.4	2.21	10	0.14	0.63
40.2	1.33	1.5	1.6	2.21	20	0.15	0.72
40.2	1.33	1.5	1.8	2.21	30	0.16	0.81

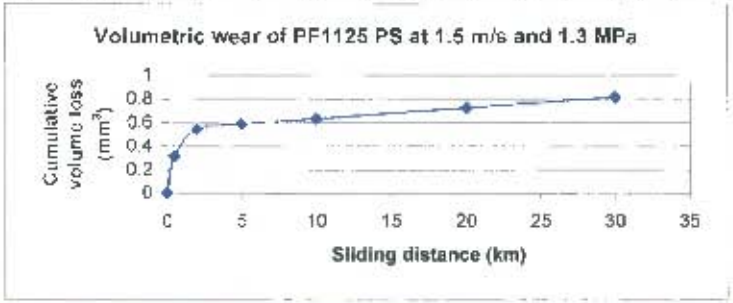

Load N	Pressure MPa	Velocity m/s	Mass loss mg	Density g/cm^3	Sliding distance km	Coeff.of friction	Volume loss mm^3
			0		0		0
60.4	2.00	1.5	0.6	2.21	0.5	0.13	0.27
60.4	2.00	1.5	1.8	2.21	2	0.13	0.81
60.4	2.00	1.5	1.9	2.21	5	0.13	0.86
60.4	2.00	1.5	2.0	2.21	10	0.14	0.90
60.4	2.00	1.5	2.3	2.21	20	0.17	1.04
60.4	2.00	1.5	2.6	2.21	30	0.18	1.18

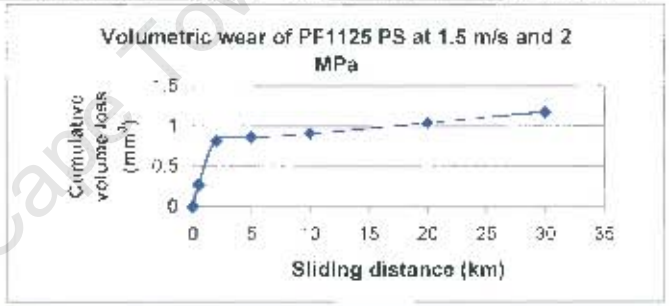

Load N	Pressure MPa	Velocity m/s	Mass loss mg	Density g/cm^3	Sliding distance km	Coeff. of friction	Volume loss mm^3
			0		0		0
50.3	1.67	1.5	0.3	2.21	0.5	0.13	0.14
50.3	1.67	1.5	0.7	2.21	2	0.14	0.32
50.3	1.67	1.5	1.2	2.21	5	0.14	0.54
50.3	1.67	1.5	1.5	2.21	10	0.15	0.68
50.3	1.67	1.5	1.8	2.21	20	0.16	0.81
50.3	1.67	1.5	2.1	2.21	30	0.18	0.95

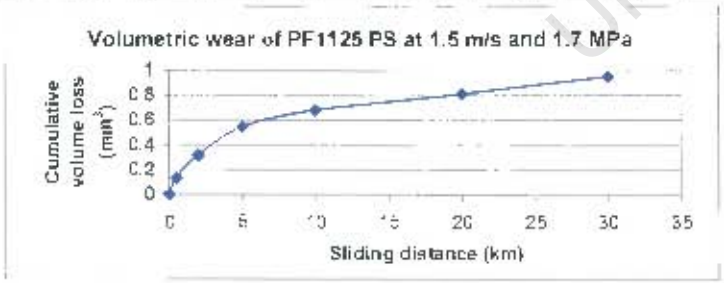

Load N	Pressure MPa	Velocity m/s	Mass loss mg	Density g/cm^3	Sliding distance km	Coeff. of friction	Volume loss mm^3
			0		0		0
75.6	2.50	1.5	0.9	2.21	0.5	0.13	0.41
75.6	2.50	1.5	1.1	2.21	2	0.13	0.50
75.6	2.50	1.5	1.2	2.21	5	0.15	0.54
75.6	2.50	1.5	1.5	2.21	10	0.17	0.68
75.6	2.50	1.5	2.1	2.21	20	0.18	0.95
75.6	2.50	1.5	2.8	2.21	30	0.20	1.27

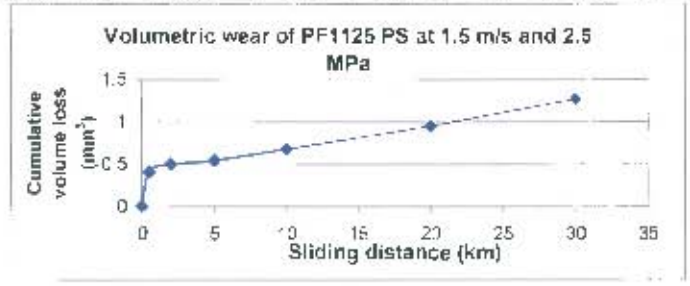

Wear data for T097/02

Load N	Pressure MPa	Velocity m/s	Mass loss mg	Density g/cm^3	Sliding distance km	Coeff. of friction	Vol. loss mm^3
			0		0		0
40.2	1.33	1.5	1.6	1.65	0.5	0.16	0.97
40.2	1.33	1.5	2.2	1.65	2	0.19	1.33
40.2	1.33	1.5	2.7	1.65	5	0.19	1.64
40.2	1.33	1.5	3.1	1.65	10	0.21	1.88
40.2	1.33	1.5	3.8	1.65	20	0.22	2.30
40.2	1.33	1.5	4.3	1.65	30	0.23	2.61

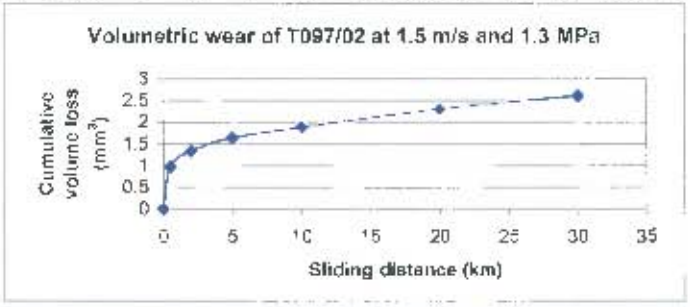

Load N	Pressure MPa	Velocity m/s	Mass loss mg	Density g/cm^3	Sliding distance km	Coeff. of friction	Volume loss mm^3
			0		0		0
60.4	2.00	1.5	1.8	1.74	0.5	0.19	1.03
60.4	2.00	1.5	2.3	1.74	2	0.18	1.32
60.4	2.00	1.5	3	1.74	5	0.19	1.72
60.4	2.00	1.5	3.6	1.74	10	0.21	2.07
60.4	2.00	1.5	4.6	1.74	20	0.23	2.64
60.4	2.00	1.5	5.8	1.74	30	0.23	3.33

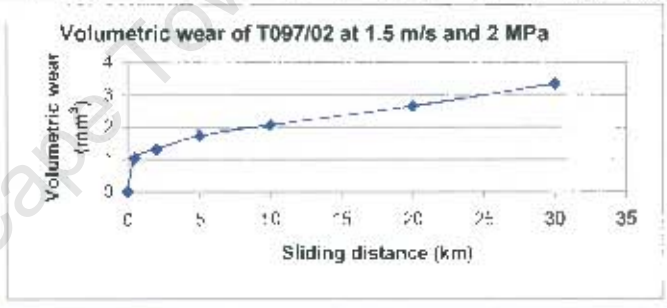

Load N	Pressure MPa	Velocity m/s	Mass loss mg	Density g/cm^3	Sliding distance km	Coeff. of friction	Volume loss mm^3
			0		0		0
50.3	1.67	1.5	1.0	1.65	0.5	0.18	0.61
50.3	1.67	1.5	1.5	1.65	2	0.18	0.91
50.3	1.67	1.5	1.9	1.65	5	0.19	1.15
50.3	1.67	1.5	2.5	1.65	10	0.20	1.52
50.3	1.67	1.5	3.7	1.65	20	0.24	2.24
50.3	1.67	1.5	4.6	1.65	30	0.25	2.79

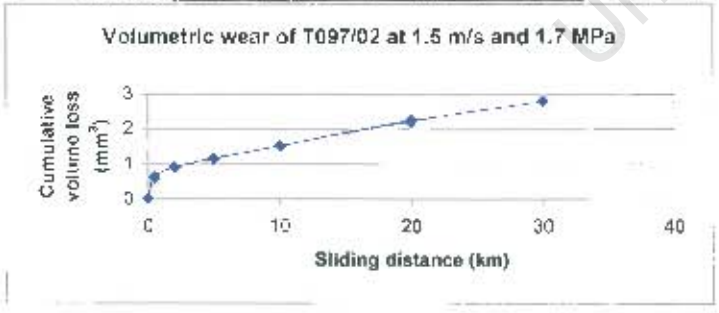

Load N	Pressure MPa	Velocity m/s	Mass loss mg	Density g/cm^3	Sliding distance km	Coeff. of friction	Volume loss mm^3
			0		0		0
75.6	2.50	1.5	2.9	1.65	0.5	0.19	1.76
75.6	2.50	1.5	3.8	1.65	2	0.20	2.30
75.6	2.50	1.5	4.6	1.65	5	0.20	2.79
75.6	2.50	1.5	5.8	1.65	10	0.24	3.52
75.6	2.50	1.5	7.7	1.65	20	0.26	4.67
75.6	2.50	1.5	9.0	1.65	30	0.27	5.45

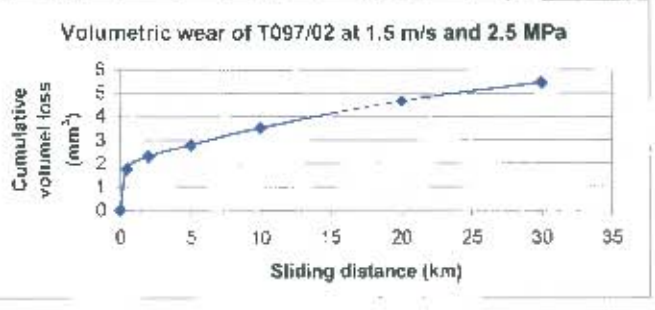

Wear data for PF1125 BP

Load N	Pressure MPa	Velocity m/s	Mass loss mg	Density g/cm^3	Sliding distance km	Coeff. of friction	Volume loss mm^3
			0		0		0
40.2	1.33	1.5	0.3	2.21	0.5	0.14	0.14
40.2	1.33	1.5	0.4	2.21	2	0.17	0.18
40.2	1.33	1.5	0.5	2.21	5	0.19	0.23
40.2	1.33	1.5	0.7	2.21	10	0.21	0.32
40.2	1.33	1.5	1.3	2.21	20	0.23	0.59
40.2	1.33	1.5	2.1	2.21	30	0.26	0.95

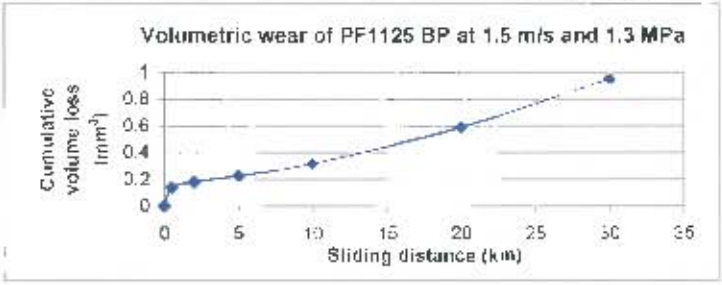

Load N	Pressure MPa	Velocity m/s	Mass loss mg	Density g/cm^3	Sliding distance km	Coeff. of friction	Volume loss mm^3
			0		0		0
60.4	2.00	1.5	0.3	2.21	0.5	0.13	0.14
60.4	2.00	1.5	0.3	2.21	2	0.17	0.14
60.4	2.00	1.5	0.5	2.21	5	0.19	0.23
60.4	2.00	1.5	0.6	2.21	10	0.24	0.27
60.4	2.00	1.5	1.5	2.21	20	0.25	0.66
60.4	2.00	1.5	2.7	2.21	30	0.30	1.22

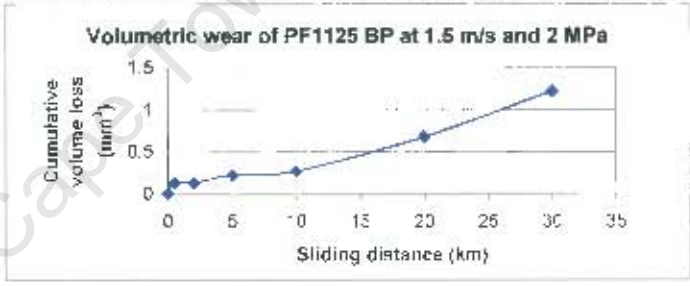

Load N	Pressure MPa	Velocity m/s	Mass loss mg	Density g/cm^3	Sliding distance km	Coeff. of friction	Volume loss mm^3
			0		0		0
50.3	1.67	1.5	0.5	2.21	0.5	0.14	0.23
50.3	1.67	1.5	0.9	2.21	2	0.16	0.41
50.3	1.67	1.5	1.2	2.21	5	0.18	0.54
50.3	1.67	1.5	1.4	2.21	10	0.19	0.63
50.3	1.67	1.5	1.8	2.21	20	0.21	0.81
50.3	1.67	1.5	2.4	2.21	30	0.22	1.09

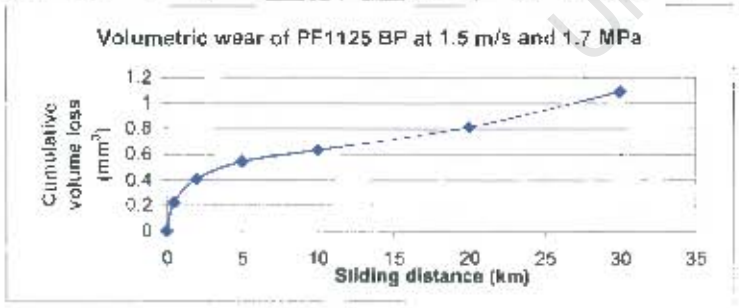

Load N	Pressure MPa	Velocity m/s	Mass loss mg	Density g/cm^3	Sliding distance km	Coeff. of friction	Volume loss mm^3
			0		0		0
75.6	2.50	1.5	0.6	2.21	0.5	0.15	0.27
75.6	2.50	1.5	0.8	2.21	2	0.15	0.36
75.6	2.50	1.5	1	2.21	5	0.16	0.45
75.6	2.50	1.5	1.3	2.21	10	0.20	0.59
75.6	2.50	1.5	2.5	2.21	20	0.23	1.13
75.6	2.50	1.5	3.3	2.21	30	0.25	1.49

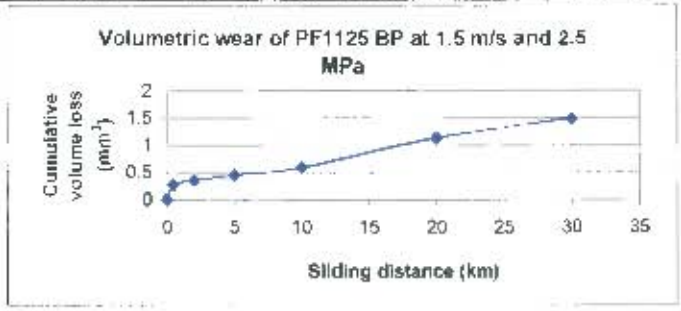

Wear data for PF1125

Load	Pressure	Velocity	Mass loss	Density	Sliding distance	Coeff. of friction	Volume loss
N	MPa	m/s	mg	g/cm^3	km		mm^3
			0		0		0
40.2	1.33	1.5	0.5	2.17	0.5	0.12	0.23
40.2	1.33	1.5	0.6	2.17	2	0.13	0.28
40.2	1.33	1.5	0.7	2.17	5	0.15	0.32
40.2	1.33	1.5	0.9	2.17	10	0.17	0.41
40.2	1.33	1.5	1.1	2.17	20	0.22	0.51
40.2	1.33	1.5	1.4	2.17	30	0.25	0.65

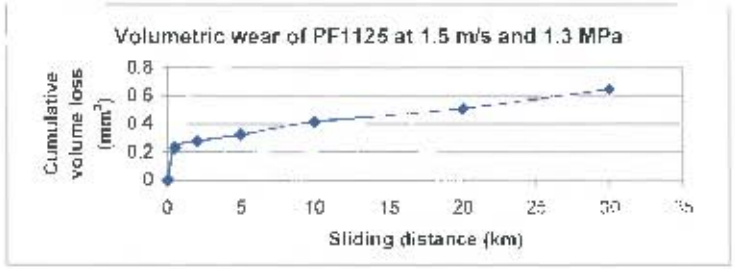

Load	Pressure	Velocity	Mass loss	Density	Sliding distance	Coeff. of friction	Volume loss
N	MPa	m/s	mg	g/cm^3	km		mm^3
			0		0		0
60.4	2.00	1.5	0.8	2.17	0.5	0.13	0.37
60.4	2.00	1.5	1.2	2.17	2	0.14	0.55
60.4	2.00	1.5	1.4	2.17	5	0.14	0.65
60.4	2.00	1.5	1.6	2.17	10	0.15	0.74
60.4	2.00	1.5	2.0	2.17	20	0.15	0.92
60.4	2.00	1.5	2.2	2.17	30	0.16	1.01

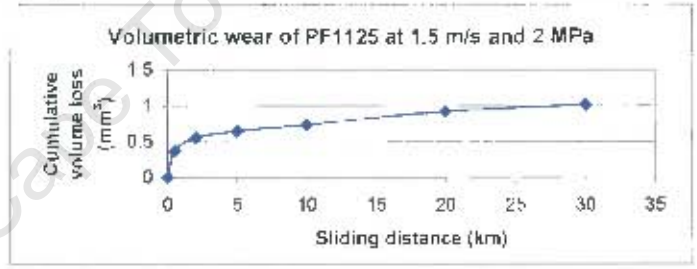

Load	Pressure	Velocity	Mass loss	Density	Sliding distance	Coeff. of friction	Volume loss
N	MPa	m/s	mg	g/cm^3	km		mm^3
			0		0		0
50.3	1.67	1.5	0.8	2.17	0.5	0.16	0.37
50.3	1.67	1.5	1.2	2.17	2	0.16	0.55
50.3	1.67	1.5	1.4	2.17	5	0.17	0.65
50.3	1.67	1.5	1.6	2.17	10	0.19	0.74
50.3	1.67	1.5	2.0	2.17	20	0.21	0.92
50.3	1.67	1.5	2.6	2.17	30	0.23	1.20

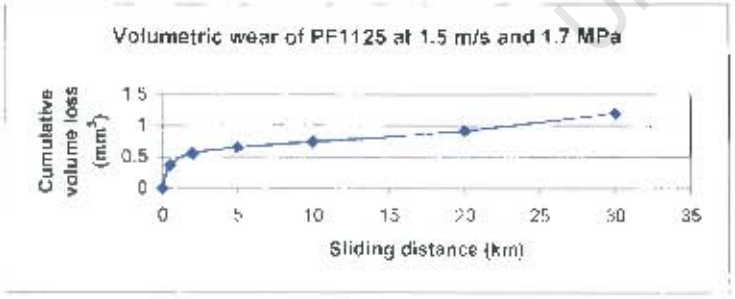

Load	Pressure	Velocity	Mass loss	Density	Sliding distance	Coeff. of friction	Volume loss
N	MPa	m/s	mg	g/cm^3	km		mm^3
			0		0		0
75.6	2.50	1.5	0.6	2.17	0.5	0.13	0.28
75.6	2.50	1.5	0.8	2.17	2	0.14	0.37
75.6	2.50	1.5	1	2.17	5	0.17	0.46
75.6	2.50	1.5	1.3	2.17	10	0.18	0.60
75.6	2.50	1.5	2	2.17	20	0.19	0.92
75.6	2.50	1.5	2.6	2.17	30	0.19	1.20

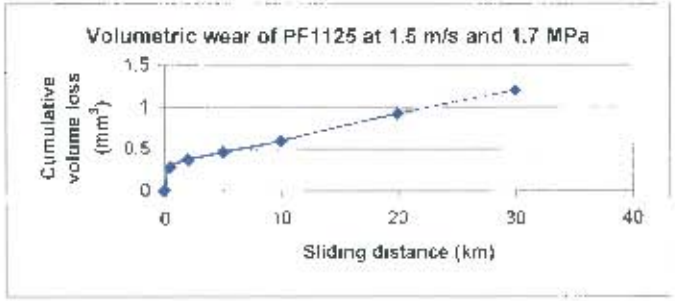

APPENDIX D: THE XRD SCANS OF THE BULK PTFE COMPOSITE MATERIALS

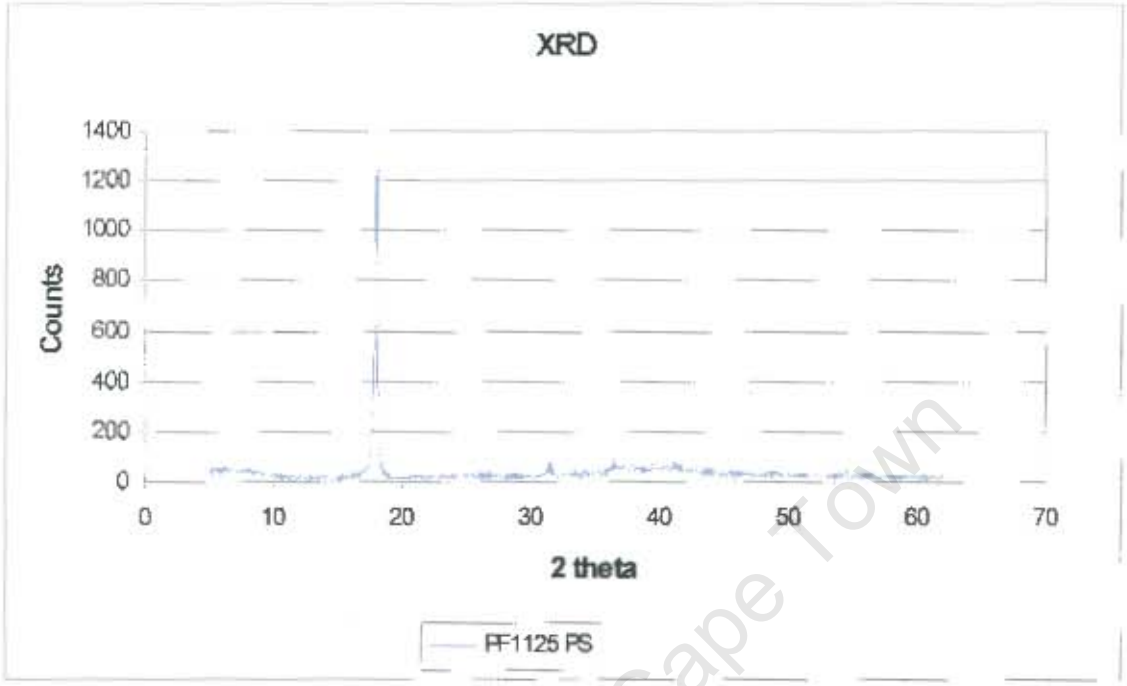

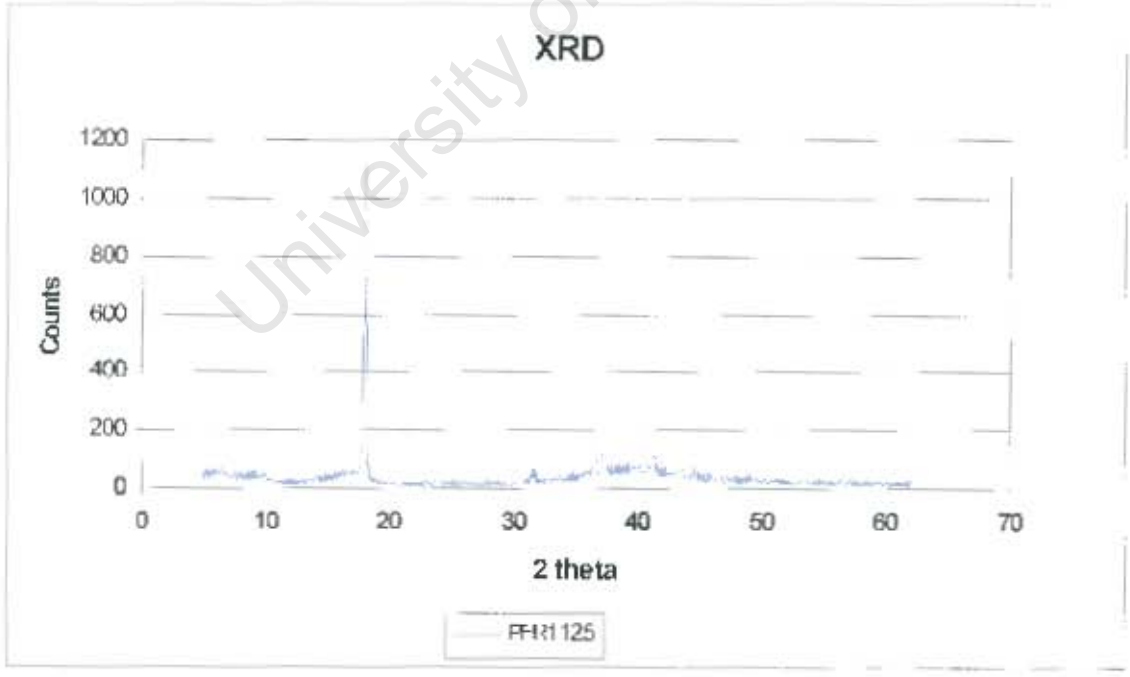

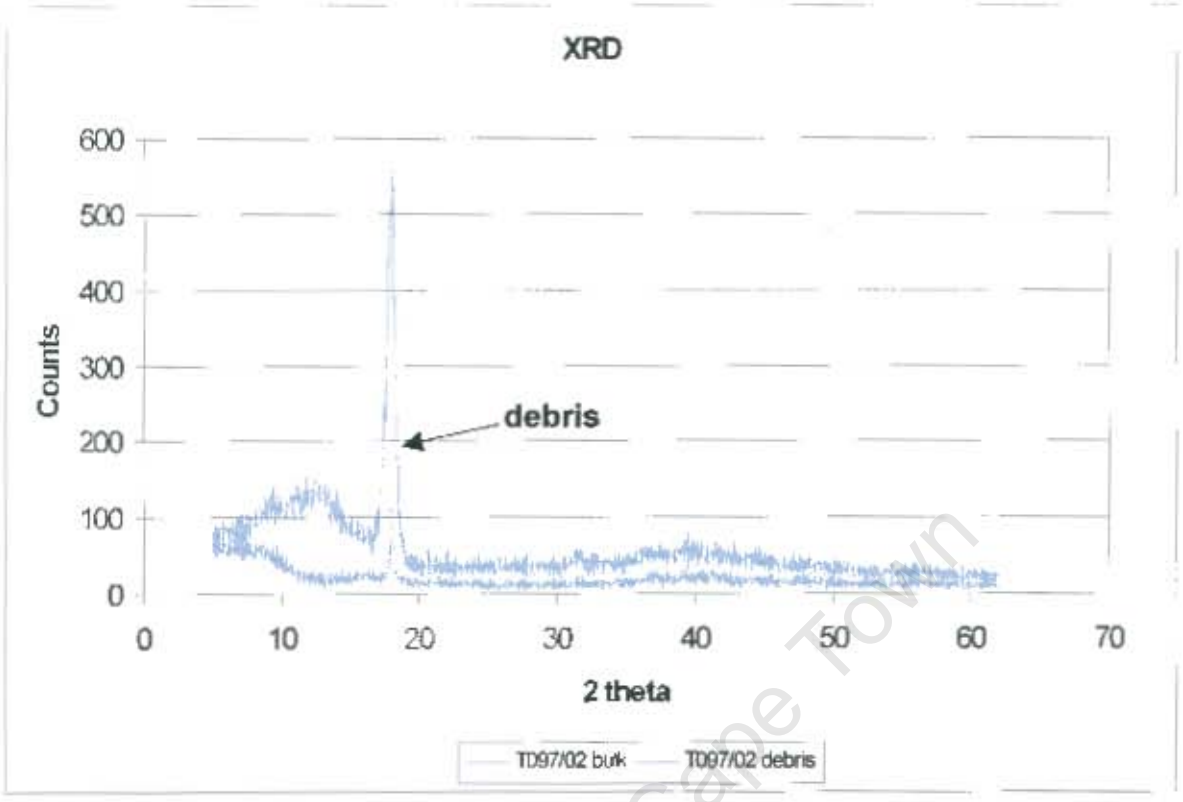

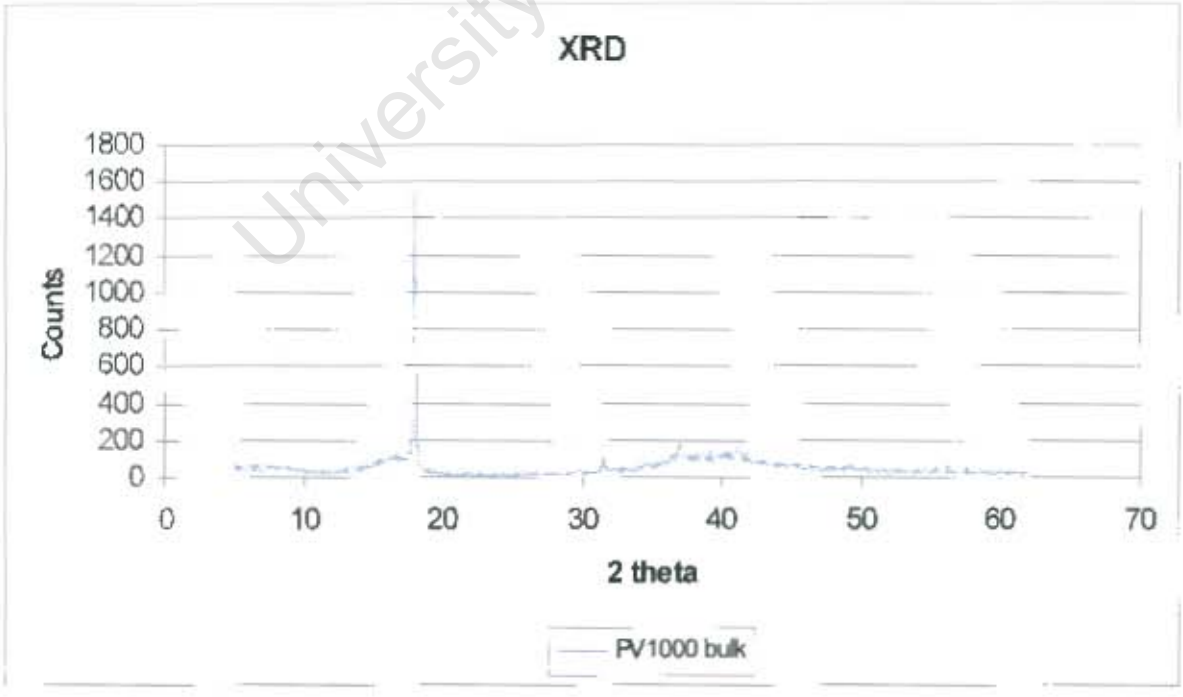

APPENDIX E: DSC Scans of T103-02